Phase IV experimental uncertainty analysis for ice tank ship resistance and manoeuvring experiments using PMM

Lau, M.; Derradji-Aouat, A.

Technical Report (National Research Council of Canada. Institute for Ocean Technology); no. TR-2006-03, 2006

DOCUMENTATION PAGE

REPORT NUMBER	NRC REPORT NUMBER	DATE
	TR-2006-03	January, 2004

REPORT SECURITY CLASSIFICATION	
Unclassified	**Unlimited**

TITLE

Phase IV Experimental Uncertainty Analysis for Ice Tank Ship Resistance and Manoeuvring Experiments using PMM

AUTHOR(S)
Michael Lau and Ahmed Derradji-Aouat

CORPORATE AUTHOR(S)/PERFORMING AGENCY(S)

Institute for Ocean Technology

PUBLICATION

SPONSORING AGENCY(S)

Institute for Ocean Technology, Marine Institute

IMD PROJECT NUMBER	NRC FILE NUMBER
42_953_10	

KEY WORDS	PAGES	FIGS.	TABLES
uncertainty analysis, PMM, manoeuvring, ice, Terry Fox	72	18	14

SUMMARY

The Institute for Ocean Technology (IOT) of the National Research Council of Canada (http://www.iot-ito.nrc-cnrc.gc.ca/) has conducted physical, numerical and mathematical modeling of ship manoeuvring characteristics in ice**,** as part of a larger effort to develop reliable modeling techniques to assist in the design of new ice-worthy vessels and in the simulation of their navigating characteristics. Preliminary tests were conducted for a range of model speeds and radii and an Experimental Uncertainty Analysis (EUA) was conducted on this test series as part of the data analysis.

This report describes the model test program, and the results of the EUA. For consistency, this test series is referred to as Phase IV of the EUA.

ADDRESS National Research Council
Institute for Ocean Technology
P. O. Box 12093, Station 'A'
St. John's, Newfoundland, Canada
A1B 3T5
Tel.: (709) 772-5185, Fax: (709) 772-2462

National Research Council Canada
Institute for Ocean Technology

Conseil national de recherches Canada
Institut des technologies océaniques

PHASE IV EXPERIMENTAL UNCERTAINTY ANALYSIS FOR ICE TANK SHIP RESISTANCE AND MANOEUVRING EXPERIMENTS USING PMM

Michael Lau and Ahmed Derradji-Aouat

January 2006

ABSTRACT

The Institute for Ocean Technology (IOT) of the National Research Council of Canada (http://www.iot-ito.nrc-cnrc.gc.ca/) has conducted physical, numerical and mathematical modeling of ship manoeuvring characteristics in ice**,** as part of a larger effort to develop reliable modeling techniques to assist in the design of new ice-worthy vessels and in the simulation of their navigating characteristics. Preliminary tests were conducted for a range of model speeds and radii and an Experimental Uncertainty Analysis (EUA) was conducted on this test series as part of the data analysis.

This report describes the model test program, and the results of the EUA. For consistency, this test series is referred to as Phase IV of the EUA.

ACKNOWLEDGMENTS

The investigations presented in this report were partially funded by the Atlantic Innovation Fund through the Marine Institute, Newfoundland. Work term student A. van Thiel provided assistance in performing the experimental uncertainty analysis. Their support is gratefully acknowledged.

TABLE OF CONTENTS

APPENDICES

LIST OF TABLES

LIST OF FIGURES

PHASE IV EXPERIMENTAL UNCERTAINTY ANALYSIS FOR ICE TANK SHIP RESISTANCE AND MANOEUVRING EXPERIMENTS USING PMM

1.0 INTRODUCTION

Recent development of offshore oil and gas reserves in several countries, together with economic studies to increase transportation through the Arctic, has led to a renewed interest in the manoeuvrability of vessels in ice. Despite a sizeable volume of work, there is not yet a universally accepted analytical method of predicting ship performance in ice. In 2003, the Institute for Ocean Technology (IOT) of the National Research Council of Canada (http://www.iot-ito.nrc-cnrc.gc.ca/) initiated a comprehensive physical, numerical and mathematical modeling of ship manoeuvring characteristics in ice, as part of a larger effort to develop reliable modeling techniques to assist in the design of new ice-worthy vessels and in the simulation of their navigating characteristics.

Considering the complexity of the loads imposed by ice during ship manoeuvres, a preliminary series of ship manoeuvring experiments in ice were conducted for a range of model speeds and radii to provide insights to assist in the subsequent numerical and mathematical modeling. An Experimental Uncertainty Analysis (EUA) was conducted on the results of these tests as a step towards developing a procedure for EUA for ship manoeuvring in ice and to gain an acceptable level of confidence in the truthfulness of experimental results. As the objective of this series was primarily on the manoeuvring characteristics of vessels in ice, a full examination was not completed of the applicability of the EUA procedure as developed in Phases I to III of the EU project (Derradji-Aouat and van Thiel, 2004). However, EUA was performed to give a measure of the EU of the ice properties and the reported ice resistance and yaw moment data.

This report accompanies IOT report TR-2006-02 (Lau and Derradji-Aouat, 2006), which documents the results of the manoeuvring tests, whereas this report documents the results of the EUA calculations. The description of the model test program is taken from TR-2006-02 for completion. Conclusions are made and recommendations for future works are provided. For consistency, this test series is referred to as Phase IV of the EUA.

2.0 TESTS PROGRAMS

In the ice tank, the *Terry Fox* model (scale = 1:21.8) was towed in five ice sheets using the PMM with the model restrained in roll. The model was outfitted with a rudder. Tests with different rudder angles were tested in open water only. Both moving straight and turning circle manoeuvres were tested. The target flexural strength and ice thickness of the ice sheets was the same for all experiments (35 kPa and 40 mm). During the turning circle manoeuvring tests, the drift angle β was set to zero degrees. Bubble ice was required for all ice sheets.

Three different types of experiments were conducted. They were:

1) Experiments in Level Ice
2) Experiments in Pre-sawn Ice (Resistance runs only)
3) Experiments in Open Water

2.1 Test Set-up

In these tests, the main components of the test set up are the ice tank, the *Terry Fox* ship model, the Planar Motion Mechanism (PMM), the Data Acquisition System (DAS), and video cameras.

2.1.1 Ice tank

The ice tank is 96 m long, 12 m wide and 3 m deep, with useable ice sheets of 76 m in length, making this tank the longest in the world. Thus, it allows for tests at higher speeds and longer test runs (more data is obtained per run). The 12 m width of the tank enables ship experiments in various manoeuvres, and for straight test runs in continuous ice, three tracks may be used (center channel, north quarter point and south quarter point) in each ice sheet. The ability to perform three continuous ice tests per sheet significantly improves the cost effectiveness. The effect of the tank walls on the center channel is also reduced because there is less confinement due to the tank walls with the wider ice tank.

2.1.2 *Terry Fox* ship model

The experiments were carried out with a 1:21.8 scaled model of the Canadian Coast Guard's icebreaker Terry Fox (IOT model # 417) (Figure 1). The model hydrostatics are provided in Appendix A. The model was mounted to the towing carriage through the PMM at the model's center of gravity. The model was towed at a controlled planar motion through a level ice sheet. The model surface was finished to a friction coefficient of 0.01 with Dupont's Imron paint.

2.1.3 Planar Motion Mechanism (PMM)

Marineering Limited (1997) provided details on the development and commissioning of the PMM. The PMM was designed to study the manoeuvring of ships in both ice and open water.

The PMM apparatus (Figure 2) consists of two primary components: a sway sub-carriage that is mounted beneath the main towing carriage, and a yaw assembly that is connected to the sway sub-carriage. The apparatus allows the model to yaw and sway in a controlled manner, while measuring the sway and surge forces as well as the yaw moment. The combination of sway and yaw allows a variety of manoeuvres to be performed.

The PMM dynamometer has 3 cantilever-type load cells for measuring surge force, sway force, and yaw moment. A load cell aligned along the model's surge axis measures surge force. The other two load cells aligned along the model's sway axis measure sway force. Yaw moment is measured by resolving the outputs from the two sway load cells. The specifications for the PMM are given in Table 1.

2.1.4 Data Acquisition System (DAS) and video

In each experiment, tow force, turning moment, and ship motions were measured. The transducer for outputs were sampled digitally at 50 Hz and filtered at 200 Hz.

Two video recordings were made of each test, one on the starboard side that is manually controlled to follow the model's manoeuvres, and the other looking down ahead of the model at the port side.

All details regarding the instrumentation used in this test program and their calibration sheets are provided in Appendix B.

2.2 Ice Conditions

The experiments were carried out in CD-EG/AD/S ice (Spencer and Timco, 1990). With inclusions of air bubbles into the growing ice sheet, the model ice significantly improves the scaling of ice density, elastic, and fracture properties. For each ice sheet, flexural, compressive, and shear strengths were measured frequently throughout the test period. Strength versus time curves were created for each ice sheet and the strength values reported at each test time were interpolated from these curves. Flexural strength, σ_f, was measured using *in-situ* cantilever beams. A number of shear strength measurements were performed immediately after the flexural strength test to provided index values for

comparison with the measured flexural strengths. The ratio of shear strength to downward breaking flexural strength varied from 1.03 to 3.16. The reported ice thickness, *h*, is the average thickness of approximately 65 measurements of the ice sheet thickness along the test path. The IOT standards and work procedures were followed for producing and characterizing level ice sheets.

All work procedures are given in the IOT documentations for system quality. The procedures followed to prepare the ice tank, seed and grow the ice sheet are given in the IOT work procedures TNK 22, TNK 23, and TNK 37, respectively. The mechanical properties of the ice are determined according to the following work procedures: TNK 26 (for measuring the flexural strength), TNK 27 (for measuring the elastic modulus), TNK 28 (for measuring compressive strength), and TNK 30 (for measuring ice density). Ice thickness measurements were performed as per the work procedure TNK 25.

It should be noted that all of the above work procedures are valid for both bubbly ice and non-bubbly ice. Simply, in the case of non-bubbly ice, the bubbler system is turned off.

The test program required five (5) different ice sheets with a nominal thickness of 40 mm and a nominal flexural strength of 35 kPa at beginning of test day. The flexural strengths were tempered throughout the test day. A summary of the five ice sheets and their properties are presented in Appendix C.

2.3 Test Matrix

The overall test matrix is summarized in Appendix D. For the tests described in this program, the ice sheets had a target ice thickness of 40 mm and a target flexural strength of 35 kPa. The following manoeuvres were utilized: (1) resistance runs in which the model was towed along a straight line at a zero drift angle, and (2) pure yaw through a constant radius manoeuvre so that the heading of the model was always tangential to the path of its center of gravity resulting in zero sway force and a yaw moment. All tests in ice were performed with a zero degree rudder angle and a model velocity ranging from 0.02 m/s to 0.6 m/s. The constant radius manoeuvre was conducted with two turning radii (50 m and 10 m). Additional resistance tests were also conducted at a model velocity of 0.9 m/s. Concurrent to the testing in ice, manoeuvres in open water were also conducted. The open water runs were performed with a rudder angle of 0, 20, and 30 degrees.

2.4 Description of the Experiments in Ice

The experiments conducted in ice included level ice resistance runs, pre-sawn ice resistance runs, and arc manoeuvring runs in level ice. Figure 3 shows a

picture of a typical test run in ice. Ship model speeds of 0.02 m/s, 0.05 m/s, 0.1 m/s, 0.2 m/s, 0.3 m/s, 0.4 m/s, 0.5 m/s, 0.6 m/s, and 0.9 m/s were tested in ice (see Appendix D).

Appendix E summarizes the channel width measurements obtained in ice tests and shows the run schematics for manoeuvring tests in ice. Figures E.1 to E.5 show schematics for the ice test runs in each sheet. For the first ice sheet, NMS1, the runs conducted are shown in Figure E.1. The second ice sheet, NMS2, used the same test matrix as Runs 1- 3 for Phase III (Figure E.2). The schematics for the ice sheets NMS3, NMS4 and NMS5 are shown in Figures E.3, E.4, and E.5, respectively.

For the straight runs, the following test run scenario was performed in the first two ice sheets (NMS1 and NMS2). Initially, a level ice test run was conducted along the centerline of the tank. In NMS1, the model was towed at a constant speed of 0.1, 0.6 and 0.9 m/s with an approximately 20 m run distance each, and a creep test performed at the end (0.02 m/s). Afterwards, the model was tested at the quarter-point (on either side of the center-line). Again, the model was towed at the set constant speeds of 0.1, 0.6, 0.9, and 0.02 m/s (creep speed). For the south quarter point test, a pre-sawn ice test run was performed (same procedure as per the standard resistance test). In NMS2, the same schematic was used and speeds tested were 0.1, 0.3, and 0.6 m/s, followed by a creep test.

For turning circle tests, the model was towed at a constant yaw rate with the prescribed arc radius (10 m and 50 m) and run length. The runs were conducted in the last three ice sheets (NMS3, NMS4 and NMS5).

2.5 Description of the Experiments in Open Water

The open water tests for the corresponding ice test runs were baseline open water tests. The experiments conducted in open water included resistance runs and arc manoeuvring. Ship model speeds of 0.02 m/s, 0.05 m/s, 0.1 m/s, 0.2 m/s, 0.3 m/s, 0.4 m/s, 0.5 m/s, 0.6 m/s and 0.9 m/s were tested with three rudder angles (0, 20, and 30 degrees) (See Appendix D). Note that all open water tests were conducted in the ice tank, for calm water conditions (no waves).

3.0 TEST RESULTS

Plots for typical test results are given in Appendix F.

3.1 Resistance Tests

Open water

Baseline open water resistance tests were completed in the ice tank for test speeds corresponding to the ice tests conducted. Figure 4 shows the measured tow force versus model velocity for the open water resistance runs. The numerical values for the mean tow force at each speed are:

Model Velocity (m/s)	Mean Tow Force (N)
0.1	0.18
0.3	1.41
0.6	4.81
0.9	10.48

The resistance (given in N) in baseline open water, R_{ow}, can be obtained from the regression line in Figure 4:

$$R_{ow} = 11.717 \cdot V^2 + 1.0809 \cdot V - 0.0182 \qquad (1)$$

where V is the tow velocity (in m/s).

Ice Tests

Figure 5 shows the measured tow force versus model velocity for the resistance tests in both pre-sawn and continuous ice. The numerical values for the mean tow force at each speed are:

Model Velocity (m/s)	Presawn Ice Mean Tow Force (N)	Level Ice Mean Tow Force (N)
0.02	4.50	9.02
0.1	5.95	10.38
0.3	9.01	15.74
0.6	16.36	23.85

3.2 Manoeuvring

3.2.1 Tow forces

Open water

Baseline open water manoeuvring tests were completed in the ice tank for test speeds corresponding to the ice tests conducted. Figure 6 shows the measured tow (surge) force versus model velocity curves for the open water manoeuvring runs grouped according to rudder angle. The numerical values for the mean tow (surge) force at each speed are:

Model Velocity (m/s)	**Rudder Angle 0 degrees**		**Rudder Angle 20 degrees**		**Rudder Angle 30 degrees**	
	Mean Surge Force (N)		**Mean Surge Force (N)**		**Mean Surge Force (N)**	
	R = 10 m	R = 50 m	R = 10 m	R = 50 m	R = 10 m	R = 50 m
0.1	1.09	0.88	3.73	0.49	4.23	0.40
0.3	2.57	1.18	n/a	n/a	n/a	n/a
0.6	8.43	4.54	12.11	7.51	14.65	8.92
0.9	42.79	10.50	27.36	14.52	25.53	19.41

The resistances in baseline open water manoeuvring, $R_{ow,}$ for the two turning radii with zero rudder angle can be obtained from the regression lines in Figure 6:

$$\textit{Arc radius} = 10m$$
$$R_{ow} = -33.135 \cdot V^2 + 5.4 \cdot V + 0.6609 \quad (2a)$$

$$\textit{Arc radius} = 50m$$
$$R_{ow} = -13.653 \cdot V^2 + 0.4821 \cdot V + 0.1673 \quad (2b)$$

Ice tests

Figure 7 shows the measured tow force versus model velocity curves for the ice manoeuvring runs. The results for Runs 132, 133, 148, and 153 are not shown, as those measurements were suspicious due to problem with the model's initial alignment. These results were not corrected for ice strength, which may contribute to the scattering of data. The numerical values for the mean tow (surge) force at each speed are:

Model Velocity (m/s)	Level Ice	
	Mean Surge Force (N)	
	R = 10 m	R = 50 m
0.05	n/a	28.91
0.1	15.43	n/a
0.2	16.11	33.82
0.3	19.12	n/a
0.4	29.01	40.42
0.5	29.33	n/a
0.6	41.08	n/a

3.2.2 Yaw moments

Open water

Figure 8 shows the measured yaw moment versus model yaw rate curves for the open water manoeuvring runs grouped according to rudder angle. The numerical values for the mean yaw moment at each model speed[1] are:

Model Velocity (m/s)	Rudder Angle 0 degrees		Rudder Angle 20 degrees		Rudder Angle 30 degrees	
	Mean Yaw Moment (Nm)		Mean Yaw Moment (Nm)		Mean Yaw Moment (Nm)	
	R = 10 m	R = 50 m	R = 10 m	R = 50 m	R = 10 m	R = 50 m
0.1	0.93	0.07	3.04	-0.04	3.39	0.09
0.3	-0.63	-0.90	n/a	n/a	n/a	n/a
0.6	-7.96	-4.47	-5.06	-4.96	-5.99	-5.27
0.9	-21.02	-10.41	-23.30	-10.54	-24.45	-11.78

The yaw moment (given in N·m) in baseline open water manoeuvring, $N_{ow,}$ for the 2 turning radii with zero rudder angle can be obtained from the regression lines in Figure 8:

$$N_{ow} = 0.4516 \cdot r^2 - 0.7781 \cdot r \qquad (2c)$$

where r is the yaw rate (in deg/s).

Ice Tests

Figure 9 shows the measured yaw moment versus model yaw rate curves for the ice manoeuvring runs. The results for Runs 132, 133, 148, and 153 are not shown, as those measurements were suspicious due to problems with the

[1] Yaw Rate = Model Speed / Turning Radius

model's initial alignment. These results were not corrected for ice strength, which may contribute to the scattering of data. The numerical values for the mean yaw moment at each speed are:

Model Velocity (m/s)	Level Ice	
	Mean Yaw Moment (Nm)	
	R = 10 m	R = 50 m
0.02	n/a	15.86
0.05	67.91	n/a
0.1	77.58	38.24
0.2	84.26	n/a
0.3	113.52	25.96
0.4	93.42	n/a
0.5	114.19	n/a
0.6	123.00	84.81

4.0 EXPERIMENTAL UNCERTAINTY ANALYSIS (EUA)

Experimental Uncertainty Analysis is used to gain an acceptable level of confidence in the truthfulness of experimental results. As the objective of this series was primarily on the manoeuvring characteristics of vessels in ice, a full examination was not completed of the applicability of the EUA procedure as developed in Phases I to III of the EU project (Derradji-Aouat and van Thiel, 2004). However, EUA was performed to give a measure of the EU of the ice properties and the reported ice resistance data. For consistency, this test series is referred to as Phase IV of the EUA.

4.1 EUA for Ice Tank Testing – A Procedure Development

A literature review of the history and development of EUA in marine/ocean testing facilities was given by Derradji-Aouat (2002) and the mathematical basis of the EUA procedure was adopted from Coleman and Steele (1998).

In a typical experiment, the total uncertainty, *U*, is the geometric sum of a bias uncertainty component, *B*, and a random uncertainty component, *P*:

$$U = \pm\sqrt{\left(B^2 + P^2\right)} \tag{3}$$

The bias component, *B*, consists of uncertainties in instrumentation and equipment calibrations. Examples of bias uncertainty sources are the load cells, RVDT's (Rotary Variable Differential Transformers), yoyo potentiometers, and the Data Acquisition System (DAS). On the other hand, the precision component, *P*, deals with environmental and human factors that may affect the repeatability of the test results (i.e. if a test was to be repeated several times, would the same results be obtained each time?). Examples of random uncertainty sources are the changing test environment (such as fluctuations in room temperature during testing), small misalignments in the initial test setup, human factors, etc.

Derradji-Aouat (2002) showed that in a typical ice tank ship resistance test, the bias uncertainty component *B* is much smaller than the random uncertainty component *P*. He reported that, in Phase I ship model tests in ice, the value of *B* is at least one order of magnitude smaller than the value of *P*. He concluded, therefore, that in routine ship resistance ice tank testing, the total uncertainty *U* can be taken as equal to the random uncertainty component. Simply, without a loss of accuracy, the bias uncertainty component can be neglected. It follows that:

$$U = \pm P \tag{4}$$

4.2 EUA Procedure for Ice Tank Testing

There are two major considerations when applying the EUA procedure to ice tank testing: the segmentation hypothesis and the steady state requirement.

4.2.1 Segmentation hypothesis

For the ice test runs, several factors have contributed to the decision for keeping the speed of the ship model constant for a longer length than required for a test run, i.e., > 1.5 times the length of the model as required by the ITTC (ITTC, 2002). The main hypothesis is that the time history from one long test run can be divided into segments, and each segment can be analyzed as a statistically independent test. The hypothesis states that (Derradji-Aouat, 2002 and 2003, and Derradji-Aouat and van Thiel, 2004):

> *"The history for a measured parameter (such as tow force versus time) can be divided into 10 (or more) segments, and each segment is analyzed as a statistically independent test. Therefore, the 10 segments in one long test run in ice are regarded as 10 individual (independent but identical) tests."*

Coleman and Steel (1998) reported that, in statistical uncertainty analysis, a population of at least 10 measurements (10 data points) is needed. Precision uncertainty is calculated using the mean and the standard deviation of that population. However, in ice tank testing, it is recognized that conducting the same test 10 times is very costly and very time consuming. Therefore, the principle of segmenting the time history of a measured parameter over a long test run into multiple segments results in significant savings in project costs and efforts. By demonstrating that each segment can be analyzed as a statistically independent test, uncertainties are calculated from the means and standard deviations of the individual segments. The segmentation hypothesis is further illustrated in the Phase II report (Derradji-Aouat, 2003).

Using the segments, the first calculation step is to obtain mean and standard deviation for each segment. The second step is to calculate the mean of the means and the standard deviation of the means. The mean of the means and standard deviation of the means are needed to compute random uncertainties in the results of the test run (as it will be shown in the subsequent sections). These two basic calculations steps are repeated for all test runs in all five (5) ice sheets.

It should be cautioned that the segmentation hypothesis is valid only if the following three conditions are satisfied (Derradji-Aouat, 2004):

1) Each segment should span over 1.5 to 2.5 times the length of the ship model,

2) Each segment should include at least 10 events for ice breaking (10 load peaks) or at least 10 collision events (in the case of pack ice test runs), and
3) General trends (of a measured parameter such as tow force versus time) are repeated in each segment.

Condition # 1 is based on the fact that the ITTC procedure for resistance tests in level ice (ITTC-4.9-03-03-04.2.1) requires that a test run should span over at least 1.5 times the model length. For high model speeds (> 1 m/s), however, the ITTC procedure requires test spans of 2.5 times the model length.

Condition # 2 is based on the fact that in EUA, for an independent test, a population of at least 10 data points is needed to achieve the optimal value of 2 for the factor t (Coleman and Steele, 1998). For tests in ice tanks, 10 to 15 segments are recommended. The gain in any further reduction in the value of t (by having more than 10 to 15 segments) is minimal.

Condition # 3 is introduced to ensure that the overall trends in a measurement (such as tow force versus time) are repeated in each segment. This condition serves to provide further assurance into the main hypothesis ("*…Therefore, the 10 segments in one long test run are regarded as 10 individual, independent but identical, tests"*). Fundamentally, if the trends are not repeated, reasonably, then the segments could not be analyzed as "*independent but identical*" tests.

For these tests, Condition #1 was relaxed, as the shorter runs only allow for the extractions of a smaller numbers (up to 5) of repeating segments for each run. This will affect the calculations of the random uncertainties as explained in Section 4.3.

It is important to emphasize the fact that the division of the time history of a measured parameter into consecutive segments is valid only for long test runs at constant speed and heading. If the model speed or heading is changed during the test run, then the segments cannot be analyzed as "identical".

Note that the time histories measured in creeping speed test are not subjected to the segmentation hypothesis. Furthermore, it is recognized that the division of the results of a test run into segments is valid only for the steady state portion of the measured data, and only the steady state portion of the measured time history is to be used. This is required to eliminate the effects of the initial ship penetration into the ice (transient stage), and the effects of the slowdown and full stop of the carriage during the final stages of the test run.

4.2.2 Steady state requirements

In ice tank testing, for any given ice sheet, the ice properties are not completely uniform (same thickness) and homogeneous (same mechanical properties) throughout the ice sheet. This is attributed, mainly, to the ice growing processes and the refrigeration system in the ice tank. An example to illustrate the spatial variability of the material properties is provided by Derradji-Aouat and van Thiel (2004).

In addition to the spatial variability of the material properties of ice during an ice test run, the carriage speed may or may not be maintained at exactly the required nominal constant speed[2]. Due to this inherent non-uniformity of ice sheets, the non-homogeneity of ice properties, and the small fluctuations in the carriage speed, a steady state condition in the time history of a measurement may not be achieved.

Theoretically, if the time history of a measured parameter is changing drastically, then the segments could not be analyzed as "identical" tests (condition # 3). The steady state requirement, therefore, calls for a corrective action to account for the effects of non-uniform ice thickness, non-homogenous ice mechanical properties, and small fluctuations in carriage speed on the test measurements.

To identify whether or not the time history for a measured parameter has reached its steady state, the following procedure was recommended (Derradji-Aouat, 2002). The measured time histories for all parameters were plotted along with their linear trend lines. A linear trend line with a zero slope (or a slope very close to zero) indicates that a steady state in a measured parameter is achieved.

Figures 10a to 10f shows the time histories for the measured tow forces in Phase IV testing. Time histories for Phases I to III testing were provided in the previous reports by Derradji-Aouat (2002), Derradji-Aouat (2003) and Derradji-Aouat and van Thiel (2004), respectively.

Figures 10g to 10h show the time histories for the measured yaw moments in Phase IV testing for the manoeuvring runs.

After drawing the linear trend lines through all measured tow forces and yaw moments, it was observed that, in a majority of cases, a true steady state was never achieved (Tables 2 and 3). For example, the linear trend lines for representative tow force time histories are shown in Fig. 10. A steep sloping trend line reflects the fact that the tow force or yaw moment did not reach their steady state.

[2] The control system maintains the carriage speed; however, when ice breaks, small fluctuations in carriage speed may take place.

As shown in Tables 2 and 3, the non-steady state led to some significant changes in the tow forces and yaw moments over the towing distance (up to 284.83% and 49.38%, respectively). This non-steady state condition may be attributed to one (or all) of the following three factors:

1) A changing carriage speed (or small fluctuations in carriage speed) during testing,
2) Non-uniform ice thickness, and
3) Non-uniform mechanical properties of the ice (flexural/compressive strengths, elastic modulus, and density of ice).

The contribution of each factor is further investigated as follows:

Effects of changing model speed

Figure 11 shows the time histories of the measured model speed in Phase IV testing. The linear trend lines point to the fact that, during testing, the actual changes in the model speed were very small and so, consequently, they can be neglected. Trend lines through the model velocity histories had slopes between 4 X 10^{-7} and 5 X 10^{-4}. Table 4 shows that, over the towing distance for run with a particular velocity, the changes in the model velocity ranged between 0.01% and 0.88%.

By and large, the model speed is very much steady, therefore, it was assumed that the contribution of the changing model speed into the development of non-steady state time history of the measured parameters could be ignored. Consequently, no corrections for model speed fluctuations are needed. The same conclusions were reached in previous phases of testing (Derradji-Aouat, 2002 and 2003, and Derradji-Aouat and van Thiel, 2004).

Effect of changing model yaw rate and drift angle in the manoeuvring runs

The manoeuvring runs in this test series require the PMM to maintain a constant yaw rate and drift angle, in addition to a constant model (tangential) speed. Therefore, the controllability of the carriage on these two variables was assessed.

Figure 12 shows the time histories of the measured yaw rate in Phase IV testing. The linear trend lines point to the fact that, during testing, the actual changes in the yaw rate were small and so, consequently, they can be neglected. Trend lines through the yaw rate histories had slopes between 2 X 10^{-6} and 0.0062, and the changes were larger with larger yaw rate as shown in Figure 12. Table 5 shows that, over the towing distance for run with a particular yaw rate, the changes in the yaw rate ranged between 0.27% and 2.66%.

Figure 13 shows the time histories of the drift angle in Phase IV testing. The drift angle was computed as the difference between the targeted yaw angle

(corresponding to zero drift angle)[3] and the measured model yaw angle. The linear trend lines point to the fact that, during testing, the actual changes in the drift angle were not small and so, consequently, they cannot be neglected. Trend lines through the drift angle histories had slopes between 8 X 10^{-5} and 0.1862, and the changes were larger with larger yaw rate, as shown in Figure 13. Table 6 shows that, over the towing distance for run with a particular yaw rate, the changes in the drift angle ranged between 1.49% and 79.33%. It should be noticed that the derivation from the target drift angle (zero degree) increased with yaw rate (Lau and Derradji, 2004).

Effects of non-uniform ice thickness

Measured ice thickness profiles along the channels created by test runs in the ice tank are given in Figure 14a. Each profile consisted of a series of ice thickness measurements (every 2 m) along the length of the ice tank.

Mean thickness profiles are given in Figure 14b, whereby each mean profile is the average of all measurements at the same tank length location. The linear trends, through the mean profiles, indicate that the ice thickness varied within the range of 4.36% (NMS3) to 8.02% (NMS2), as can be shown in Table 7.

To correct for the effects of non-uniform ice thickness on the test measurements, the following correction methodology and rational are used (Derradji-Aouat, 2002):

a. Uncertainty analyses for both mean and maximum tow forces may be calculated. In ice engineering, maximum tow forces are indicators for maximum ice loads on the ship structure, while mean tow forces are used in the standard ship resistance calculations. For this phase, only the mean tow force is examined.

b. In the following discussion, mean ice resistance values are used to show how the EUA method is conceptualized and developed. The same procedure and equations are used for maximum ice resistance values (Derradji-Aouat, 2002).

c. Ice thickness corrections are applied only to the resistance of ice. In ice resistance analysis, the total ice resistance, R_{Ice}, is equal to the measured resistance in ice tests, R_t, minus the resistance measured in the baseline open water tests, R_{ow} (Derradji-Aouat and van Thiel, 2004).

$$\left(R_{Ice}\right)_{Mean} = \left(R_t\right)_{Mean} - \left(R_{ow}\right) \quad (5)$$

[3] The targeted yaw angle was computed from the PMM controlled model motion as follows:

$$\beta = \tan^{-1}\left(\frac{V_y}{V_x}\right) - r_{meas}$$

where R_{ow} is obtained from the correlation obtained from the baseline open water test results. For resistance tests Equation 1 is used, and for manoeuvring tests with arc radii of 10m and 50 m, Equations 2a and 2b are used, respectively.

d. For a given ice sheet, with nominal thickness h_o, the following equation is used to calculate mean total ice resistance (Derradji-Aouat, 2003):

$$\left(R_{Ice}\right)_{Correct\ Mean} = \left(R_{Ice}\right)_{Measured\ Mean} \cdot \left(\frac{h_o}{h_m}\right) \tag{6}$$

where $(R_{Ice})_{Correct\ Mean}$ is the corrected total ice resistance for the nominal ice thickness h_o (h_o = 40 mm), $(R_{Ice})_{Measured\ Mean}$ is the measured total ice resistance for the nominal ice thickness h_o. The parameter h_m is the ice thickness averaged over the measurements taken at an area within which the corresponding resistance time history segment is corrected.

Note that Equations 5 and 6 are also valid when using maximum ice resistance values. This is achieved by substituting the subscript “mean” in Equations 5 and 6 by the subscript “max”.

Figures 15a and 15b show the plots for corrected versus measured (uncorrected) mean tow force for the resistance and manoeuvring tests, respectively.

Note that only the results of tests in continuous ice were subjected to ice thickness corrections. Note, also, that the time histories measured in the creeping speed test runs were not subjected to corrections for ice thickness variation. The length of each creeping speed test run was small (only one ship length ≈ 3.8 m), and the variation of ice thickness over this small length can be ignored.

Effects of non-homogeneous ice properties

Measured flexural strength profiles along the length of the ice tank are given in Figure 16a. Mean flexural strength profiles are given in Figure 16b. *In-situ* cantilever beam flexural strength measurements were conducted along the ice tank. The beam dimensions have the proportions of 1:2:5 (thickness: width: length). The flexural strength, σ_f, is calculated as:

$$\sigma_f = \frac{6PL}{wh_f^2} \tag{7}$$

where L is the length, w *is* the width, h_f is the thickness, and P is the point load.

The uncertainty in the measured flexural strength is $U_{\sigma f}$:

$$U\sigma_f = \sqrt{U_P^2 + U_L^2 + U_W^2 + 2U_{h_f}^2} \tag{8}$$

where U_L, U_W, and U_{hf} are the uncertainties in the measured dimensions *L, w and* h_f, respectively, and U_p is the uncertainty in the measured point load.

The uncertainties in the flexural strength profiles were calculated using Equation 14, and they are given in Table 8. Uncertainties varied between 33.03% and 88.44%.

Measured ice density values in the ice tank are given in Table 9 and shown in Figure 17. The density of ice, ρ_i, is:

$$\rho_i = \rho_w - \frac{M}{V} \tag{9}$$

where ρ_w is the density of water. *M* and *V* are the mass and volume of the ice. The uncertainty involved in the ice density is:

$$U_{\rho_i} = \sqrt{U_H^2 + U_L^2 + U_W^2 + U_M^2} \tag{10}$$

The value of U_M is neglected because it is considered a bias uncertainty (Derradji-Aouat, 2002). The variation of density in the ice tank ranged between 5.60% and 11.59%. From the ice tank operational point of view, in non-bubby ice sheets, density values could not be controlled but uniformity is reasonably assured. In bubbly-ice, however, the opposite is true, the target density values can be achieved but the spatial uniformity of the ice density is compromised.

4.3 Calculations for Random Uncertainties

Step # 1: In Tables 10 and 11, after the calculations of the mean of means, $Mean\_TF_{Mean}$, and standard deviation of means, STD_TF_{Mean}, the Chauvenet's criterion was applied to identify the outliers (outliers are discarded data points). The Chauvenet number for mean tow forces is:

$$(Chauv\ \#)_{Mean} = \left| \frac{TFMean - (\ Mean\_TFMean)}{(\ STD\_TFMean)} \right| \tag{11}$$

The Chauvenet's criterion dictates that the *Chauv #* for each data point should not exceed a certain prescribed value (Coleman and Steele, 1998). For 10 to 15

segments, the *Chauv #* should not exceed 1.96 to 2.13. The Chauvenet numbers for other sample sizes are given in Table 12.

A new mean of means and a new standard deviation of means were then calculated from the remaining data points (remaining segments).

Step # 2: After calculating the new mean of the means and the new standard deviation of the means (from the remaining segments - data points), random uncertainties in the mean tow force are:

$$\left(U(TF_{Mean}) \right) = \frac{t \cdot (STD\_TF_{Mean})}{\sqrt{N}} \tag{12}$$

where the variable t is a function of the degrees of freedom and the confidence limit, and N is the number of the remaining data points (segments). For example, for a sample size N larger than 10 and a confidence limit of 95%, t is approximately equal to 2.

Step # 3: Random uncertainties, calculated using Equation 18, are expressed in terms of uncertainty percentage, *UP*:

$$\left(UP(TF_{Mean}) \right) = \frac{U(TF_{Mean})}{Mean\_TF_{Mean}} \cdot 100 \tag{13}$$

4.3.1 Random uncertainties in resistance tests in ice

The calculated uncertainties in mean resistance are summarized in Table 10. The uncertainties range from 0.53% to 80.15%.

4.3.2 Random uncertainties in manoeuvring tests in ice

The calculated uncertainties in mean surge force are summarized in Table 11. The uncertainties range from 16.39% to 35.3%. The calculated uncertainties in mean yaw moment are summarized in Table 13. The uncertainties range from 10.01% to 62.96%.

4.3.3 Effect of correction for ice thickness on random uncertainties

Corrections for variations in ice thickness profiles (using Equation 6) are made only for tests in continuous ice. Figures 18a and 18b show the comparison between corrected and uncorrected random uncertainties in mean tow force for

resistance and manoeuvring tests, respectively. The correction for variation in ice thickness did not have much effect of the random uncertainty in both the resistance and manoeuvring tests.

4.3.4 Effects of Data Reduction Equation (DRE)

Equation 6 was proposed to correct effects of ice thickness variations on the values of random uncertainties. It should be recognized that the corrected resistance curves are not direct laboratory measurements, but they are calculated from the analytical equation (Equation 6). The process of using analytical equations to correct measured parameters is called "Application of Data Reduction Equations (DRE)".

In EUA, there are additional random uncertainties involved in the application of the DRE. The uncertainty involved in using Equation 6 is:

$$\left(\frac{U_R}{R}\right) = \left(\left(\frac{U_{R_0}}{R_0}\right)^2 + \left(\frac{U_h}{h_0}\right)^2\right)^{\frac{1}{2}} \tag{14}$$

In the above equation, (U_R/R) is the total uncertainty in resistance, R. Both (U_{R0}/R_0) and (U_h/h_0) are the relative uncertainty in the measured ice resistance (as calculated in Tables 10 and 11), and the relative uncertainty in the measured ice thickness, respectively (the uncertainties in ice thickness are shown in Table 4). Note that, in Equation 14, the value of (U_h/h_0) is an additional relative uncertainty, which is induced by the application of the DRE. The total relative uncertainty is the geometric sum of both relative uncertainties (U_{R0}/R_0) and (U_h/h_0).

Tables 14a and 14b summarize the mean tow forces, random uncertainties before and after the use of the DRE for the resistance and manoeuvring tests, respectively. After adding the effect of the DRE, in mean tow force, final uncertainties ranged between 4.58% and 80.27% for resistance tests and ranged between 16.96% and 35.57% for manoeuvring tests.

4.4 Bias and Total Uncertainties

In ice tank testing bias uncertainties are neglected (Derradji-Aouat, 2002), and therefore, the total uncertainties are taken as equal to the random ones.

4.5 Comparison with Previous Phases

Total uncertainties obtained in previous phases of testing were generally between 3% and 10% for continuous ice resistance tests. For Phase IV tests, the

total uncertainties were mainly under 20% for resistance tests and mainly under 35% for manoeuvring tests. The uncertainties obtained in this phase of testing are generally larger than uncertainties calculated in previous phases; this is partially due to the fact than a smaller sample size was used (smaller number of segments) in Phase IV analysis. Another possible explanation may be the effect of the changing boundary conditions when performing arc tests. The model position relative to the tank wall changes during manoeuvring tests, therefore varying the ice boundary conditions. Boundary conditions may also be affected by the testing of several arcs in close proximity within an ice sheet.

5.0 CONCLUSIONS

A total of 42 ice test runs (using five different ice sheets) were used to generate data to analysis the manoeuvring characteristics (28 resistance test and 14 manoeuvring tests).

The uncertainties obtained in this phase of testing are generally larger than uncertainties calculated in previous phases; this is partially due to the fact than a smaller sample size was used (smaller number of segments) in Phase IV analysis. The development of a EUA procedure for manoeuvring in ice is not possible due to the limited usable data currently available. The work completed for this test series is a preliminary analysis, as a step towards developing a EUA procedure for ice manoeuvring tests. Further manoeuvring tests are required to provide more data for EUA.

REFERENCES

Coleman, H. W. and Steele, W. G. (1998), "Experimentation and Uncertainty Analysis for Engineers." 2nd edition, John Wiley & Sons publications, New York.

Derradji-Aouat, A. (2002). "Experimental Uncertainty Analysis for Ice Tank Ship Resistance Experiments." IMD/NRC report # TR-2002-04, Institute for Ocean Technology, St. John's, Newfoundland.

Derradji-Aouat, A. (2003). "Phase II Experimental Uncertainty Analysis for Ice Tank Ship Resistance Experiments." IMD/NRC report # TR-2003-09, Institute for Ocean Technology, St. John's, Newfoundland.

Derradji-Aouat, A. (2004). "A Method for Calculations of Uncertainty in Ice Tank Ship Resistance Testing." Proceedings of the 19th International Symposium on Sea Ice, Mombetsu, Japan.

Derradji-Aouat, A. and van Thiel, A. (2004). "Terry Fox Resistance Tests – Phase III (PMM Testing). The ITTC Experimental Uncertainty Analysis Initiative." IOT/NRC report # TR-2004-05, Institute for Ocean Technology, St. John's, Newfoundland.

ITTC (2002). "Testing and Extrapolation Methods, Ice Testing, Resistance Test in Level Ice." ITTC Recommended Procedures, Section ITTC-4.9-03-03-04.2.1, ITTC.

Lau, M. and Derradji-Aouat, A. (2004) "Preliminary Modelling of Ship Manoeuvring in Ice Using a PMM", IOT/NRC report # TR-2006-02, Institute for Ocean Technology, St. John's, Newfoundland.

Marineering Limited (1997). "The Development and Commissioning of a Large Amplitude Planar Motion Mechanism. Volume 1: Main Report." IMD/NRC report # CR-1997-05, Institute for Ocean Technology, St. John's, Newfoundland.

Spencer, D.S. and Timco, G.W. (1993) "CD Model Ice – A Process to Produce Correct Density (CD) Model Ice." Proceedings of the 10th International IAHR Symposium on Ice, Vol. 2, Espoo, Finland, pp. 745-755.

Table 1: Specifications of the PMM

Max Sway Amplitude (m)	± 4.0
Max Yaw Amplitude (º)	± 175
Max Sway Velocity (m/s)	± 0.70
Max Yaw Rate (º/s)	± 60.0
Max Sway Force (N)	± 2200
Max Yaw Moment (N-m)	± 3000

Table 2: Change in tow force time history

Run Name	Change in measured Tow Force	Slope for Tow Force Time Histories
LIR_022 (0.1m/s)	10.66%	0.0422
LIR_022 (0.6m/s)	0.27%	0.0074
LIR_022 (0.9m/s)	13.91%	0.6214
PS_SQP_023 (0.1m/s)	1.94%	0.0019
PS_SQP_023 (0.6m/s)	8.42%	0.0982
PS_SQP_023 (0.9m/s)	9.43%	0.2601
LIR_CC_111 (0.1m/s)	0.76%	0.0024
LIR_CC_111 (0.3m/s)	17.28%	0.1192
LIR_CC_111 (0.6m/s)	6.51%	0.1284
Presawn_SQP_HB_112 (0.1m/s)	8.11%	0.0125
Presawn_SQP_HB_112 (0.3m/s)	1.06%	0.0041
Presawn_SQP_HB_112 (0.6m/s)	2.82%	0.0431
Presawn_SQP_SC_113 (0.1m/s)	23.04%	0.0076
Presawn_SQP_SC_113 (0.3m/s)	15.87%	0.0267
Presawn_SQP_SC_113 (0.6m/s)	6.30%	0.0575
LIR_NQP_114 (0.1m/s)	5.67%	0.0081
LIR_NQP_114 (0.3m/s)	24.26%	0.2333
LIR_NQP_114 (0.6m/s)	18.19%	0.4608
LIR11_0P1_AR50_128	28.55%	0.0985
LIR11A_0P1_129	137.28%	0.1736
LIR12_0P3_AR50_130	42.89%	0.4587
LIR12A_0P3_131	284.83%	0.3325
LIR13_0P3_AR10_132	24.78%	1.0867
LIR14_0P1_AR10_133	0.54%	0.0041
LIR_SQP_134 (0.1 m/s)	12.52%	0.0128
LIR_SQP_134 (0.3 m/s)	1.67%	0.0061
LIR_SQP_134 (0.6 m/s)	24.01%	0.2846
LIR21_0P6_AR50_144	57.61%	2.7376
LIR21A_0P6_145	57.17%	0.8394
LIR23A_0P6_AR10_148	1.68%	0.5723
LIR24A_SQP_149 (0.1 m/s)	21.83%	0.0916
LIR24A_SQP_149 (0.3 m/s)	8.13%	0.0689
LIR24A_SQP_149 (0.6 m/s)	45.23%	1.2073
LIR24B_SQP_150	10.91%	0.0341
LIR25_0P3_AR10_152	9.21%	0.417
LIR31_0P6_AR10_164	0.41%	0.1238
LIR32_0P5_AR10_165	0.72%	0.0888
LIR33_0P4_AR10_168	20.23%	1.4613
LIR34_0P3_AR10_169	57.61%	2.0592
LIR35_0P2_AR10_170	46.73%	0.6864
LIR36_0P1_AR10_171	21.82%	0.1396
LIR37_0P05_AR10_172	38.85%	0.0868

Table 3: Change in yaw moment time history

Run Name	Change in measured Yaw Moment	Slope for Yaw Moment Time Histories
LIR11_0P1_AR50_128	23.42%	0.0466
LIR12_0P3_AR50_130	87.23%	0.2962
LIR13_0P3_AR10_132	15.80%	0.7138
LIR14_0P1_AR10_133	20.79%	0.2771
LIR21_0P6_AR50_144	79.27%	1.7824
LIR23A_0P6_AR10_148	35.48%	4.136
LIR25_0P3_AR10_152	45.17%	1.7395
LIR31_0P6_AR10_164	17.62%	2.2625
LIR32_0P5_AR10_165	12.64%	0.8852
LIR33_0P4_AR10_168	49.38%	2.2502
LIR34_0P3_AR10_169	6.27%	0.2726
LIR35_0P2_AR10_170	28.44%	0.5857
LIR36_0P1_AR10_171	13.55%	0.1303
LIR37_0P05_AR10_172	27.44%	0.122

Table 4: Change in velocity time history

Run Name	Change in measured Model Speed	Slope for Model Speed Time Histories
LIR_022 (0.1m/s)	0.14%	1.00E-06
LIR_022 (0.6m/s)	0.19%	4.00E-05
LIR_022 (0.9m/s)	0.09%	4.00E-05
PS_SQP_023 (0.1m/s)	0.10%	7.00E-07
PS_SQP_023 (0.6m/s)	0.03%	7.00E-06
PS_SQP_023 (0.9m/s)	0.19%	0.0001
LIR_CC_111 (0.1m/s)	0.06%	4.00E-07
LIR_CC_111 (0.3m/s)	0.12%	6.00E-06
LIR_CC_111 (0.6m/s)	0.04%	9.00E-06
Presawn_SQP_HB_112 (0.1m/s)	0.12%	3.00E-06
Presawn_SQP_HB_112 (0.3m/s)	0.07%	9.00E-06
Presawn_SQP_HB_112 (0.6m/s)	0.09%	5.00E-05
Presawn_SQP_SC_113 (0.1m/s)	0.25%	4.00E-06
Presawn_SQP_SC_113 (0.3m/s)	0.03%	3.00E-06
Presawn_SQP_SC_113 (0.6m/s)	0.12%	5.00E-05
LIR_NQP_114 (0.1m/s)	0.28%	2.00E-06
LIR_NQP_114 (0.3m/s)	0.02%	5.00E-06
LIR_NQP_114 (0.6m/s)	0.02%	1.00E-05
LIR11_0P1_AR50_128	0.77%	4.00E-06
LIR11A_0P1_129	0.14%	1.00E-06
LIR12_0P3_AR50_130	0.18%	7.00E-06
LIR12A_0P3_131	0.04%	1.00E-06
LIR13_0P3_AR10_132	0.40%	4.00E-05
LIR14_0P1_AR10_133	0.43%	5.00E-06
LIR_SQP_134 (0.1 m/s)	0.24%	3.00E-06
LIR_SQP_134 (0.3 m/s)	0.02%	2.00E-06
LIR_SQP_134 (0.6 m/s)	0.15%	5.00E-05
LIR21_0P6_AR50_144	0.57%	9.00E-05
LIR21A_0P6_145	0.05%	1.00E-05
LIR23A_0P6_AR10_148	0.46%	0.0003
LIR24A_SQP_149 (0.1 m/s)	0.15%	5.00E-06
LIR24A_SQP_149 (0.3 m/s)	0.07%	1.00E-05
LIR24A_SQP_149 (0.6 m/s)	0.01%	4.00E-06
LIR24B_SQP_150	0.14%	4.00E-06
LIR25_0P3_AR10_152	0.58%	6.00E-05
LIR31_0P6_AR10_164	0.78%	0.0005
LIR32_0P5_AR10_165	0.65%	0.0002
LIR33_0P4_AR10_168	0.51%	0.0001
LIR34_0P3_AR10_169	0.88%	0.0001
LIR35_0P2_AR10_170	0.61%	3.00E-05
LIR36_0P1_AR10_171	0.73%	9.00E-06
LIR37_0P05_AR10_172	0.31%	1.00E-06

Table 5: Change in yaw rate time history

Run Name	Change in measured Yaw Rate	Slope for Yaw Rate Time Histories
LIR11_0P1_AR50_128	0.34%	2.00E-06
LIR12_0P3_AR50_130	1.11%	5.00E-05
LIR13_0P3_AR10_132	1.05%	0.0006
LIR14_0P1_AR10_133	0.76%	5.00E-05
LIR21_0P6_AR50_144	1.65%	0.0003
LIR23A_0P6_AR10_148	0.57%	0.0021
LIR25_0P3_AR10_152	0.34%	0.0002
LIR31_0P6_AR10_164	1.76%	0.0062
LIR32_0P5_AR10_165	0.57%	0.001
LIR33_0P4_AR10_168	0.27%	0.0003
LIR34_0P3_AR10_169	0.94%	0.0006
LIR35_0P2_AR10_170	0.72%	0.0002
LIR36_0P1_AR10_171	0.72%	5.00E-05
LIR37_0P05_AR10_172	2.66%	5.00E-05

Table 6: Change in drift angle time history

Run Name	Change in measured Drift Angle	Slope for Drift Angle Time Histories
LIR11_0P1_AR50_128	20.67%	8.00E-05
LIR12_0P3_AR50_130	25.58%	6.00E-04
LIR13_0P3_AR10_132	33.43%	0.0177
LIR14_0P1_AR10_133	72.47%	0.0014
LIR21_0P6_AR50_144	22.25%	0.0031
LIR23A_0P6_AR10_148	31.03%	0.1402
LIR25_0P3_AR10_152	34.93%	0.0196
LIR31_0P6_AR10_164	40.91%	0.1862
LIR32_0P5_AR10_165	1.49%	0.0024
LIR33_0P4_AR10_168	13.45%	0.0116
LIR34_0P3_AR10_169	42.50%	0.0188
LIR35_0P2_AR10_170	79.33%	0.0131
LIR36_0P1_AR10_171	47.85%	0.0015
LIR37_0P05_AR10_172	61.39%	0.0015

Table 7: Mean thickness profiles

Tank Position (m)	Thickness (mm)				
	NMS1	NMS2	NMS3	NMS4	NMS5
2	39.58	36.37	34.48	37.75	37.15
4	40.35	38.78	37.83	40.1	38.77
6	40.1	40.03	38.9	40.63	39.75
8	41.55	40.53	38.85	41.63	40.73
10	42.08	40.48	39.75	41.7	42.3
12	42.33	40.1	40.87	42.12	41.6
14	41.8	38.7	41.05	41.37	41.25
16	41.73	38.22	41.13	41.47	41.6
18	41.75	38.27	41.08	41.33	41.7
20	41.78	37.62	41.07	41	41.6
22	40.95	37.45	40.72	40.7	40.18
24	40.25	36.9	40.38	40.57	41.2
26	39.75	36.72	40.65	39.98	40.7
28	39.58	36.38	40.65	39.43	40.25
30	40.08	36.25	40.78	39.38	40.18
32	39.95	36.23	40.22	39.4	40.4
34	39.48	36.07	40.52	40.18	40.4
36	39.38	36.2	40.05	40.1	40.35
38	38.7	36.27	39.98	40.3	
40	38.98	36.95	39.83	40.1	38.55
42	39.65	37.35	39.75	39.98	39.2
44	39.6	37.2	39.18	40.3	39
46	39.43	37.22	38.6	39.4	38.45
48	39.33	37.72	38.78	39.28	38.85
50	38.93	37.98	39	38.75	39.3
52	38.38	38.33	39.95	39.5	39.13
54	39.13	38.92	39.93	39.45	39.65
56	38.75	39	39.15	39	40.85
58	38.65	39.87	39.6	39.5	39.5
60	39	40.23	40.05		41.2
62	38.85	40.32			
64	38.28	40.65			
66	36.60				
H mean	39.94	38.10	39.94	40.24	40.24
STDEV	1.19	1.53	0.87	0.90	1.08
U_h(N)	2.37	3.06	1.74	1.81	2.17
U_h(%)	5.94%	8.02%	4.36%	4.49%	5.39%

Table 8a: Mean flexural strength profile

NMS1				
Location	Length (m)	Width (m)	Thickness (m)	Load (N)
15N	0.2000	0.0868	0.0414	7.06
	0.2000	0.0849	0.0418	7.26
	0.1950	0.0835	0.0429	7.80
15S	0.2050	0.0792	0.0408	5.54
	0.2000	0.0767	0.0403	5.64
	0.2000	0.0743	0.0407	4.80
34N	0.2100	0.0853	0.0399	6.32
	0.2000	0.0838	0.0400	7.45
	0.2050	0.0832	0.0402	7.94
34S	0.2000	0.0851	0.0391	5.10
	0.2050	0.0837	0.0387	5.69
	0.2000	0.0818	0.0402	5.69
53N	0.2080	0.0819	0.0392	5.79
	0.2000	0.0869	0.0384	6.37
	0.2150	0.0840	0.0387	6.77
53S	0.2100	0.0834	0.0393	5.10
	0.2000	0.0800	0.0388	5.30
	0.2050	0.0822	0.0391	5.98
Mean	0.2025294	0.0830824	0.0398	6.2
STDEV	0.0041851	0.0026439	0.0009987	0.9718811
U (%)	4.13%	6.36%	5.02%	31.35%

NMS2				
Location	Length (m)	Width (m)	Thickness (m)	Load (N)
15N	0.2100	0.0900	0.0380	7.16
	0.2060	0.0866	0.0376	7.06
	0.2020	0.0843	0.0386	5.93
15S	0.1900	0.0859	0.0384	6.86
	0.2000	0.0865	0.0380	6.37
	0.2000	0.0850	0.0391	6.86
30N	0.2090	0.0860	0.0357	3.82
	0.2030	0.0875	0.0358	4.12
	0.2070	0.0795	0.0364	3.97
30S	0.2000	0.0898	0.0358	4.02
	0.2000	0.0934	0.0364	4.12
	0.2000	0.0935	0.0361	5.20
45N	0.2010	0.0864	0.0371	4.90
	0.2090	0.0911	0.0367	4.61
	0.1980	0.0832	0.0377	4.71
45S	0.1970	0.0870	0.0368	4.76
	0.2070	0.0901	0.0370	5.10
	0.2000	0.0930	0.0370	5.83
60N	0.1950	0.0861	0.0408	5.34
	0.1980	0.0875	0.0407	4.61
	0.1870	0.0846	0.0410	5.39
60S	0.1970	0.0850	0.0392	5.39
	0.1950	0.0942	0.0387	5.59
	0.1990	0.0965	0.0381	6.37
Mean	0.201	0.0880292	0.0373429	5.34
STDEV	0.0050632	0.0040388	0.0011066	1.0351496
U (%)	5.04%	9.18%	8.30%	38.79%

Table 8b: Mean flexural strength profile

NMS3				
Location	Length (m)	Width (m)	Thickness (m)	Load (N)
18N	0.1950	0.0883	0.0415	6.18
	0.2030	0.0901	0.0413	6.08
	0.2080	0.0918	0.0407	5.39
18S	0.2030	0.0920	0.0402	4.02
	0.1980	0.0799	0.0401	3.33
	0.2110	0.0870	0.0401	3.63
37N	0.2050	0.0901	0.0408	5.69
	0.1990	0.0943	0.0406	5.20
	0.1960	0.0936	0.0406	5.98
	0.2150	0.0953	0.0413	5.79
37S	0.2010	0.0905	0.0400	3.73
	0.1960	0.0785	0.0395	2.75
	0.1950	0.0862	0.0400	4.02
	0.1920	0.0853	0.0400	4.22
52N	0.1920	0.0912	0.0392	3.53
	0.1920	0.0951	0.0388	4.12
	0.2100	0.1002	0.0390	3.87
52S	0.1950	0.0923	0.0396	3.33
	0.2050	0.0900	0.0400	3.38
	0.2080	0.0895	0.0395	3.24
59N	0.1970	0.0927	0.0407	3.43
	0.2070	0.0915	0.0400	2.94
	0.2080	0.0965	0.0400	2.75
59S	0.2050	0.0904	0.0406	2.35
	0.1950	0.0840	0.0399	2.16
	0.1980	0.0892	0.0402	2.40
Mean	0.2011154	0.09068	0.0401615	3.9811538
STDEV	0.006605	0.0042404	0.0006783	1.2334483
U (%)	6.57%	9.35%	3.38%	61.96%

NMS4				
Location	Length (m)	Width (m)	Thickness (m)	Load (N)
18N	0.1930	0.0918	0.0423	5.98
	0.2130	0.0950	0.0418	5.59
	0.1900	0.0921	0.0416	5.00
18S	0.1980	0.0931	0.0408	4.56
	0.2040	0.0877	0.0405	3.92
	0.1900	0.0819	0.0403	3.92
37N	0.1900	0.0906	0.0409	5.10
	0.2020	0.0935	0.0406	5.39
	0.1970	0.0906	0.0407	5.20
	0.1980	0.0947	0.0400	5.30
37S	0.1900	0.0816	0.0404	3.92
	0.2000	0.0865	0.0400	3.73
	0.1910	0.0860	0.0402	4.02
	0.2010	0.0880	0.0404	4.41
46N	0.1950	0.0823	0.0397	2.99
	0.2020	0.0940	0.0394	3.19
	0.1920	0.0945	0.0394	2.99
46S	0.2120	0.0878	0.0392	2.01
	0.2020	0.0854	0.0390	1.81
	0.2080	0.0867	0.0392	2.01
55N	0.2020	0.1019	0.0387	1.67
	0.2050	0.0870	0.0394	2.11
	0.2210	0.0824	0.0394	2.40
55S	0.1850	0.0900	0.0396	1.37
	0.2050	0.0844	0.0396	0.98
	0.1990	0.0890	0.0402	1.23
Mean	0.1994231	0.088664	0.04004	3.4923077
STDEV	0.0072748	0.0042718	0.0007805	1.5267883
U (%)	7.33%	9.64%	3.90%	87.44%

Table 8c: Mean flexural strength profile

NMS5				
Location	Length (m)	Width (m)	Thickness (m)	Load (N)
5N	0.1960	0.0866	0.0398	5.00
	0.2000	0.0856	0.0397	5.39
	0.1990	0.0850	0.0395	4.85
5S	0.2000	0.0856	0.0392	4.56
	0.1950	0.0850	0.0398	4.07
	0.2050	0.0865	0.0395	4.46
14N	0.1980	0.0863	0.0412	3.63
	0.1910	0.0942	0.0410	3.82
	0.2030	0.0859	0.0412	3.33
14S	0.1900	0.0846	0.0404	3.48
	0.1920	0.0840	0.0406	3.53
	0.1970	0.0870	0.0408	3.97
20N	0.2000	0.0857	0.0412	2.94
	0.1800	0.0838	0.0412	2.50
	0.1850	0.0929	0.0402	2.50
20S	0.2020	0.0846	0.0414	2.50
	0.2180	0.0856	0.0413	2.40
	0.2040	0.0860	0.0414	2.45
28N	0.1950	0.0828	0.0395	2.40
	0.1950	0.0841	0.0399	2.26
	0.2000	0.0858	0.0395	2.40
28S	0.2090	0.0863	0.0408	2.16
	0.1890	0.0864	0.0407	2.30
	0.1850	0.0798	0.0406	2.01
37N	0.1950	0.0835	0.0378	3.04
	0.1800	0.0855	0.0400	2.84
	0.2000	0.0850	0.0396	3.38
	0.1850	0.0826	0.0389	3.19
37S	0.2050	0.0965	0.0406	3.24
	0.1910	0.0808	0.0406	2.89
	0.2110	0.0913	0.0400	3.82
	0.2120	0.0908	0.0404	3.63
45N	0.1600	0.0809	0.0378	1.42
	0.1300	0.0858	0.0385	1.62
	0.2100	0.0852	0.0381	1.27
45S	0.1950	0.0898	0.0394	1.81
	0.2040	0.0912	0.0394	1.72
	0.2100	0.0863	0.0395	1.67
58N	0.1890	0.0969	0.0400	2.06
	0.1850	0.0972	0.0405	1.72
	0.1910	0.0955	0.0408	1.81
58S	0.1930	0.0911	0.0405	2.06
	0.1890	0.0836	0.0410	1.67
	0.2010	0.0869	0.0402	1.67
Mean	0.19614	0.086966	0.0400909	2.850909
STDEV	0.010464	0.004276	0.0009333	1.048584
U (%)	10.67%	9.83%	4.66%	73.56%

Table 9: Ice density values

NMS1											
Tank Location (m)		Length (m)		Width (m)		Thickness (m)		Sub. Force (g)		Density (kg/m^3)	
		Value	Chauv #	Value	Chauv #	Value	Chauv #	Value	Chauv #	Value	Chauv #
60	North	0.1018		0.0992		0.0364		59.2		841	
60	South	0.1054		0.1023		0.0357		37.2		905.9	
Mean		0.1036		0.1007		0.036		48.2		873.45	
STDEV		0.0026		0.0022		0.0004		15.556		45.891	
Uncertainty		3.52%		3.08%		1.73%		45.64%		7.43%	

NMS2											
Tank Location (m)		Length (m)		Width (m)		Thickness (m)		Sub. Force (g)		Density (kg/m^3)	
		Value	Chauv #	Value	Chauv #	Value	Chauv #	Value	Chauv #	Value	Chauv #
62	North										
62	South	0.1032	0.650814	0.1046	0.779431	0.0409	0.880528	81	0.889857	819.2	0.908438
66	North	0.1035	0.500626	0.1067	1.127527	0.0403	0.206654	70	0.192344	845.1	0.163078
66	South										
70	North										
70	South	0.1062	1.15144	0.105	0.348095	0.0391	1.087182	49.9	1.082201	888	1.071516
Mean		0.1043		0.1054		0.0401		66.967		850.77	
STDEV		0.0017		0.0011		0.0009		15.77		34.748	
Uncertainty		1.84%		1.21%		2.67%		27.19%		4.72%	

NMS3											
Tank Location (m)		Length (m)		Width (m)		Thickness (m)		Sub. Force (g)		Density (kg/m^3)	
		Value	Chauv #	Value	Chauv #	Value	Chauv #	Value	Chauv #	Value	Chauv #
39	North	0.1052		0.1015		0.0393		66.4		844.2	
39	South	0.1045		0.1053		0.0399		66.8		850.4	
Mean		0.1048		0.1034		0.0396		66.6		847.3	
STDEV		0.0005		0.0027		0.0004		0.2828		4.3841	
Uncertainty		0.64%		3.67%		1.58%		0.60%		0.73%	

NMS4											
Tank Location (m)		Length (m)		Width (m)		Thickness (m)		Sub. Force (g)		Density (kg/m^3)	
		Value	Chauv #	Value	Chauv #	Value	Chauv #	Value	Chauv #	Value	Chauv #
39	North	0.1063		0.1064		0.0412		90.1		808.9	
39	South	0.106		0.1032		0.0401		69.5		844.1	
Mean		0.1061		0.1048		0.0406		79.8		826.5	
STDEV		0.0003		0.0022		0.0007		14.566		24.89	
Uncertainty		0.35%		3.03%		2.52%		25.81%		4.26%	

NMS5											
Tank Location (m)		Length (m)		Width (m)		Thickness (m)		Sub. Force (g)		Density (kg/m^3)	
		Value	Chauv #	Value	Chauv #	Value	Chauv #	Value	Chauv #	Value	Chauv #
37	North										
37	South	0.0991		0.0998		0.0404		34.9		915.4	
36	North	0.1062		0.1041		0.041		61.3		867.2	
36	South										
Mean		0.1027		0.102		0.0407		48.1		891.3	
STDEV		0.005		0.003		0.0004		18.668		34.083	
Uncertainty		6.94%		4.17%		1.29%		54.89%		5.41%	

Table 10a: Summary of random uncertainties in Phase 4 resistance tests

Segment #	Model Velocity	TF-mean (N)	Mean TF_corr	STD max (N)	Chauv #	Uncertainty Value (N)	Uncertainty %
LIR_022	0.1	53.33	55.28	2.34	1.15	2.70	
LIR_022	0.1	57.66	55.28	2.34	0.68		**4.88%**
LIR_022	0.1	57.15	55.28	2.34	0.47		
LIR_022	0.6	80.03	78.22	2.75	0.28	3.18	
LIR_022	0.6	76.13	78.22	2.75	1.11		**4.06%**
LIR_022	0.6	81.55	78.22	2.75	0.83		
LIR_022	0.9	91.47	86.60	5.31		7.51	**8.68%**
LIR_022	0.9	83.85	86.60	5.31			
PS_SQP_023	0.1	13.65	13.30	0.16	1.03	0.18	
PS_SQP_023	0.1	13.98	13.30	0.16	0.97		**1.38%**
PS_SQP_023	0.1	13.83	13.30	0.16	0.06		
PS_SQP_023	0.6	32.00	30.23	1.05		1.48	**4.90%**
PS_SQP_023	0.6	30.46	30.23	1.05			
PS_SQP_023	0.9	46.06	44.71				
LIR_CC_111	0.1	43.30	45.57	0.17		0.24	**0.53%**
LIR_CC_111	0.3	43.14	45.57	0.17			
LIR_CC_111	0.3	43.92	42.48	3.38	1.09	3.90	
LIR_CC_111	0.3	37.64	42.48	3.38	0.88		**9.19%**
LIR_CC_111	0.3	39.88	42.48	3.38	0.20		
LIR_CC_111	0.6	49.19	52.76	2.06		2.92	**5.53%**
LIR_CC_111	0.6	52.05	52.76	2.06			
PRESAWN_SQP_HB_112	0.1	5.95	6.27				
PRESAWN_SQP_HB_112	0.3	9.01	9.42				
PRESAWN_SQP_HB_112	0.6	16.36	16.96				
PRESAWN_SQP_SC_113	0.1	2.01	2.09				
PRESAWN_SQP_SC_113	0.3	5.12	5.03	0.39		0.55	**10.86%**
PRESAWN_SQP_SC_113	0.3	4.60	5.03	0.39			
PRESAWN_SQP_SC_113	0.6	12.68	13.03				
LIR_NQP_114	0.1	20.21	20.82	0.70		0.99	**4.78%**
LIR_NQP_114	0.1	19.30	20.82	0.70			
LIR_NQP_114	0.6	28.97	27.87	3.31		4.68	**16.80%**
LIR_NQP_114	0.6	24.55	27.87	3.31			
LIR_NQP_114	0.9	45.86	47.50				

Table 10b: Summary of random uncertainties in Phase 4 resistance tests

Segment #	Model Velocity	TF-mean (N)	Mean TF_corr	STD max (N)	Chauv #	Uncertainty Value (N)	Uncertainty %
LIR11A_0P1_129	0.1	11.11	17.50	9.11		12.89	**73.65%**
LIR11A_0P1_129	0.1	24.01	17.50	9.11			
LIR12A_0P3_131	0.3	3.57	13.72	12.29	0.83	11.00	
LIR12A_0P3_131	0.3	2.55	13.72	12.29	0.91		
LIR12A_0P3_131	0.3	8.88	13.72	12.29	0.39		**80.15%**
LIR12A_0P3_131	0.3	24.46	13.72	12.29	0.88		
LIR12A_0P3_131	0.3	29.03	13.72	12.29	1.25		
LIR_SQP_134	0.1	8.09	8.06				
LIR_SQP_134	0.3	13.49	13.56	0.13		0.19	**1.39%**
LIR_SQP_134	0.3	13.66	13.56	0.13			
LIR_SQP_134	0.6	21.81	21.84				
LIR21A_OP6_145	0.6	31.10	41.55	9.71	1.15	11.22	
LIR21A_OP6_145	0.6	48.39	41.55	9.71	0.60		**27.00%**
LIR21A_OP6_145	0.6	47.68	41.55	9.71	0.55		
LIR24A_SQP_149	0.1	12.06	11.67				
LIR24A_SQP_149	0.3	17.91	17.46				
LIR24A_SQP_149	0.6	25.89	25.50				
LIR24B_SQP_150	0.1	10.99	10.90				

Table 11: Summary of random uncertainties in Phase 4 manoeuvring tests (tow force)

Segment #	Model Velocity	TF-mean (N)	Mean TF_corr	STD max (N)	Chauv #	Uncertainty Value (N)	Uncertainty %
LIR11_0P1_AR50_128	0.1	32.92	33.72	4.79	0.20	5.53	**16.39%**
LIR11_0P1_AR50_128	0.1	39.02	33.72	4.79	1.08		
LIR11_0P1_AR50_128	0.1	29.51	33.72	4.79	0.89		
LIR12_0P3_AR50_130	0.3	45.30	40.54	8.55	0.56	9.88	**24.36%**
LIR12_0P3_AR50_130	0.3	45.50	40.54	8.55	0.59		
LIR12_0P3_AR50_130	0.3	30.53	40.54	8.55	1.15		
LIR13_0P3_AR10_132	0.3	36.23	31.74	6.66		9.41	**29.65%**
LIR13_0P3_AR10_132	0.3	26.86	31.74	6.66			
LIR14_0P1_AR10_133	0.1	27.45	23.52	5.87		8.30	**35.30%**
LIR14_0P1_AR10_133	0.1	19.20	23.52	5.87			
LIR21_OP6_AR50_144	0.6	60.32	53.80	7.10		10.04	**18.66%**
LIR21_OP6_AR50_144	0.6	49.49	53.80	7.10			
LIR23A_OP6_AR10_148	0.6	52.41	52.86				
LIR25_0P3_AR10_152	0.3	38.16	33.20	7.90		11.17	**33.63%**
LIR25_0P3_AR10_152	0.3	27.10	33.20	7.90			
LIR31_0P6_AR10_164	0.6	44.31	43.63				
LIR31_0P6_AR10_165	0.5	41.08	40.57				
LIR33_0P4_AR10_168	0.4	29.33	29.10				
LIR34_0P3_AR10_169	0.3	25.35	25.25				
LIR35_0P2_AR10_170	0.2	19.12	19.20				
LIR36_0P1_AR10_171	0.1	16.11	16.25				
LIR37_0P05_AR10_172	0.05	15.43	15.64				

Table 12: Chauvenet's numbers

Number of Observations (N)	Chauvenet's #
3	1.38
4	1.54
5	1.65
6	1.73
7	1.80
8	1.85
9	1.92
10	1.96
11	1.99
12	2.03
13	2.06
14	2.10
15	2.13

Table 13: Summary of random uncertainties in Phase 4 manoeuvring tests (yaw moment)

Ice Sheet	Segment #	Model Velocity	YM-mean (N-m)	Mean YM_corr	STD max (N-m)	Chauv #	Uncertainty Value (N-m)	Uncertainty %
NMS3	LIR11_0P1_AR50_128	0.1	29.08	38.26	11.00	0.83	12.70	**33.20%**
	LIR11_0P1_AR50_128	0.1	50.45	38.26	11.00	1.11		
	LIR11_0P1_AR50_128	0.1	35.24	38.26	11.00	0.27		
	LIR12_0P3_AR50_130	0.3	38.97	25.98	12.00	1.08	13.85	**53.33%**
	LIR12_0P3_AR50_130	0.3	15.31	25.98	12.00	0.89		
	LIR12_0P3_AR50_130	0.3	23.65	25.98	12.00	0.19		
	LIR13_0P3_AR10_132	0.3	142.80	134.64	11.54		16.32	**12.12%**
	LIR13_0P3_AR10_132	0.3	126.48	134.64	11.54			
	LIR14_0P1_AR10_133	0.1	123.24	115.18	11.40		16.12	**13.99%**
	LIR14_0P1_AR10_133	0.1	107.12	115.18	11.40			
NMS4	LIR21_OP6_AR50_144	0.6	58.14	84.85	37.78		53.43	**62.96%**
	LIR21_OP6_AR50_144	0.6	111.56	84.85	37.78			
	LIR23A_OP6_AR10_148	0.6	108.42	108.42				
	LIR25_0P3_AR10_152	0.3	117.02	111.45	7.89		11.15	**10.01%**
	LIR25_0P3_AR10_152	0.3	105.87	111.45	7.89			
NMS5	LIR31_0P6_AR10_164	0.6	253.99	123.00				
	LIR31_0P6_AR10_165	0.5	170.55	114.19				
	LIR33_0P4_AR10_168	0.4	120.98	93.42				
	LIR34_0P3_AR10_169	0.3	77.78	115.59				
	LIR35_0P2_AR10_170	0.2	43.59	84.26				
	LIR36_0P1_AR10_171	0.1	23.90	77.58				
	LIR37_0P05_AR10_172	0.05	16.27	67.91				

Table 14a: Effect of the DRE on uncertainty in resistance tests

Ice Sheet	Segment #	Model Velocity (m/s)	Corrected Mean Resistance (N)	Random Uncertainty before DRE	Random Uncertainty after DRE
NMS1	LIR_022	0.1	55.28	4.88%	7.69%
	LIR_022	0.6	78.22	4.06%	7.20%
	LIR_022	0.9	86.60	8.68%	10.51%
	PS_SQP_023	0.1	13.30	1.38%	6.10%
	PS_SQP_023	0.6	30.23	4.90%	7.70%
	PS_SQP_023	0.9	44.71		
NMS2	LIR_CC_111	0.1	45.57	0.53%	8.04%
	LIR_CC_111	0.3	42.48	9.19%	12.20%
	LIR_CC_111	0.6	52.76	5.53%	9.74%
	PRESAWN_SQP_HB_112	0.1	6.27		
	PRESAWN_SQP_HB_112	0.3	9.42		
	PRESAWN_SQP_HB_112	0.6	16.96		
	PRESAWN_SQP_SC_113	0.1	2.09		
	PRESAWN_SQP_SC_113	0.3	5.03	10.86%	13.50%
	PRESAWN_SQP_SC_113	0.6	13.03		
	LIR_NQP_114	0.1	20.82	4.78%	9.34%
	LIR_NQP_114	0.6	27.87	16.80%	18.62%
	LIR_NQP_114	0.9	47.50		
NMS3	LIR11A_0P1_129	0.1	17.50	73.65%	73.78%
	LIR12A_0P3_131	0.3	13.72	80.15%	80.27%
	LIR_SQP_134	0.1	8.06		
	LIR_SQP_134	0.3	13.56	1.39%	4.58%
	LIR_SQP_134	0.6	21.84		
NMS4	LIR21A_OP6_145	0.6	41.55	27.00%	27.37%
	LIR24A_SQP_149	0.1	11.67		
	LIR24A_SQP_149	0.3	17.46		
	LIR24A_SQP_149	0.6	25.50		
	LIR24B_SQP_150	0.1	10.90		

Table 14b: Effect of the DRE on uncertainty in manoeuvring tests

Ice Sheet	Segment #	Model Velocity (m/s)	Corrected Mean Tow Force (N)	Random Uncertainty before DRE	Random Uncertainty after DRE
NMS3	LIR11_0P1_AR50_128	0.1	33.72	16.39%	16.96%
	LIR12_0P3_AR50_130	0.3	40.54	24.36%	24.75%
	LIR13_0P3_AR10_132	0.3	31.74	29.65%	29.97%
	LIR14_0P1_AR10_133	0.1	23.52	35.30%	35.57%
NMS4	LIR21_OP6_AR50_144	0.6	53.80	18.66%	19.20%
	LIR23A_OP6_AR10_148	0.6	52.86		
	LIR25_0P3_AR10_152	0.3	33.20	33.63%	33.93%
NMS5	LIR31_0P6_AR10_164	0.6	43.63		
	LIR31_0P6_AR10_165	0.5	40.57		
	LIR33_0P4_AR10_168	0.4	29.10		
	LIR34_0P3_AR10_169	0.3	25.25		
	LIR35_0P2_AR10_170	0.2	19.20		
	LIR36_0P1_AR10_171	0.1	16.25		
	LIR37_0P05_AR10_172	0.05	15.64		

Figure 1a: *Terry Fox* model on the shop floor (model in its wooden cradle).

Figure 1b: *Terry Fox* model on the swing frame on the shop floor.

Figure 2a: Actual Planar Motion Mechanism (PMM) on the shop floor.

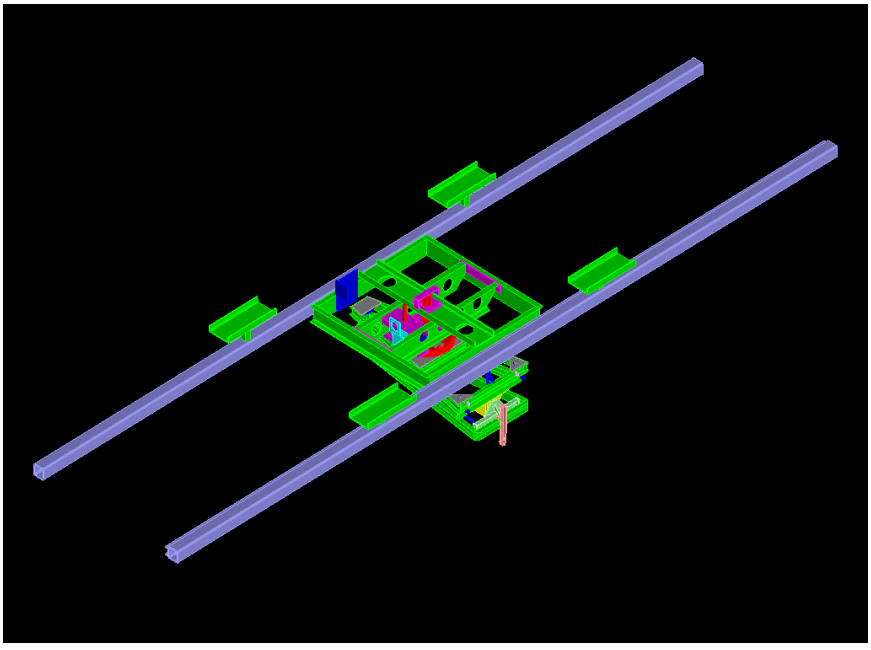

Figure 2b: CAD- top isometric - view for the Planar Motion Mechanism (PMM).

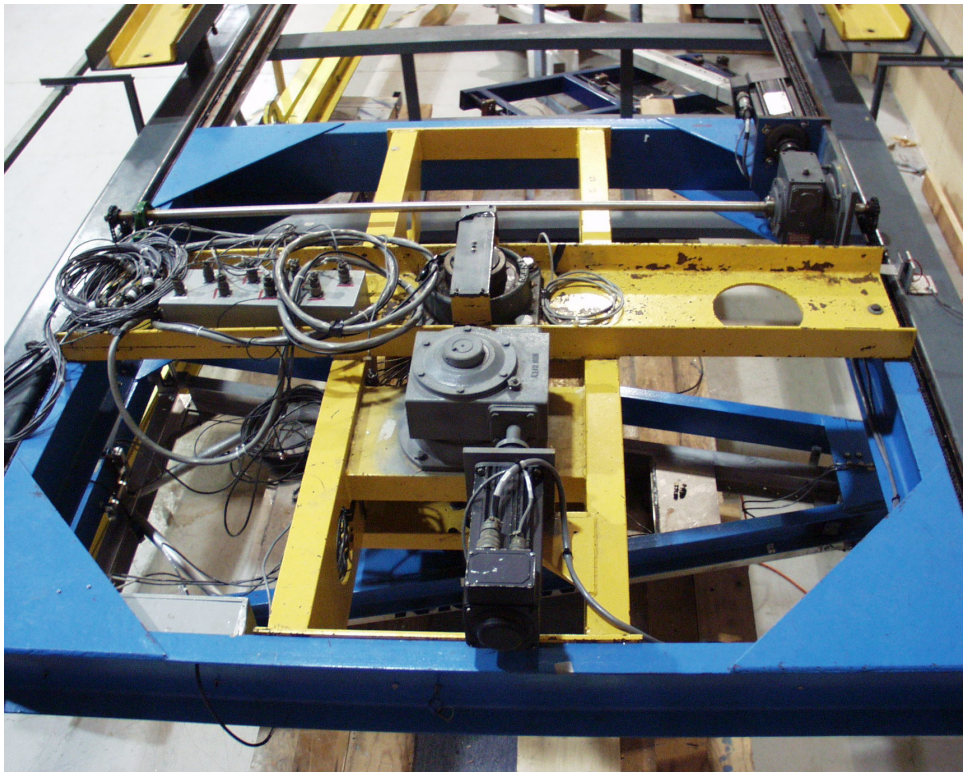

Figure 2c: Actual Planar Motion Mechanism (top view).

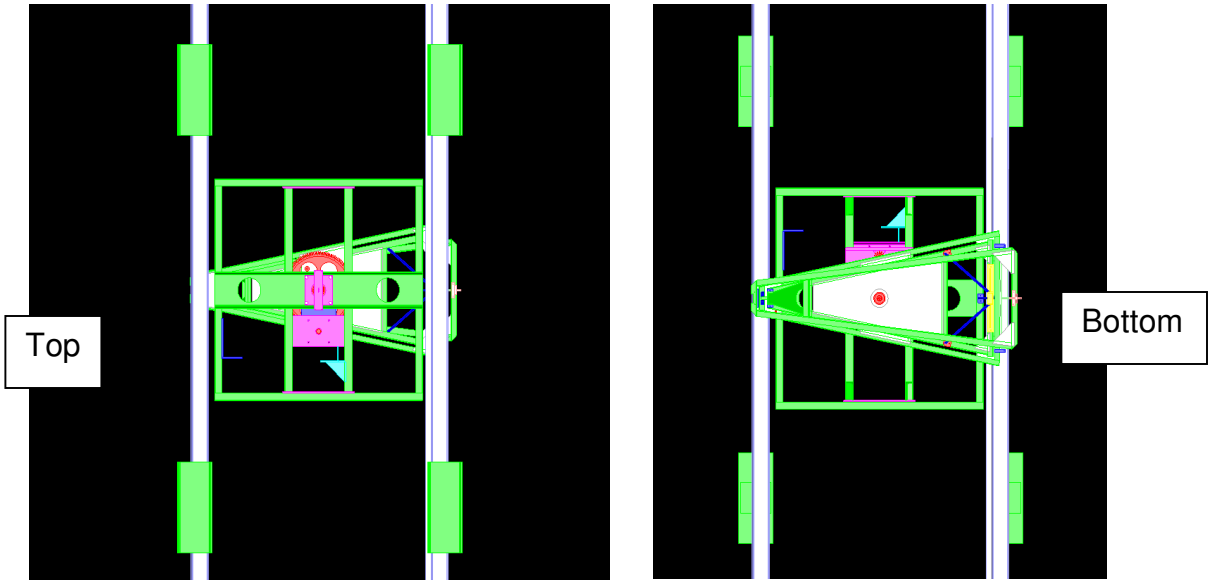

Figure 2d: Top and bottom CAD views of the PMM.

Figure 3: Typical test run in ice.

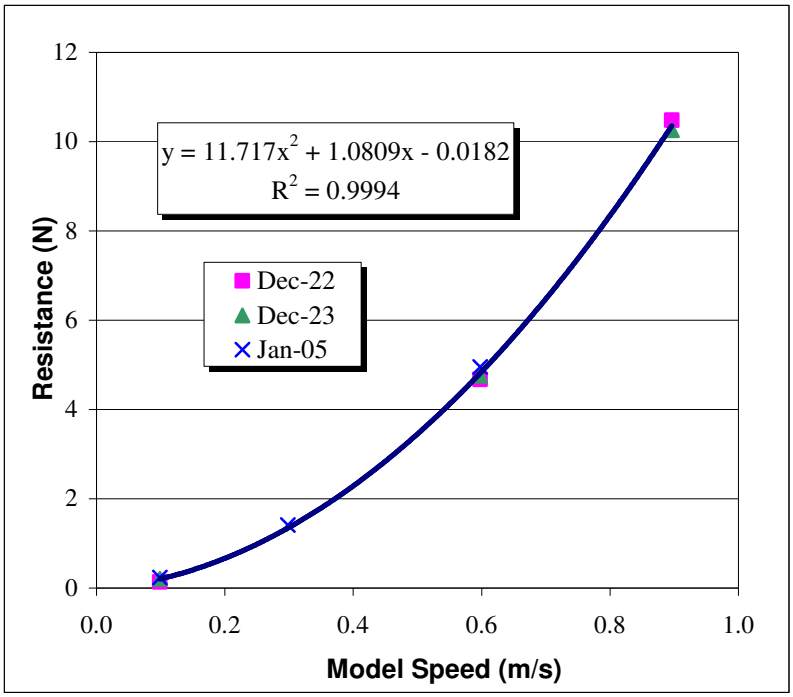

Figure 4: Open water resistance tests

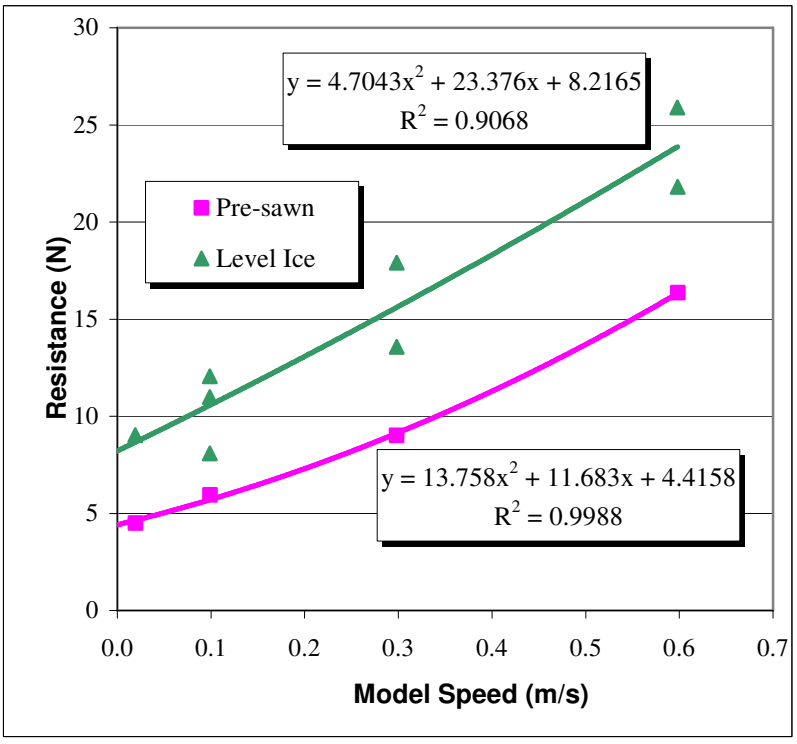

Figure 5: Ice resistance tests

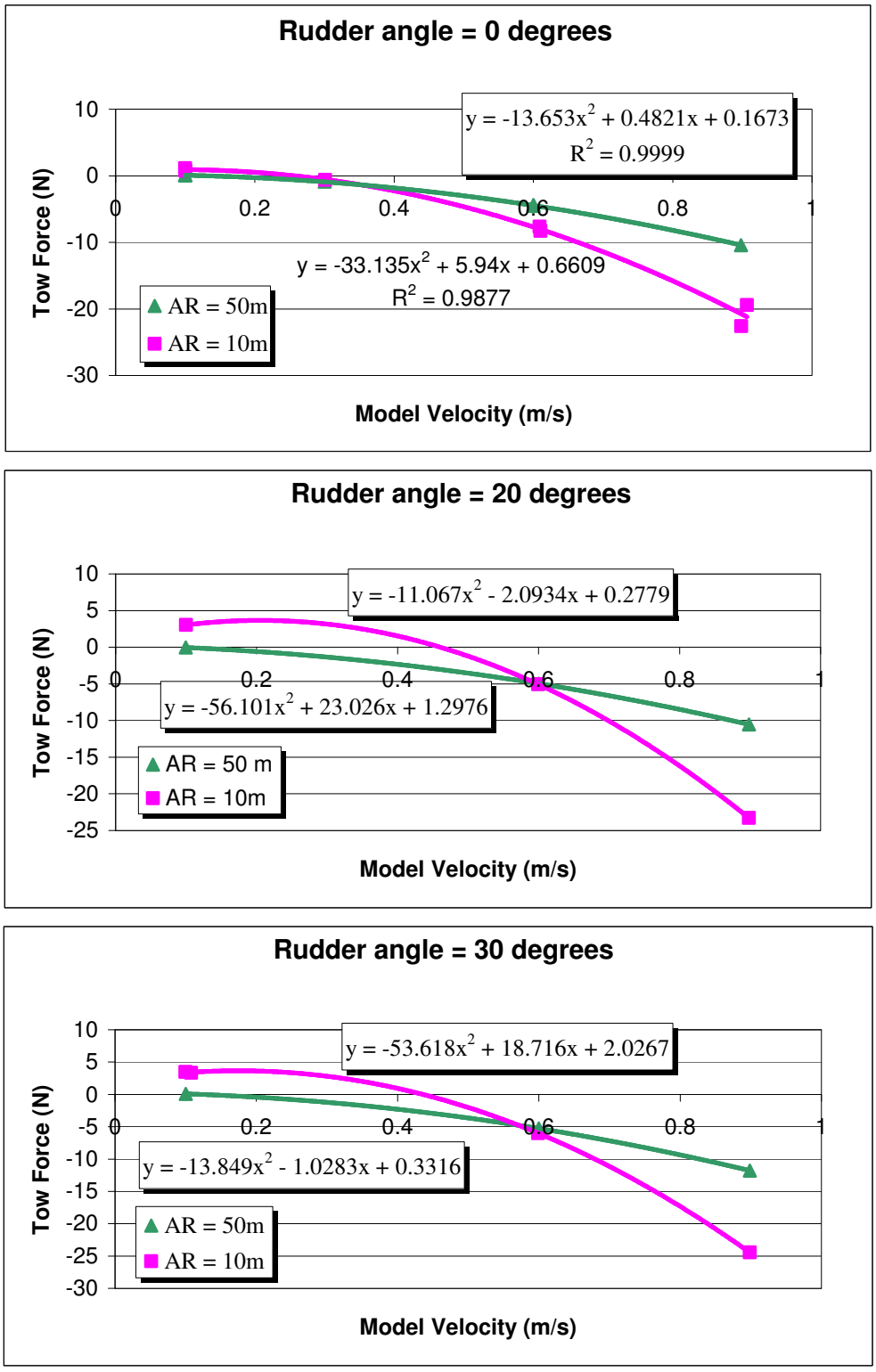

Figure 6: Results for open water manoeuvring tests (tow force)

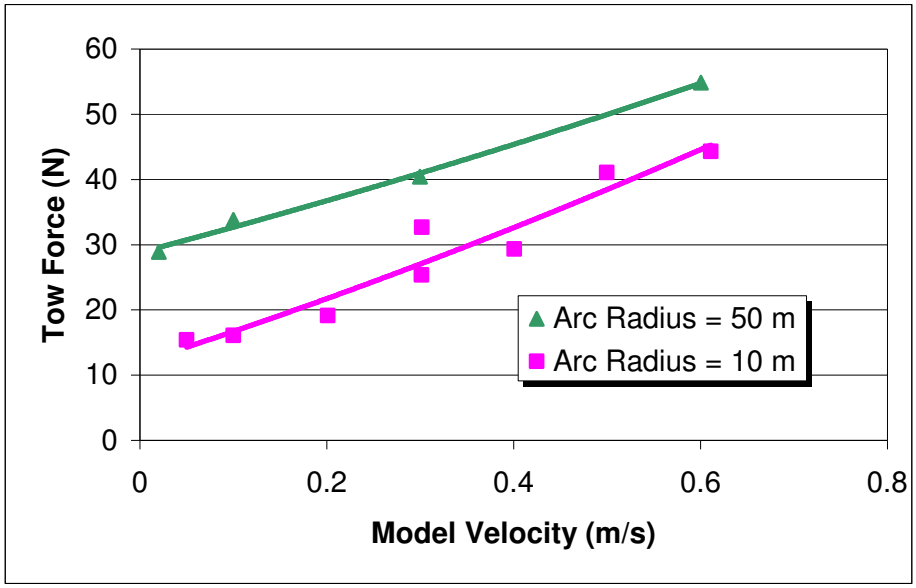

Figure 7: Results for ice manoeuvring tests (tow force)

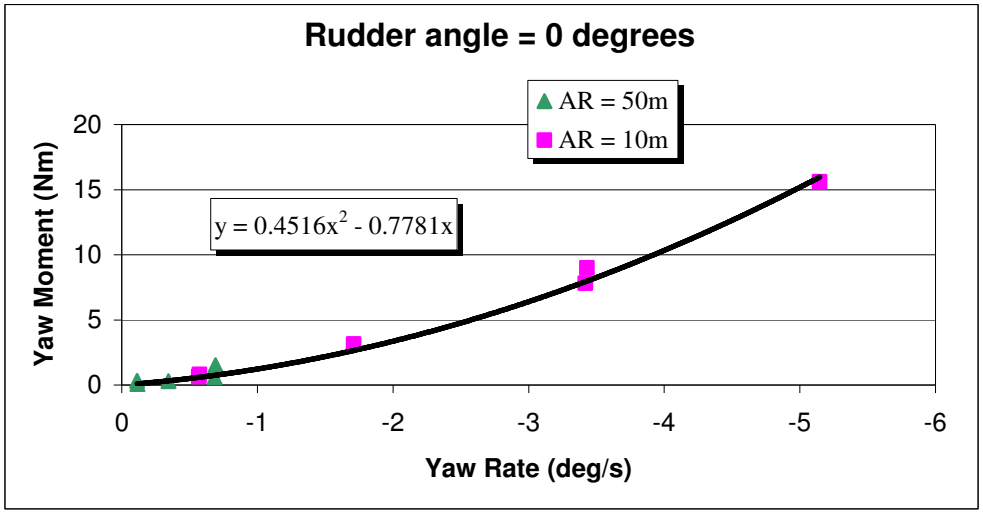

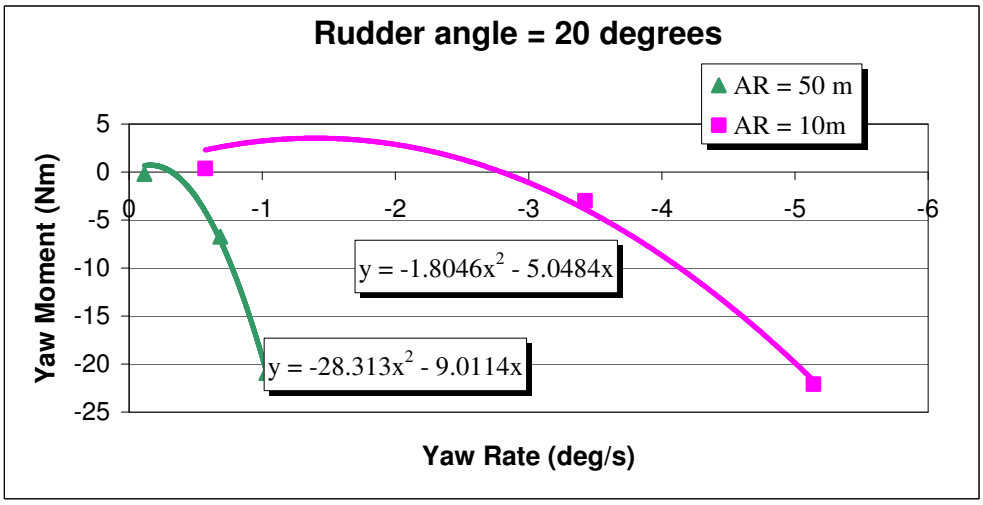

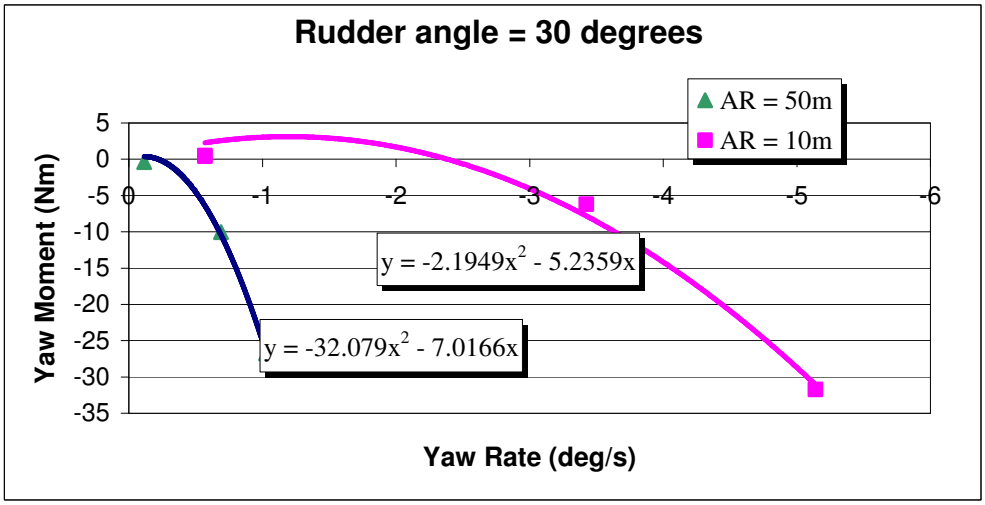

Figure 8: Results for open water manoeuvring tests (yaw moment)

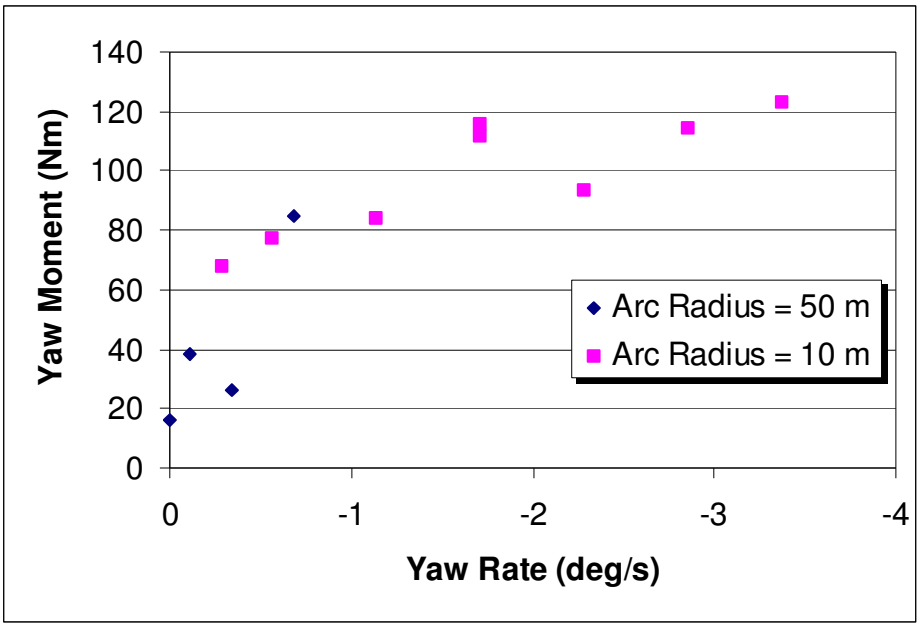

Figure 9: Results for ice manoeuvring tests (yaw moment)

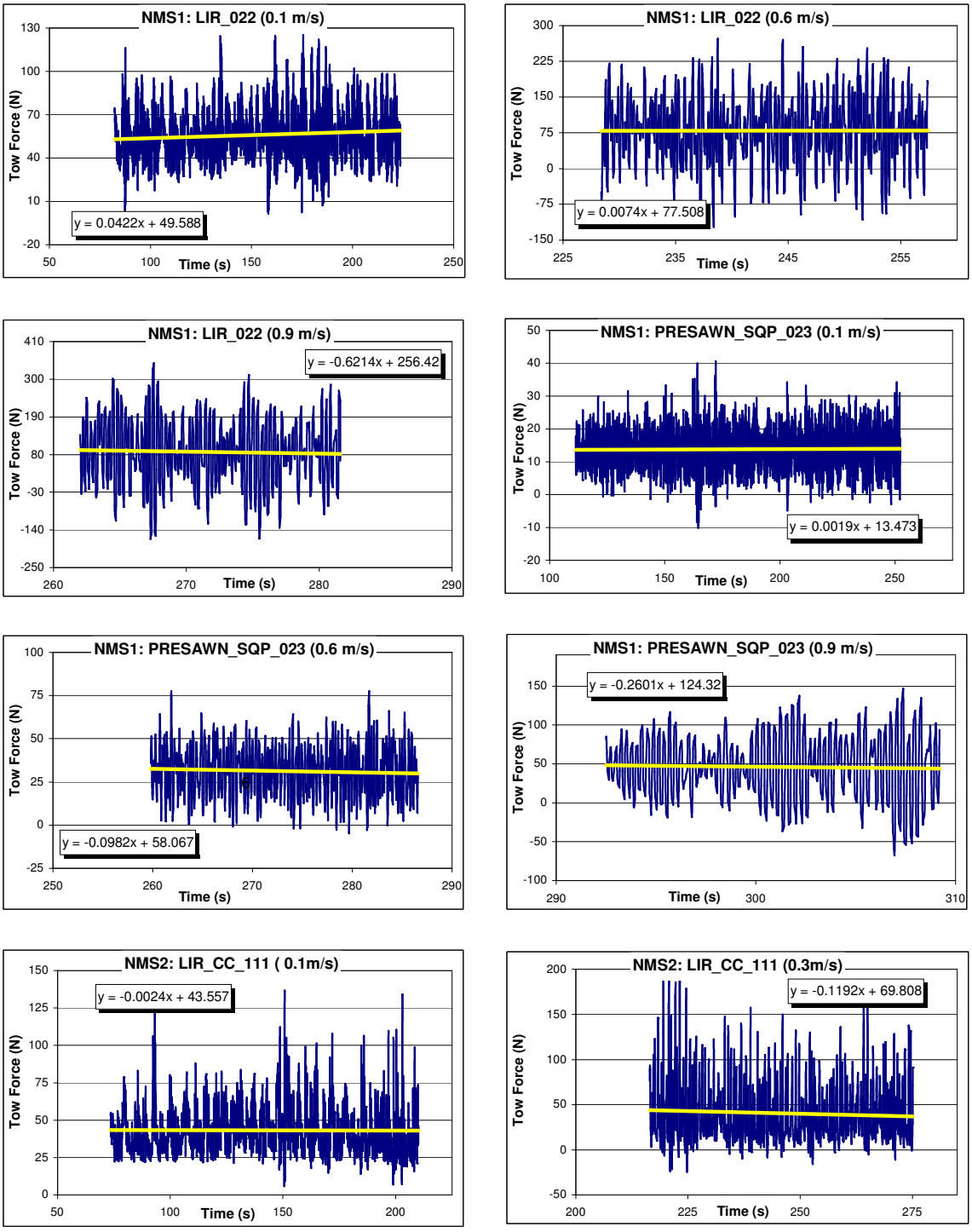

Figure 10a: Tow force-time history

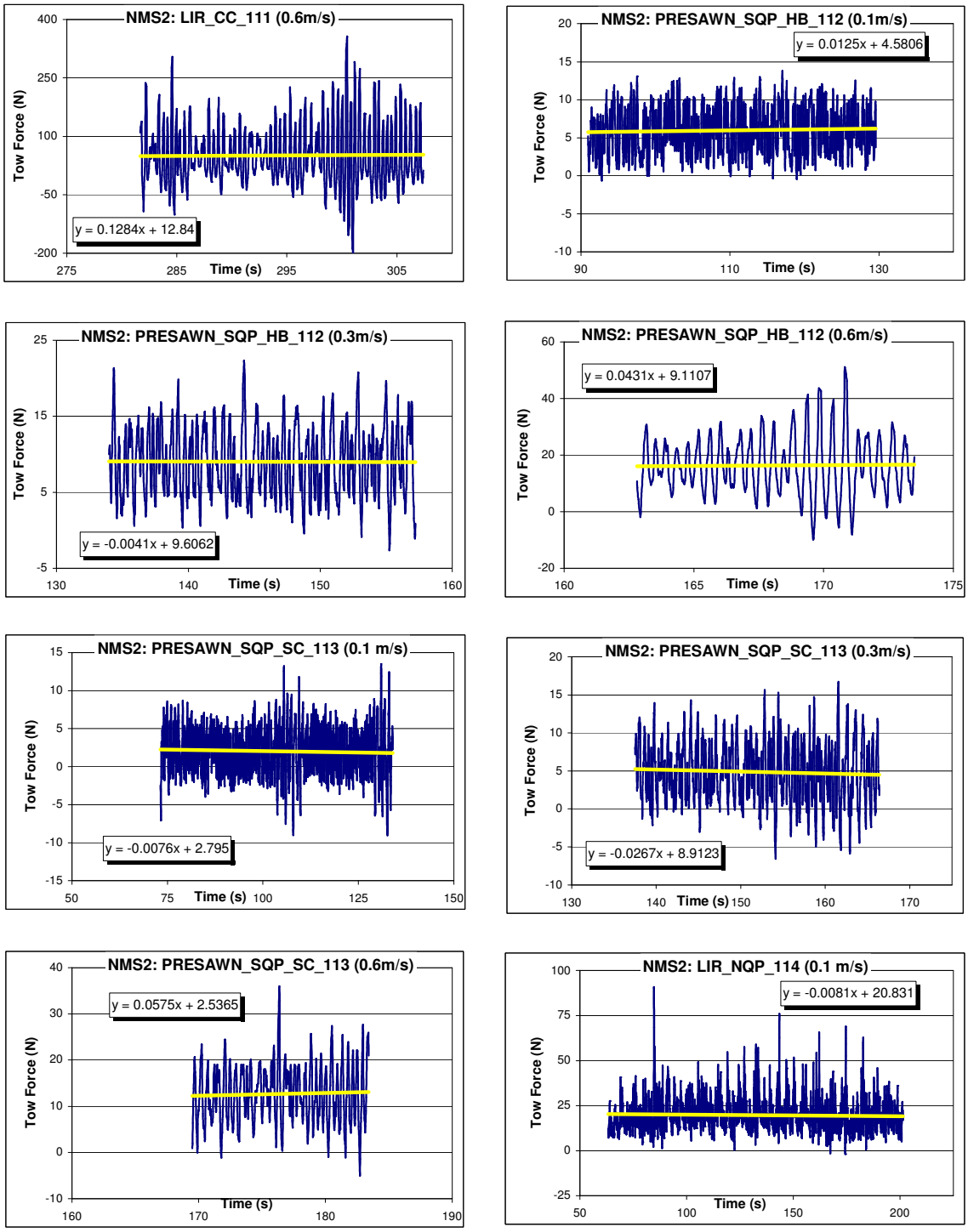

Figure 10b: Tow force-time history

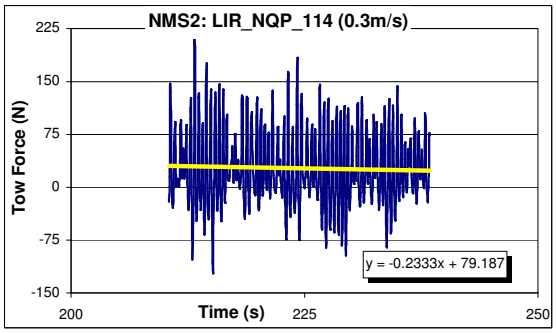

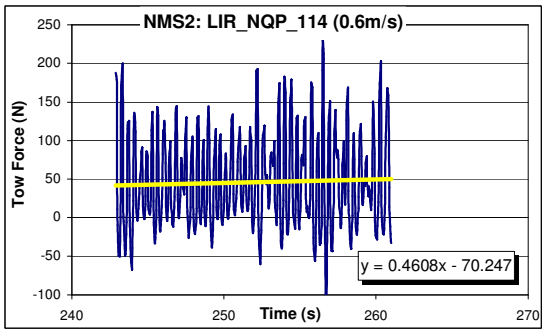

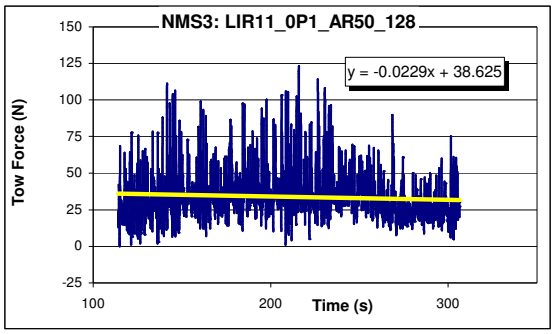

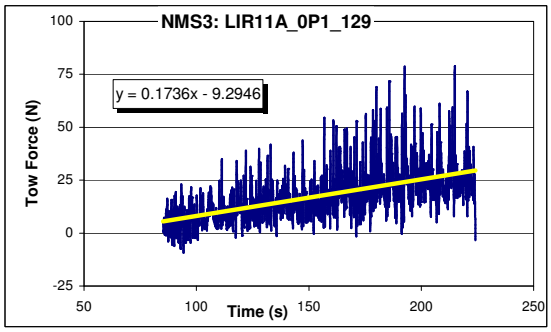

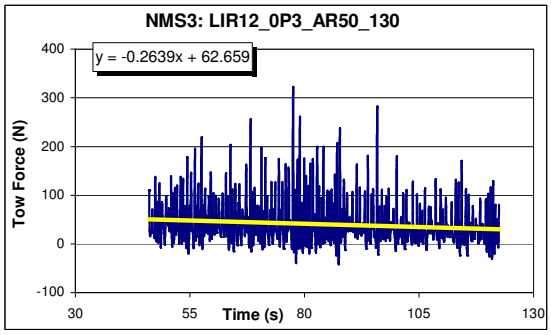

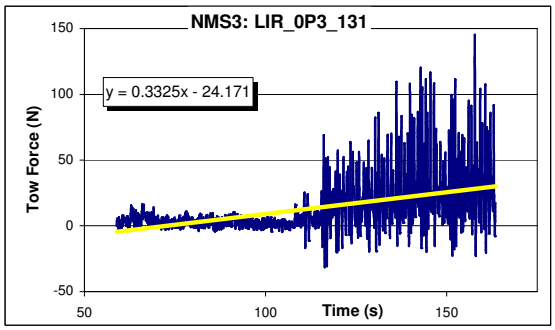

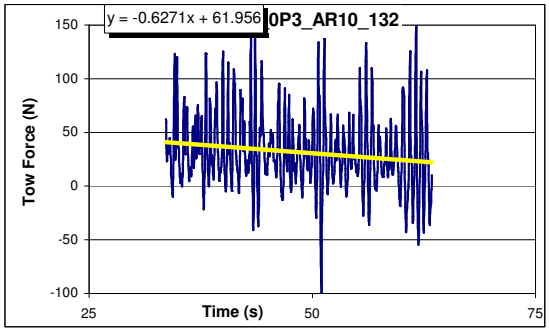

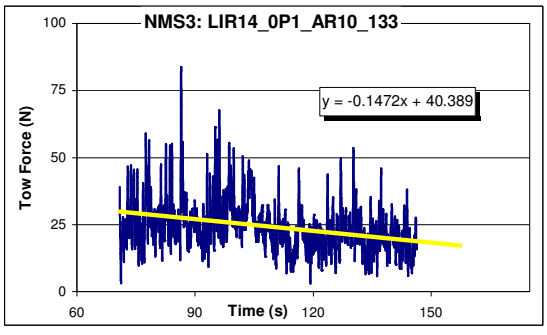

Figure 10c: Tow force-time history

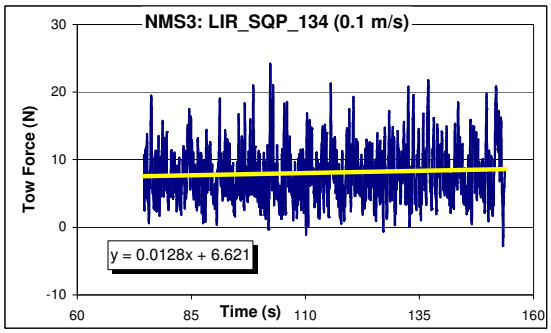

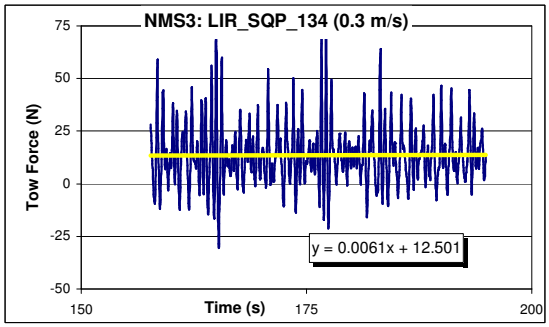

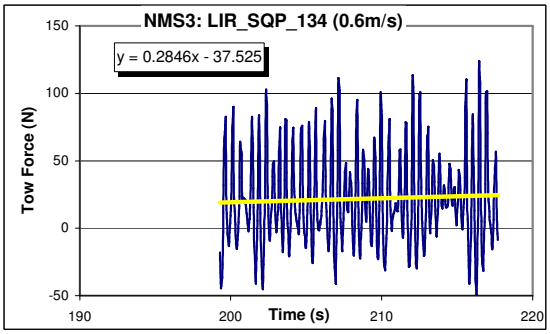

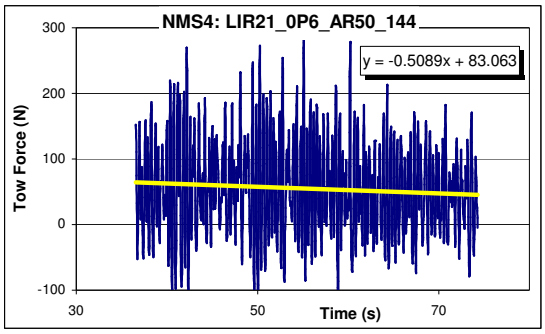

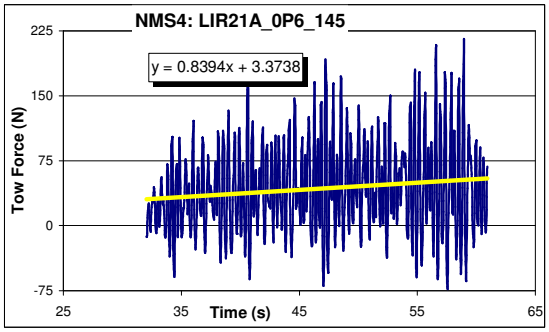

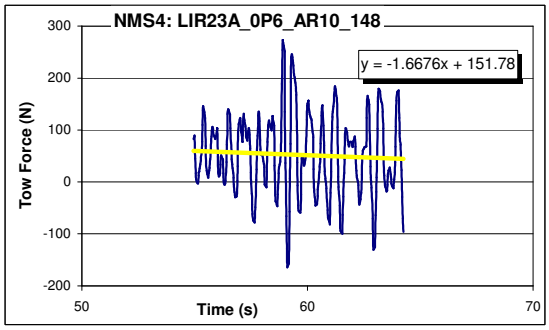

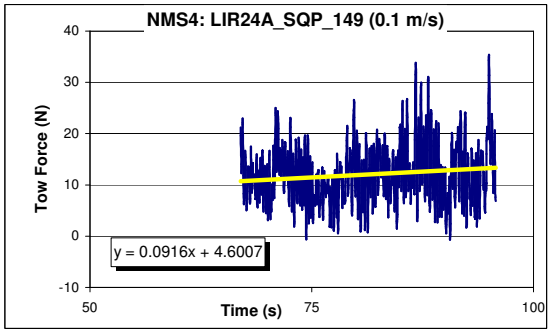

Figure 10d: Tow force-time history

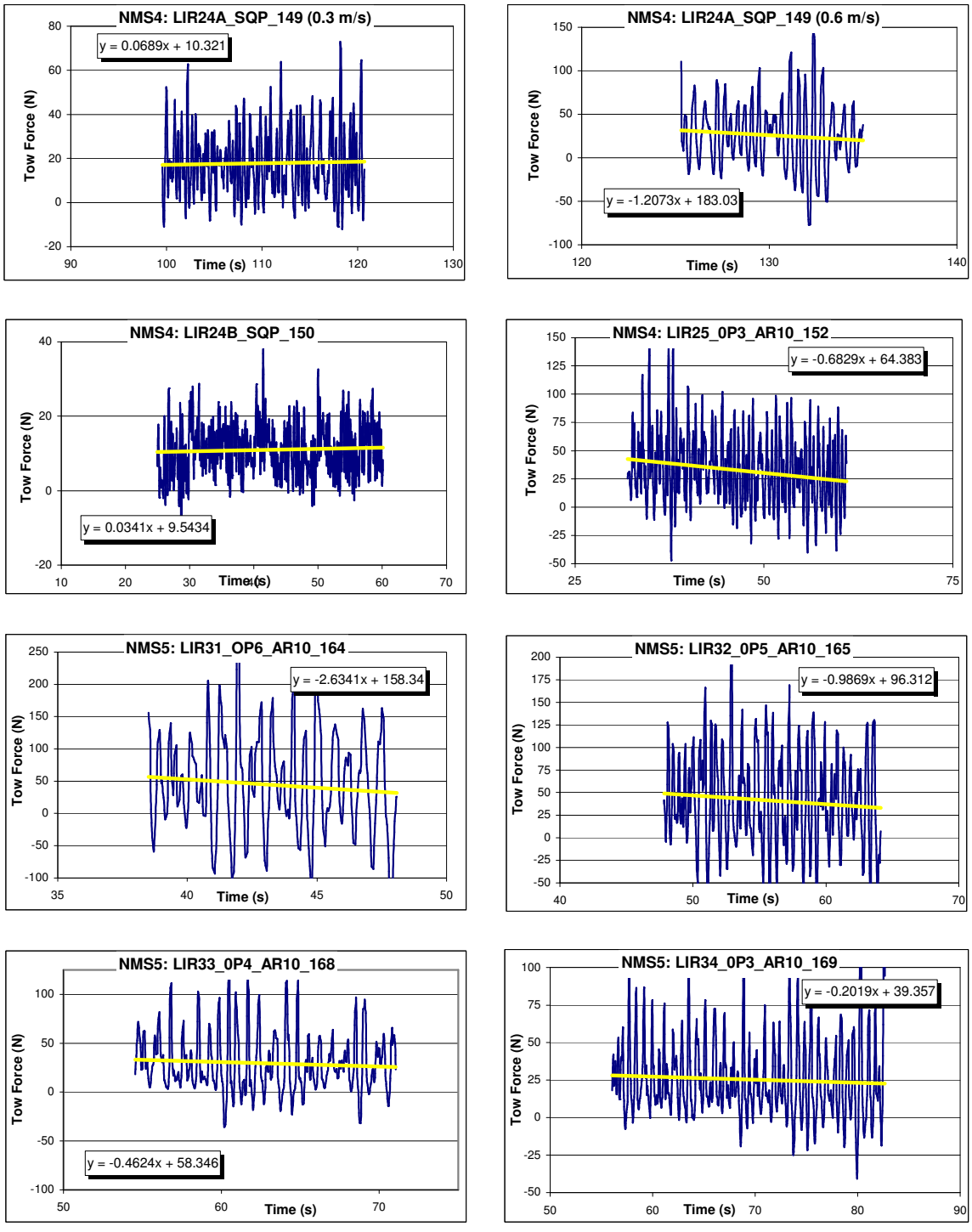

Figure 10e: Tow force-time history

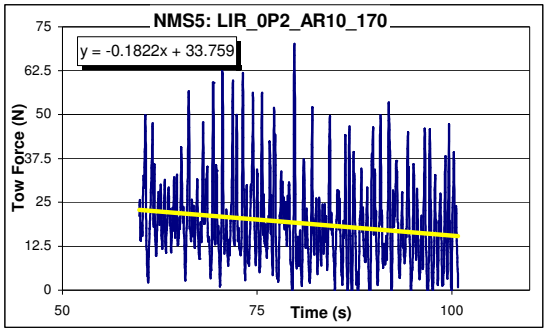

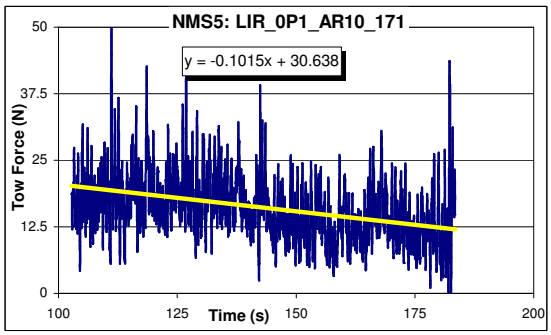

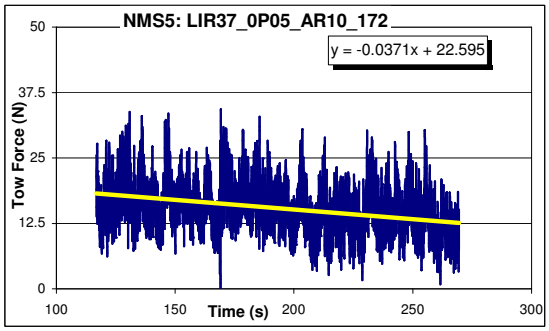

Figure 10f: Tow force-time history

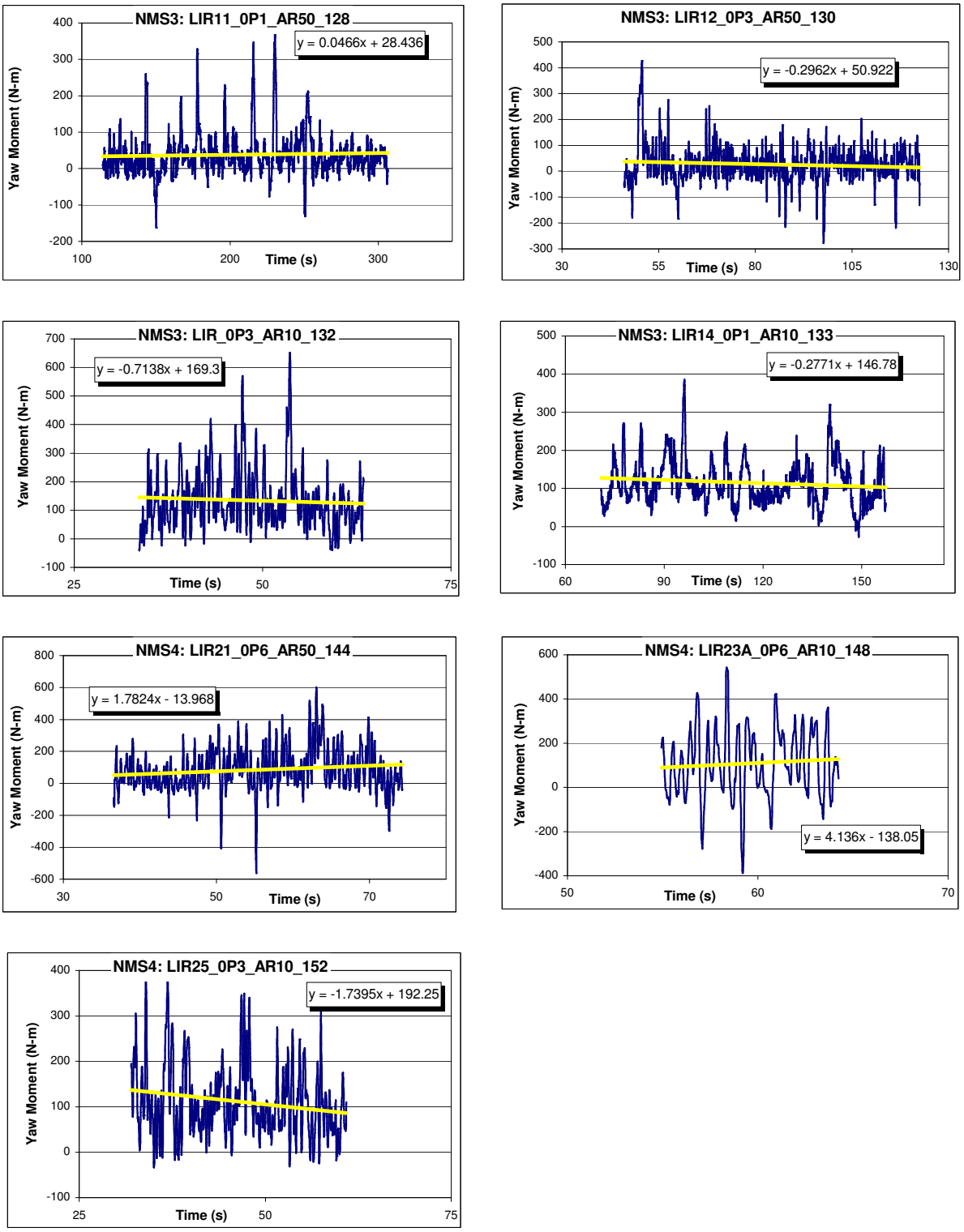

Figure 10g: Yaw moment-time history

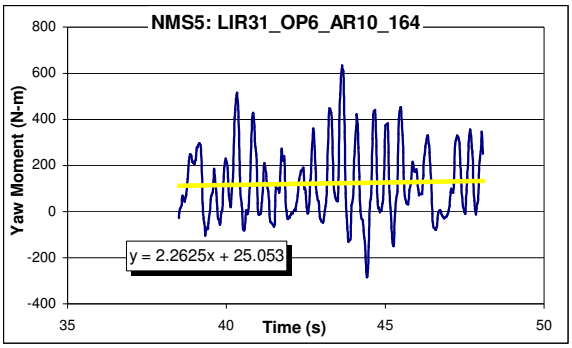

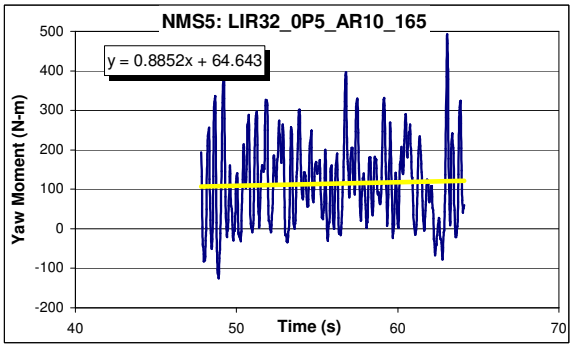

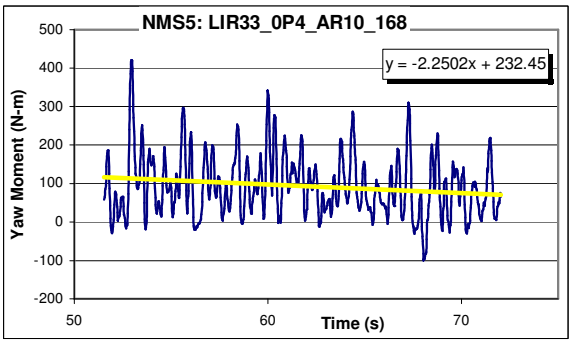

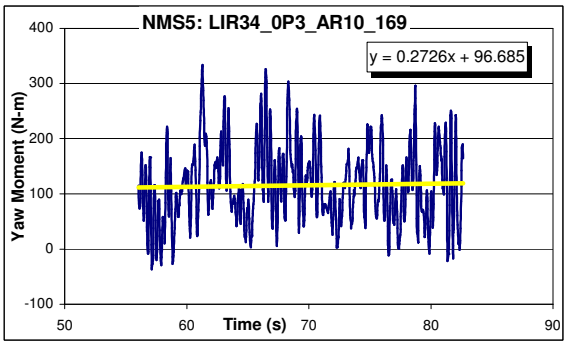

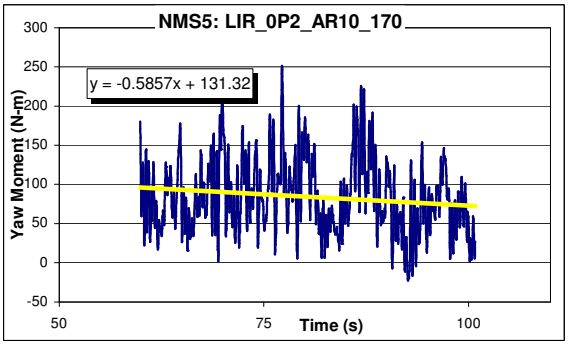

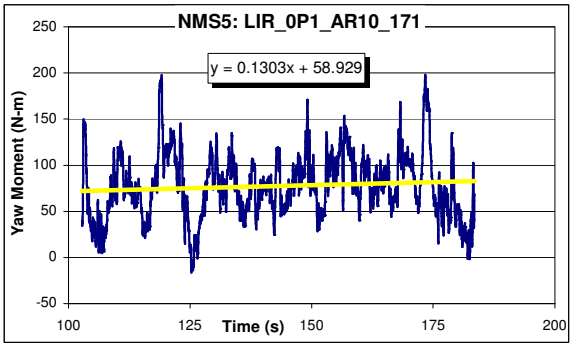

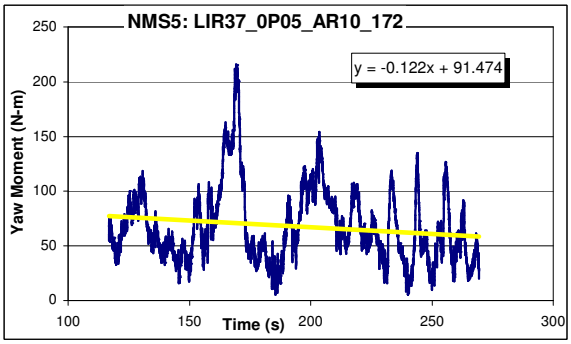

Figure 10h: Yaw moment-time history

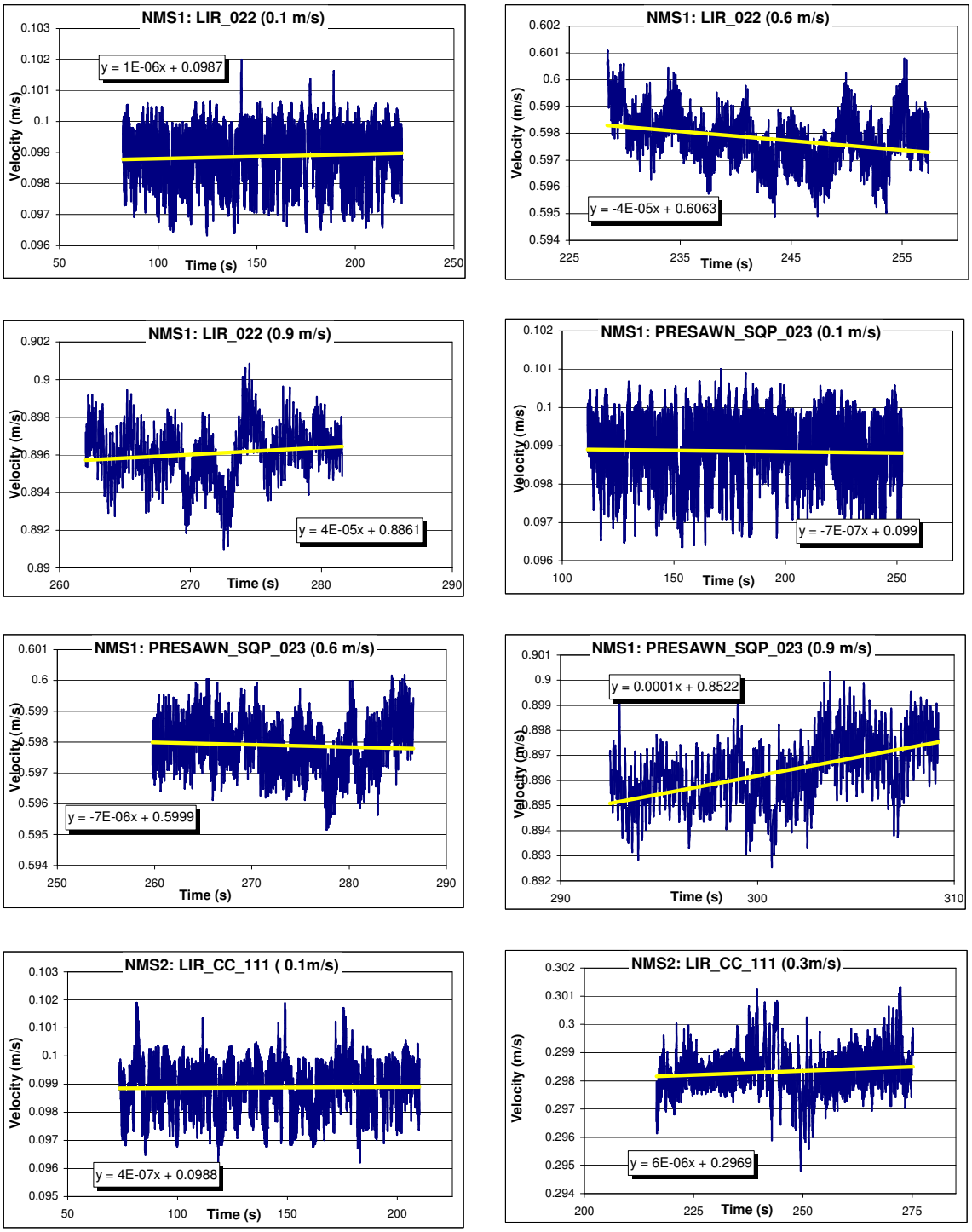

Figure 11a: Velocity-Time history

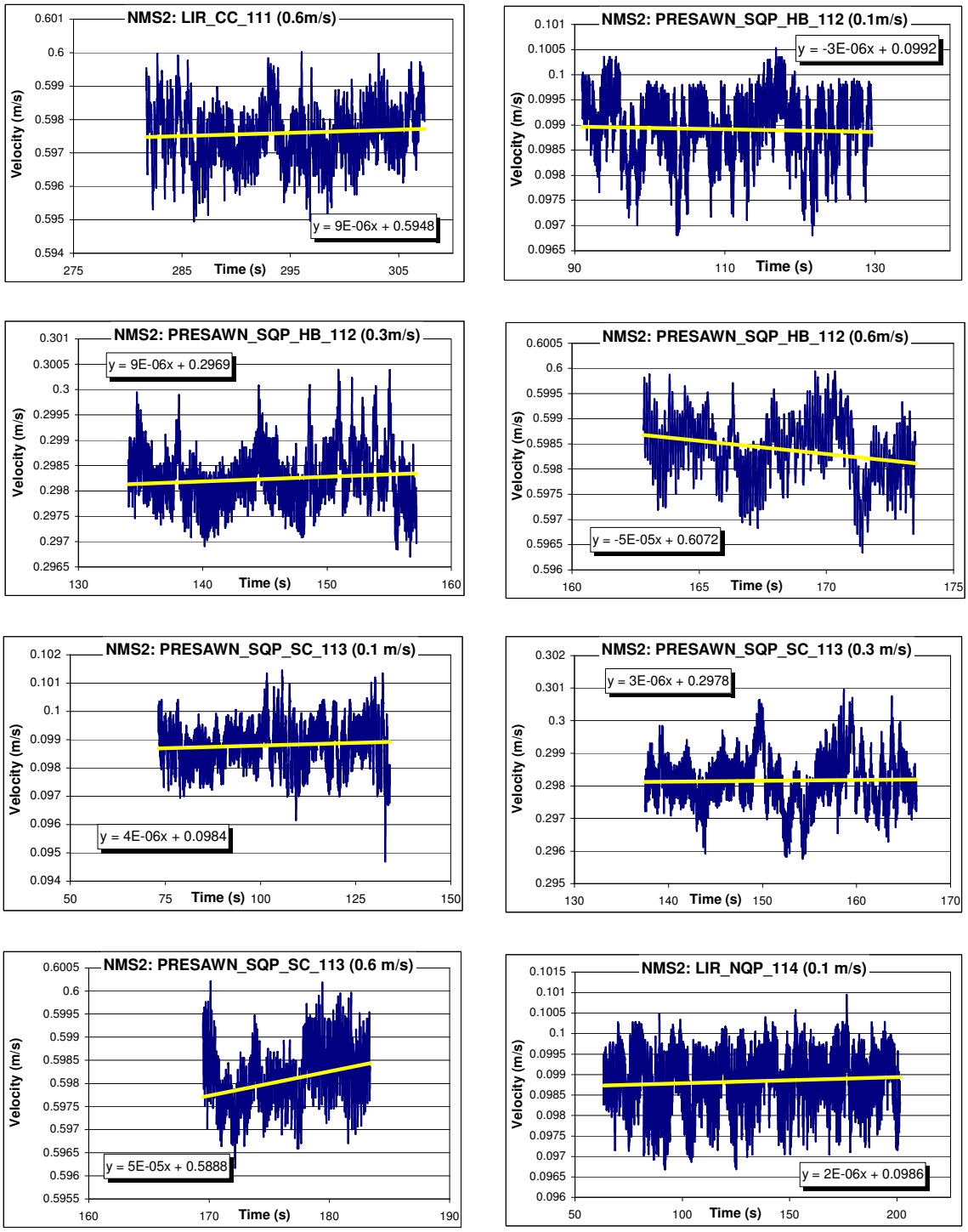

Figure 11b: Velocity-Time history

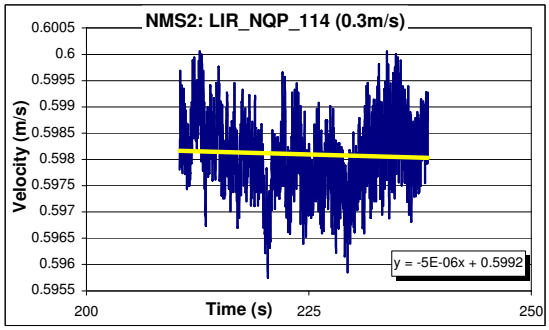

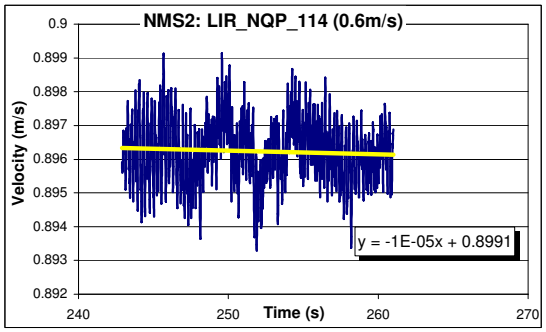

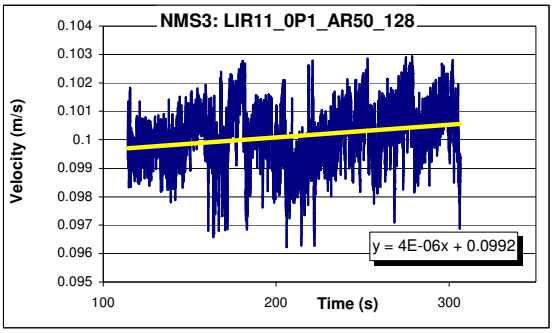

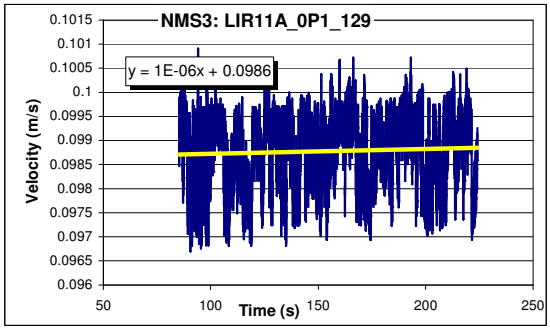

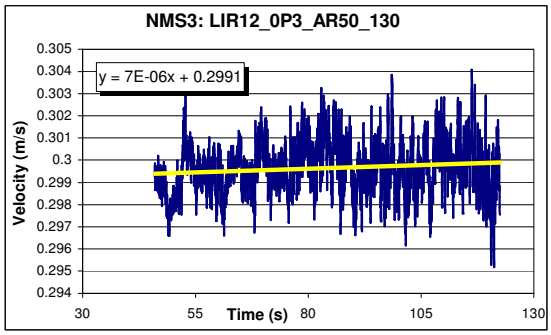

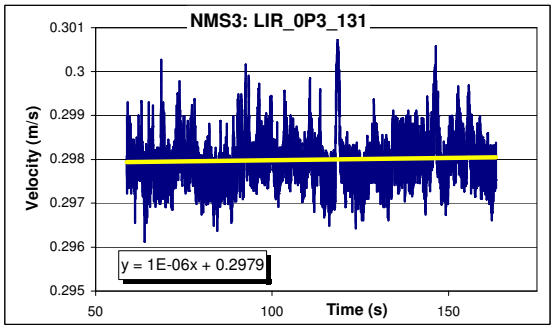

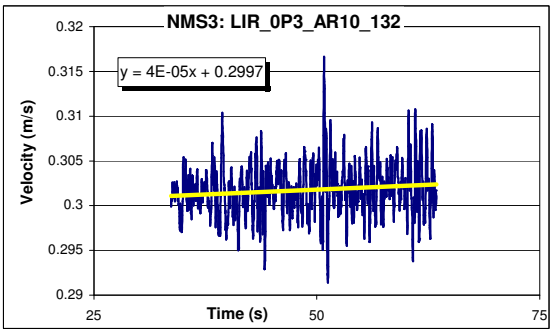

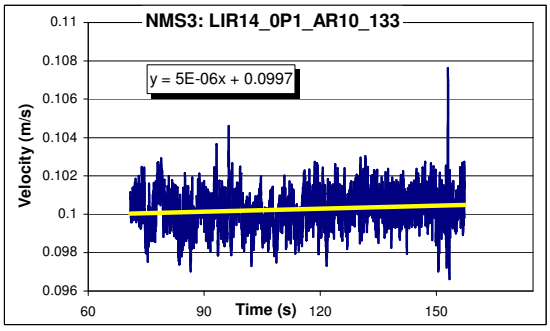

Figure 11c: Velocity-Time history

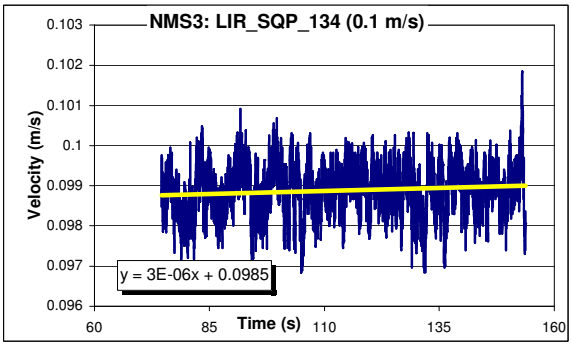

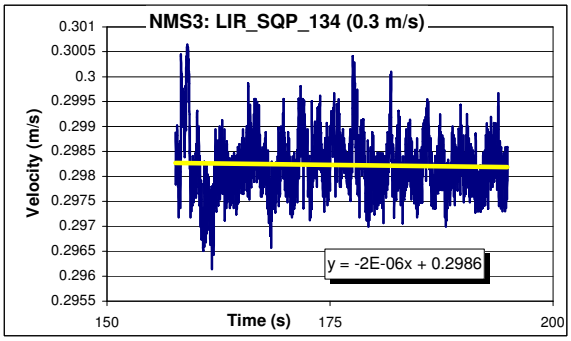

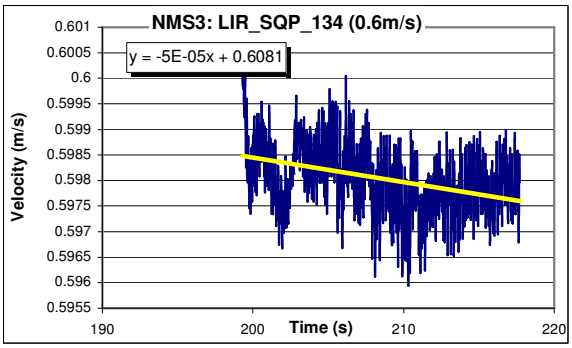

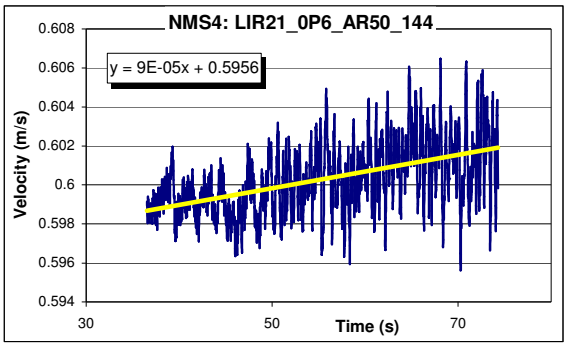

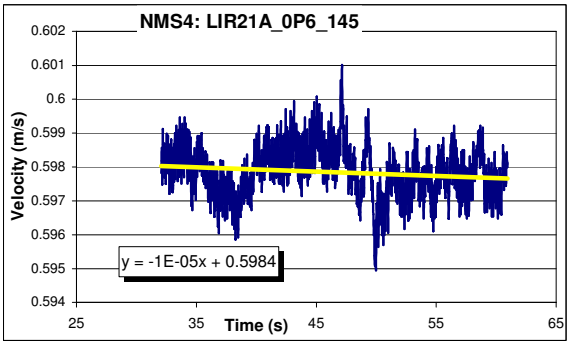

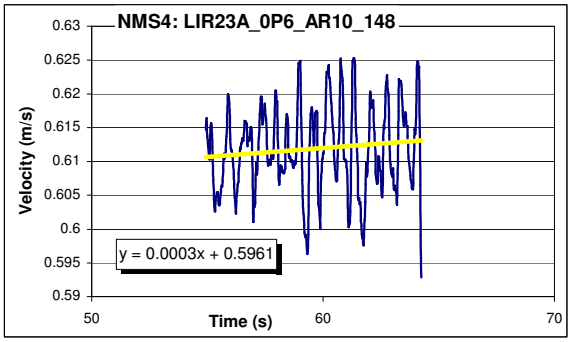

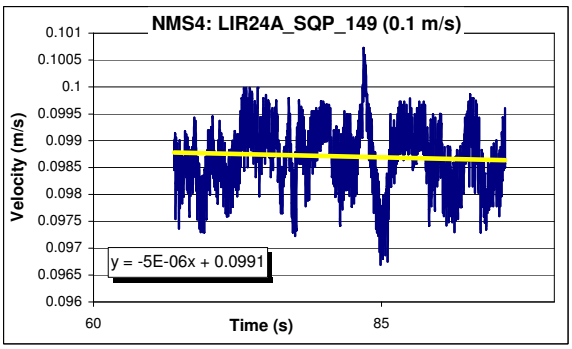

Figure 11d: Velocity-Time history

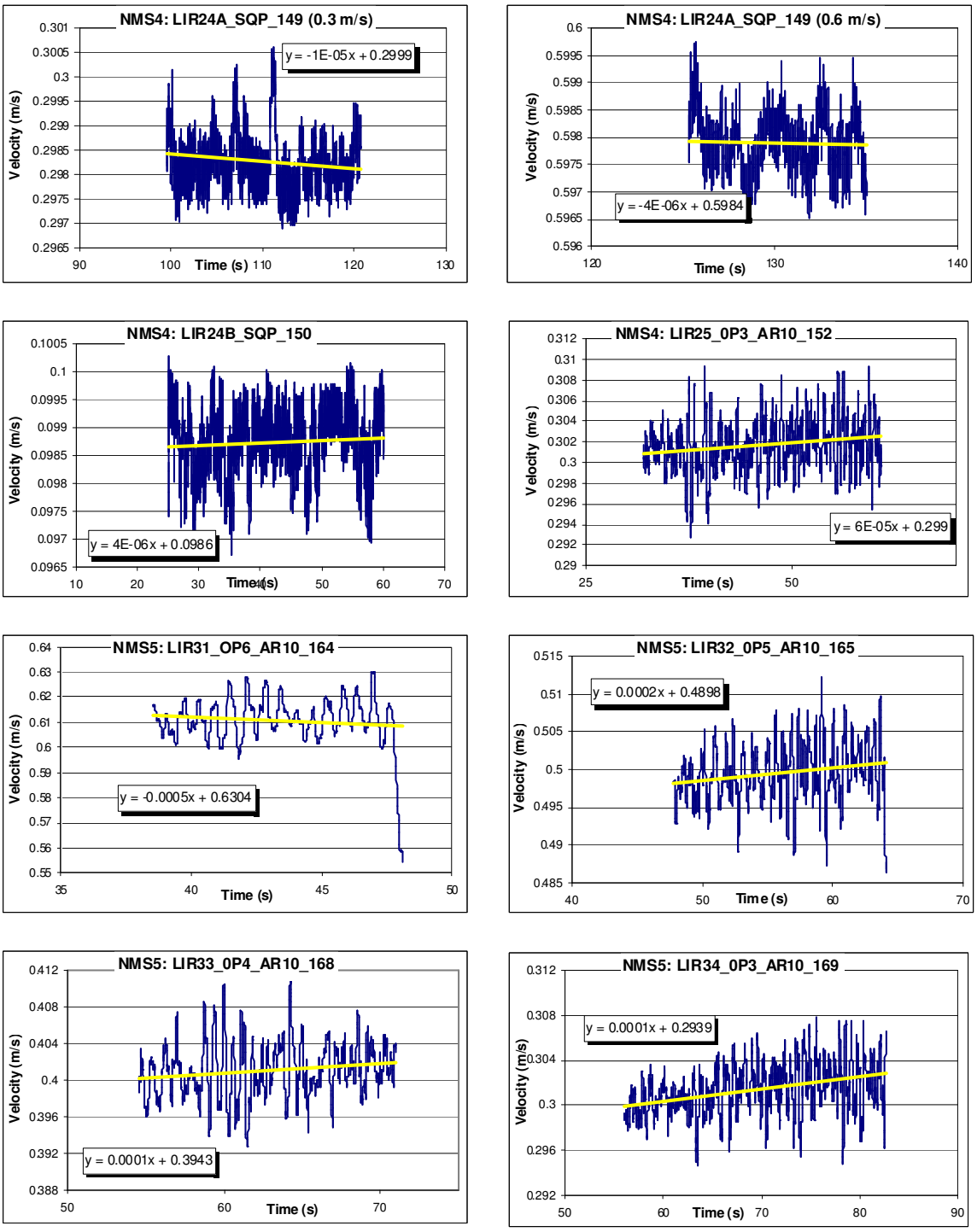

Figure 11e: Velocity-Time history

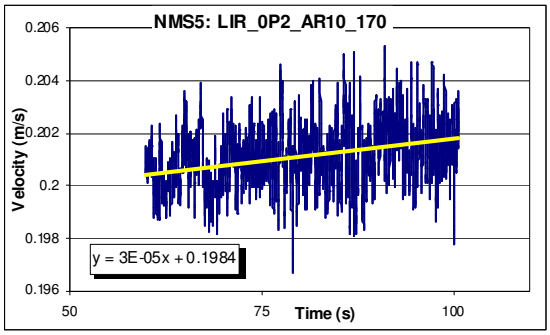

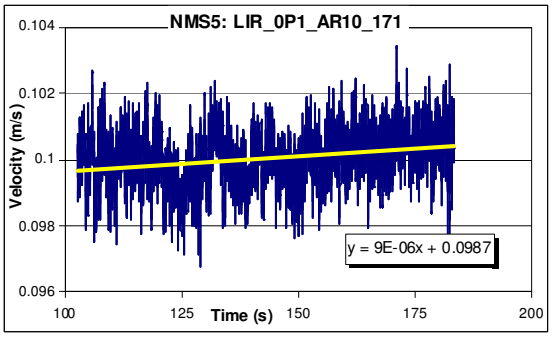

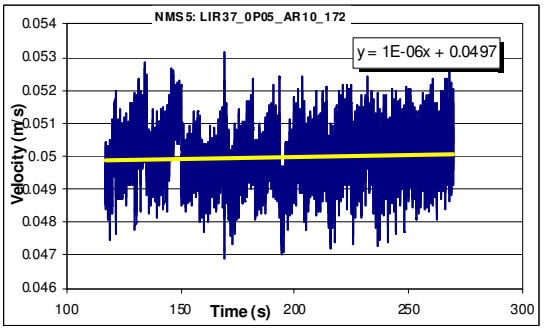

Figure 11f: Velocity -Time history

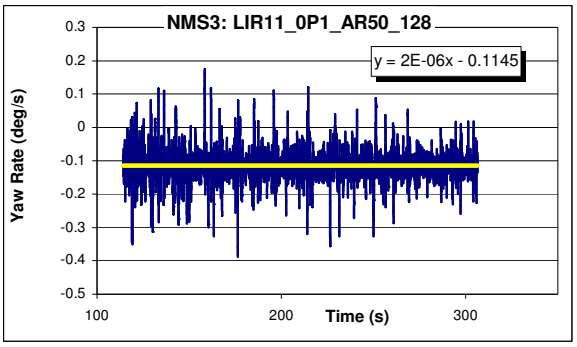

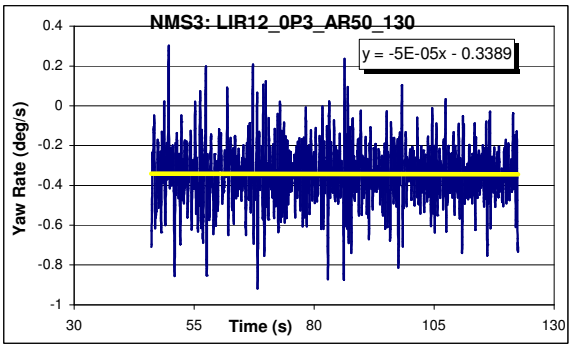

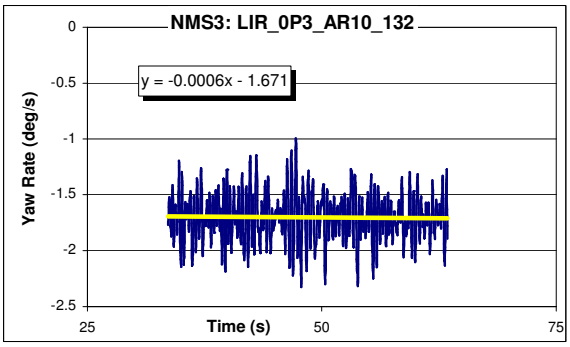

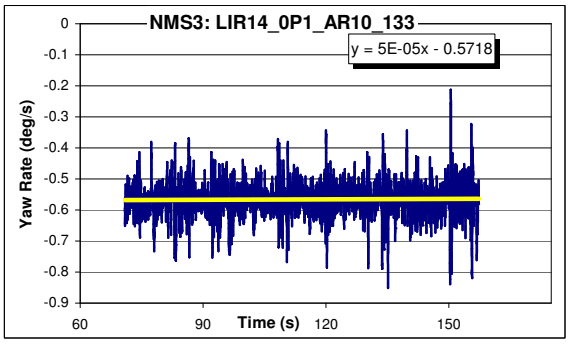

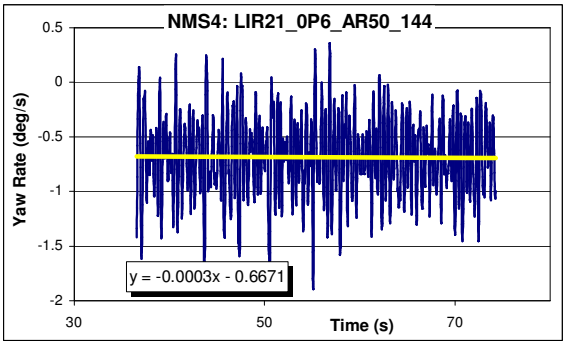

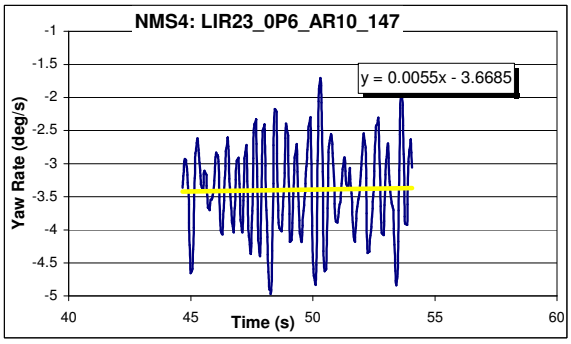

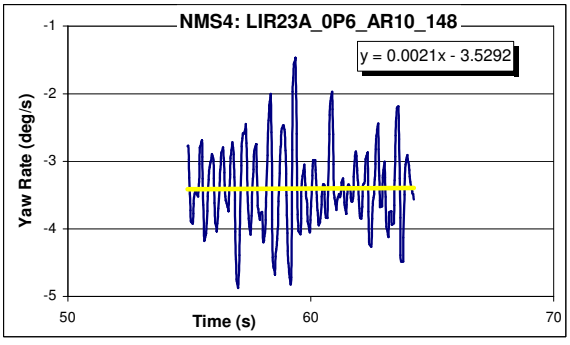

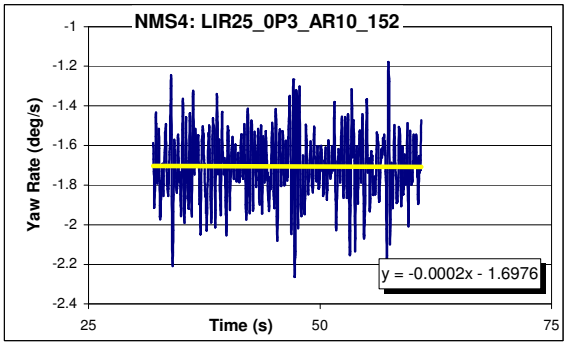

Figure 12a: Yaw rate-time history

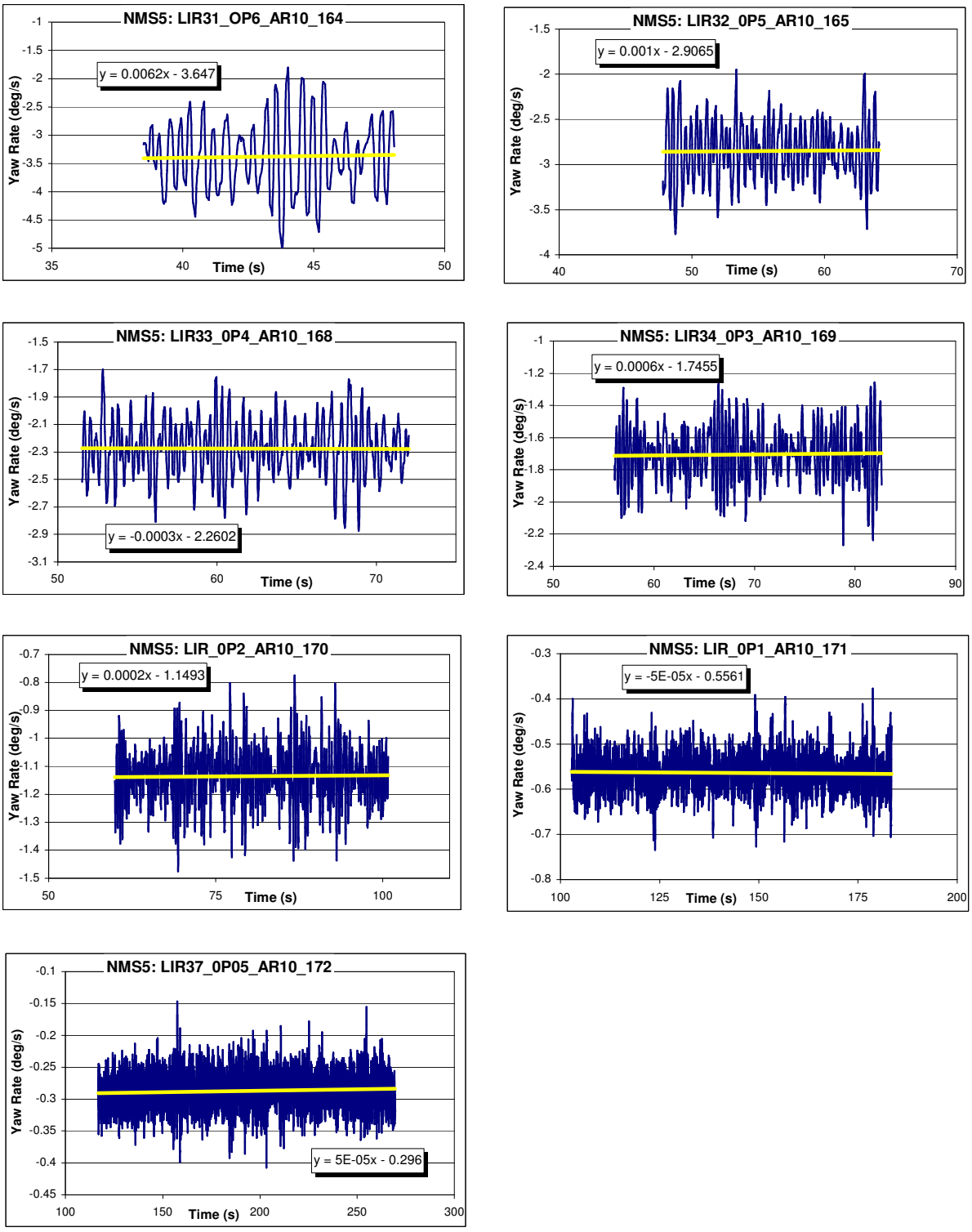

Figure 12b: Yaw rate-time history

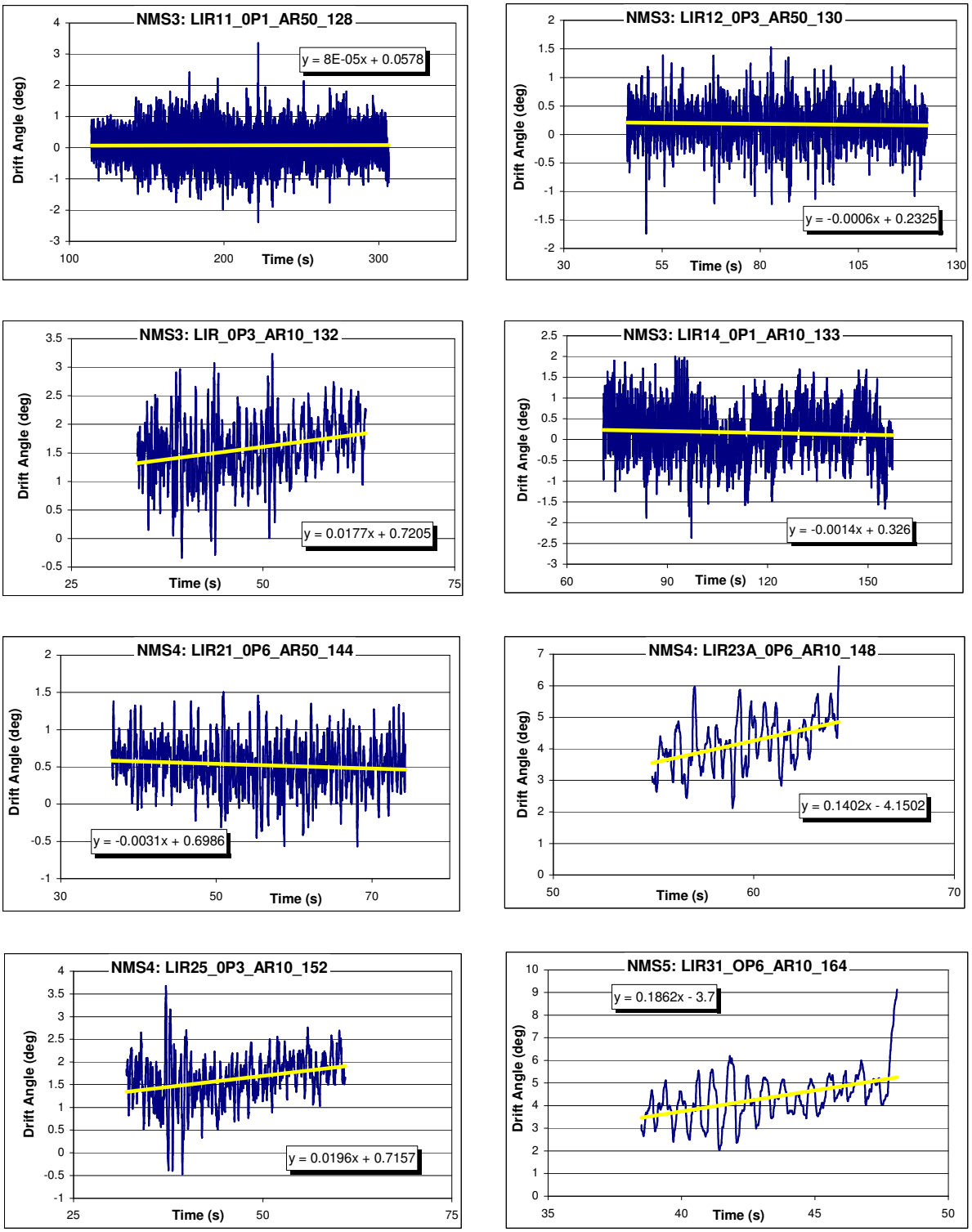

Figure 13a: Drift angle-time history

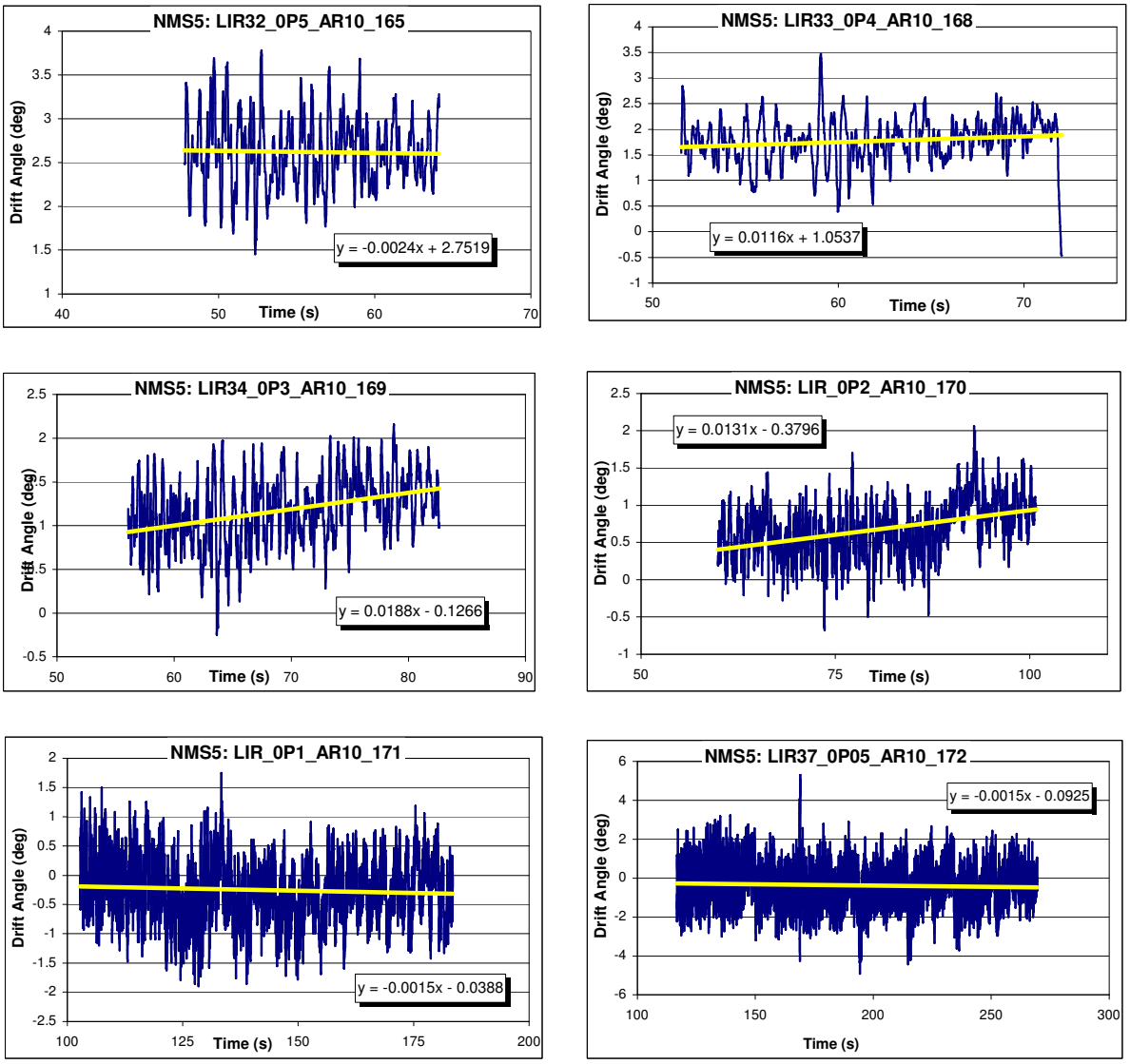

Figure 13b: Drift angle-time history

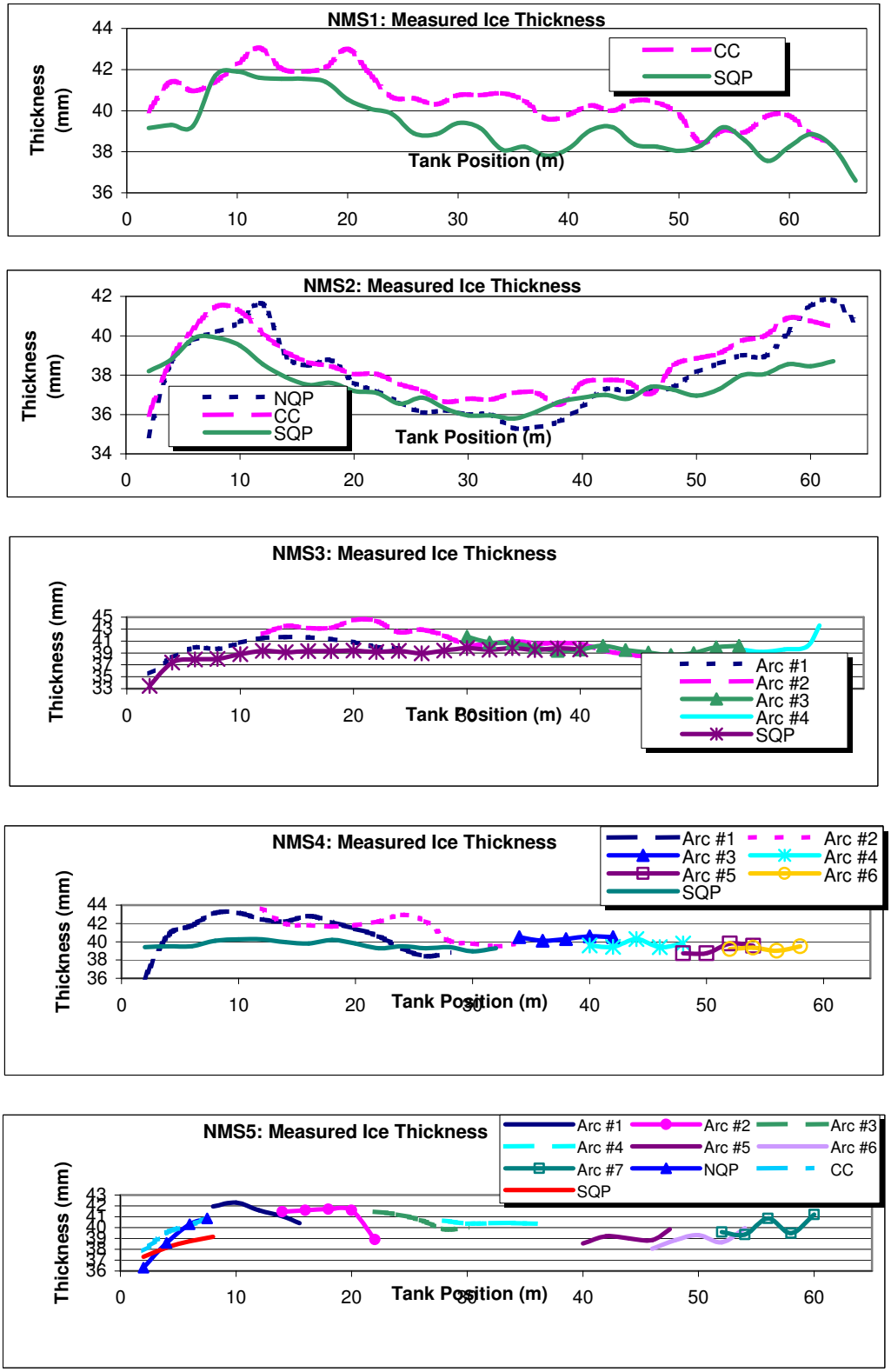

Figure 14a: Measured ice thickness profiles

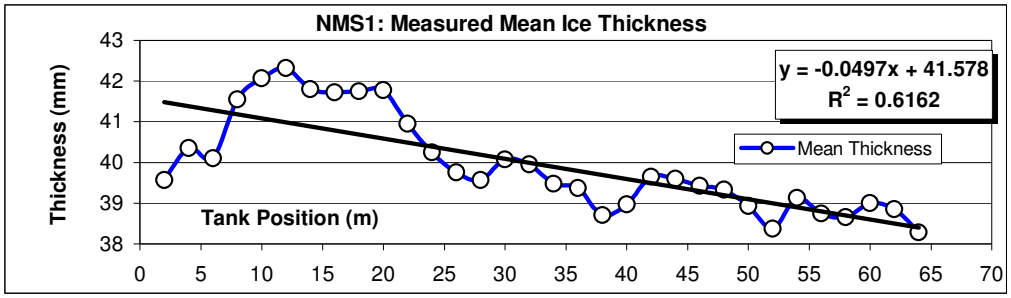

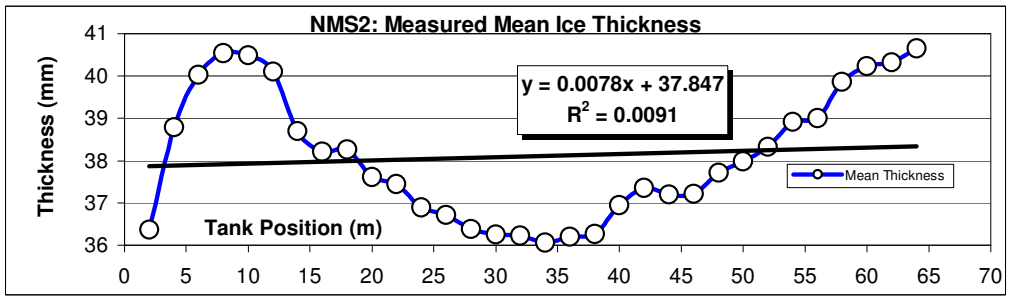

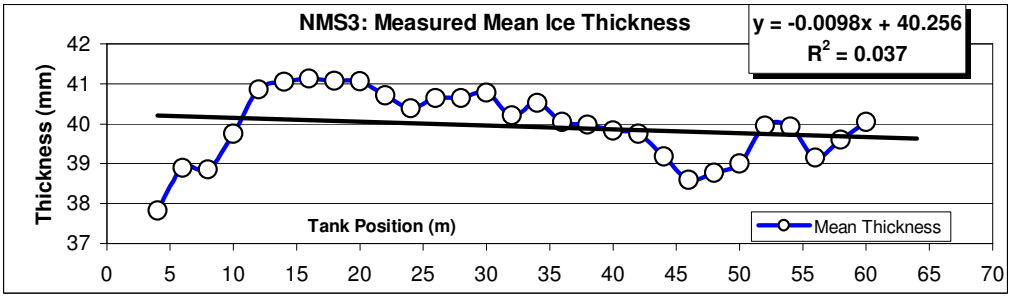

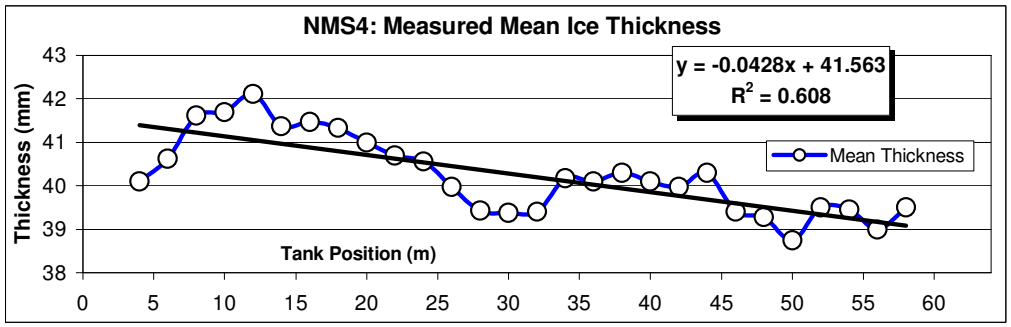

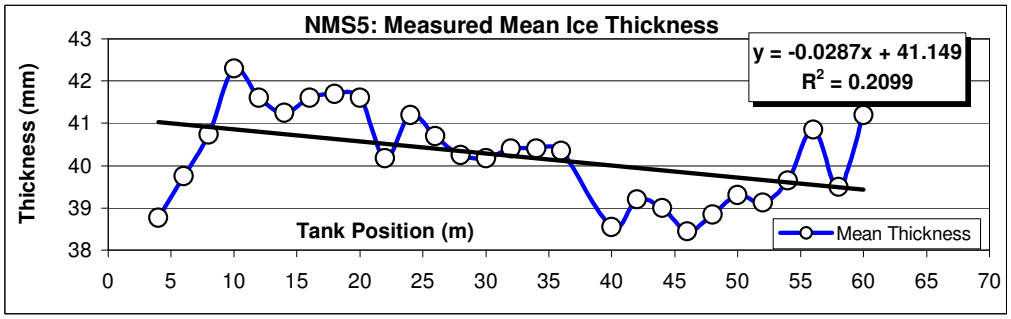

Figure 14b: Mean ice thickness profiles and the linear trends.

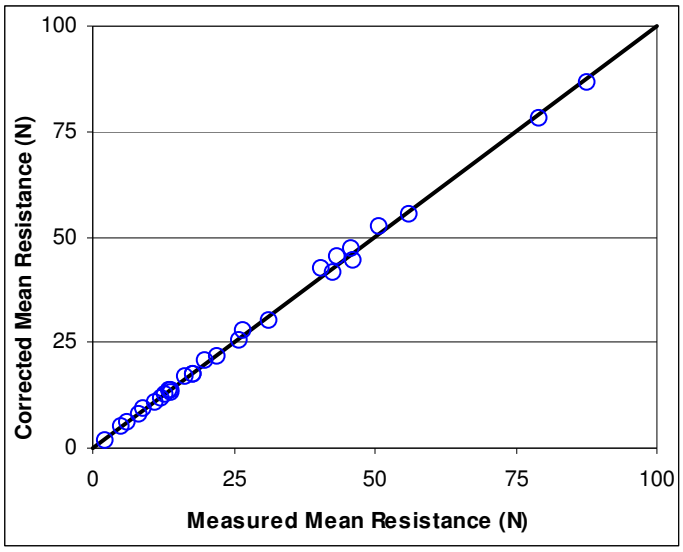

Figure 15a: Corrected versus measured (uncorrected) mean resistance.

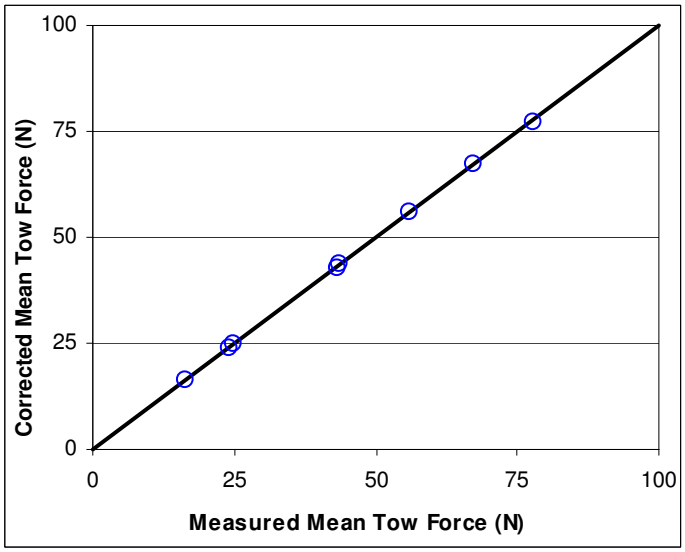

Figure 15b: Corrected versus measured (uncorrected) mean tow force.

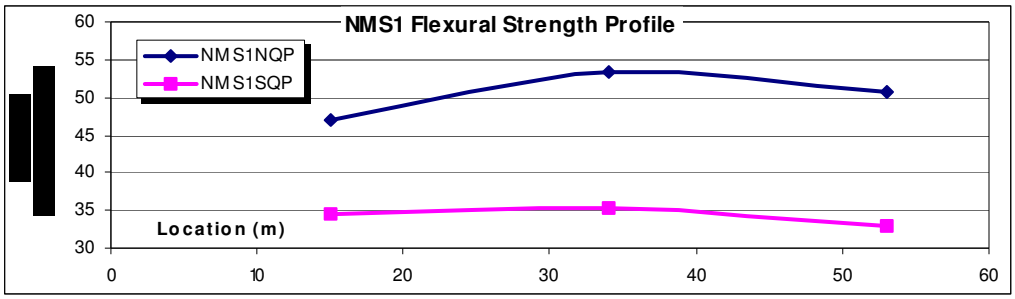

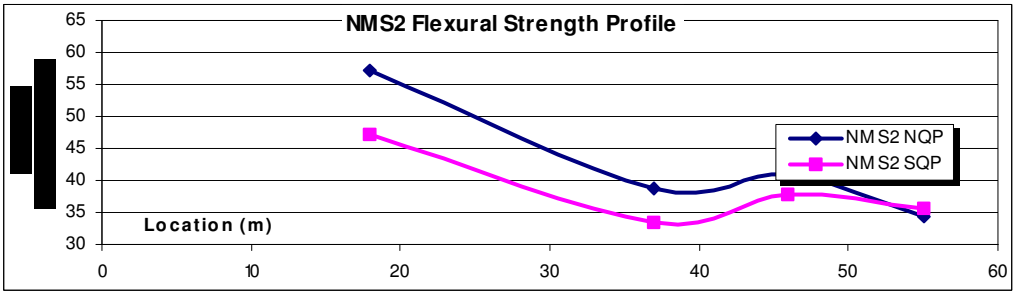

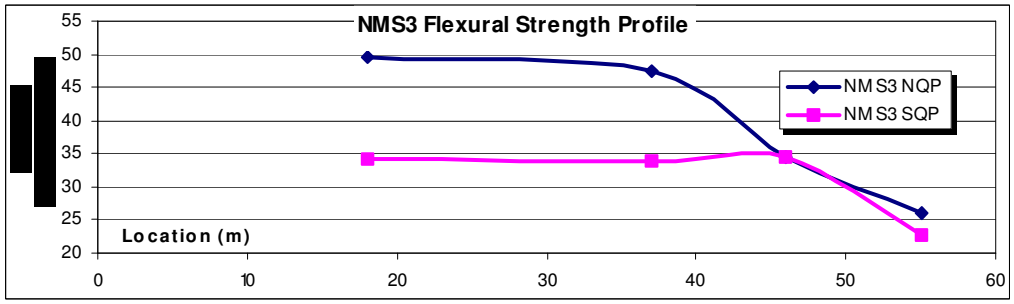

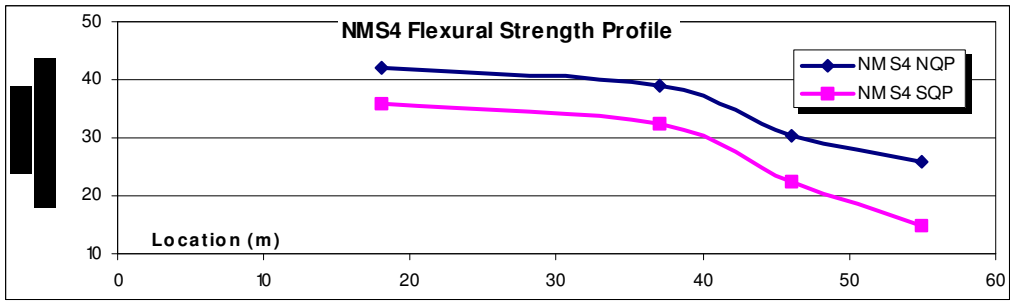

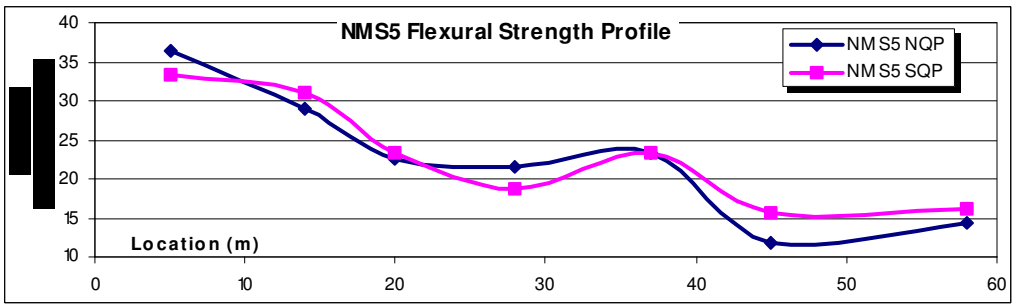

Figure 16a: Measured flexural strength profiles.

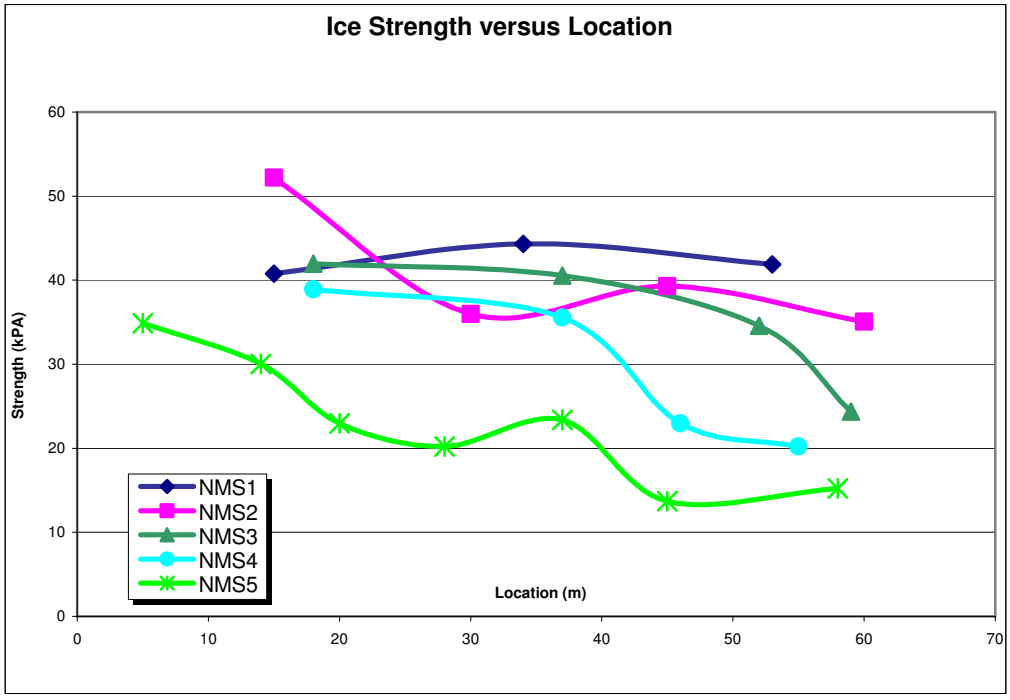

Figure 16b: Mean flexural strength profiles.

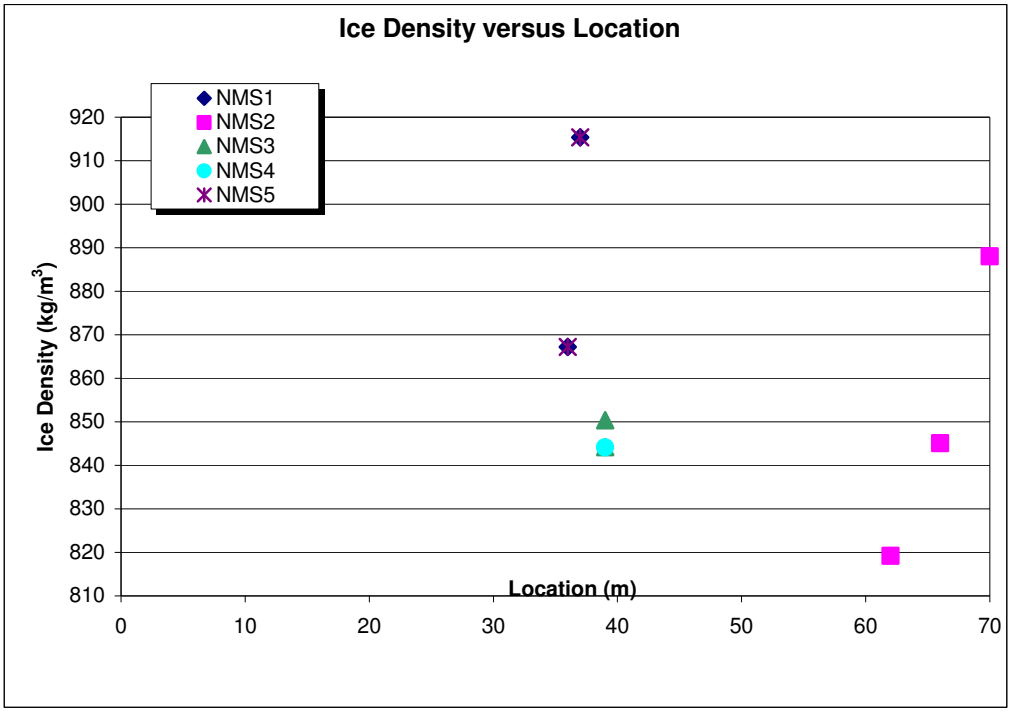

Figure 17: Measured density values.

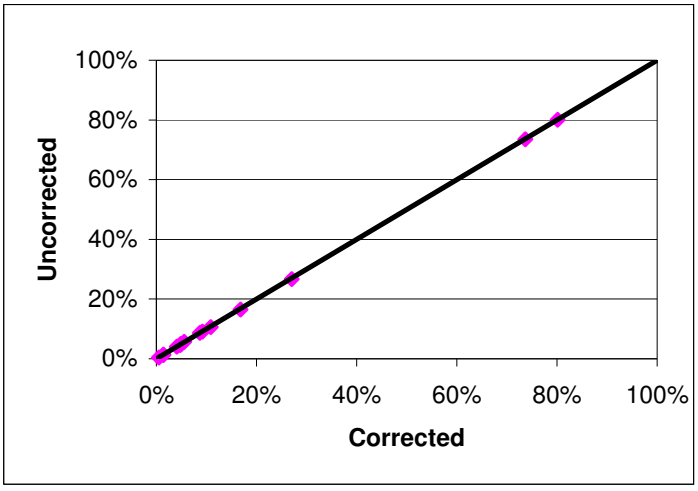

Figure 18a: Comparison between corrected and uncorrected random uncertainties in mean tow force for resistance tests using thickness correction only.

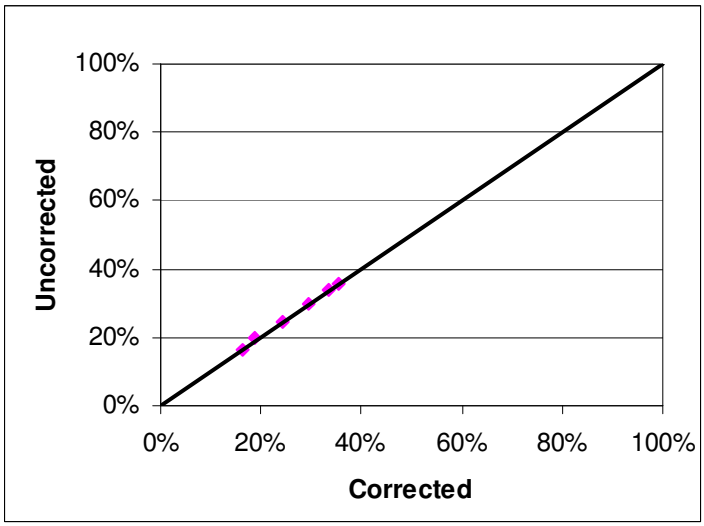

Figure 18b: Comparison between corrected and uncorrected random uncertainties in mean tow force for manoeuvring tests using thickness correction only.

Appendix A

Hydrostatics and Particulars of the *Terry Fox* Model

Hydrostatics

PARAMETER		PROTOTYPE	1/21.8 SCALE MODEL
Length Overall	LOA	86.826m	
	LBP	75.000m	
Beam Overall	BOA	17.494m	802.477064mm
	BWL	17.247 m	
Height Overall	HOA		
Draft	T	8.2m	376.147mm
Volume		6895.791 m^3	
Displacement	Δ	7068.223MT	665.602kg
Waterplane		1250.269 m^2	
Wetted Surface Area	S	2157.345m^2	
Under Water Lateral Plane		570.710 m^2	
Above Water Lateral Plane		137.790 m^2	

COEFFICIENTS (Note: Coefficients calculated based on length of 75.000 m)		
Block Coefficient	CB	0.65
Midship Coefficient	CX	0.906
Prismatic Coefficient	CP	0.718
Waterplane Coefficient	CW	0.967

RATIOS		
Length to Beam Ratio	L/B	4.963
Beam to Draft Ratio	B/T	2.133
Displacement/length		466.923
MT/ cm Immersion		12.815

CENTROIDS		
Buoyancy	LCB	35.218 fwd m
	TCB	0.000 port m
	VCB	4.742 m
Flotation	LCF	33.047 fwd m
Under Water LP		33.218 fwd m of Origin, 3.910 below waterline
Above Water LP		51.279 fwd m of Origin, 1.312 above waterline
TPcm		12.815 MT/cm
MTcm		76.964 MT-m/cm
	GML	81.666 m
GM (Solid)		1.991 m

Draft is from Baseline.
No Trim, No heel, VCG = 6.730
Water Specific Gravity = 1.025. Trim is per 75.00m

Hull Data (with appendages)
Baseline Draft: 8.200
Trim: zero
Heel: zero

Floating Status

Draft FP	8.200 m	Heel	zero	GM(Solid)	1.991 m
Draft MS	8.200 m	Equil	Yes	F/S Corr.	0.000 m
Draft AP	8.200 m	Wind	0.0 kn	GM(Fluid)	1.991 m
Trim	zero	Wave	No	KMT	8.721 m
LCG	35.218f m	VCG	6.730 m	TPcm	12.82

LIST OF TERMINOLOGY
KE = Knife edge
GoBo = Restoring moment of frame without model
GsBs = Restoring moment of frame model, and trimming mass
GcBc = Restoring moment for trimming mass used to level model
GmBm = Restoring moment for the model
Jo = Mass moment of inertia of frame without model
Js = Mass moment of inertia of frame with model, and trimming mass
Jc = Mass moment of inertia of trimming mass used to level model
Jm(ke) = Mass moment of inertia of model about the knife edge
Jm(vcg) = Mass moment of inertia of model about the VCG
K = Radius of Gyration
T = Period

Swung Test Results

CONSTANTS			
Model:			
Description:			
Condition:		Frame used:	Steel Frame
Date:	Nov-26-2003	Frame code:	
Model Length:	3.440m		
Mass of model:	665.602kg	**Frame Constants Used:**	
Model Beam	0.802477064m	G0B0t (Nm)	770.814
Supports (if not used enter 0.0 for mass):		G0b0l (Nm)	772.438
Mass:	3.1kg	l1 (m)	0.750
Length:	2.438m	l2 (m)	0.750
Width	0.609m	a (m)	0.188
Thickness:	0.0508m	d (m)	1.197
		J0t (kg-m^2)	235.098
INCLINOMETER		J0l(kg-m^2)	234.915
Mass:	0kg		
		Frame Constants Corrected for Support	
Height above KE	0m	G0B0t (Nm)	806.433
		G0b0l (Nm)	808.057
INCLINING MASS:	63.5kg	J0t (kg-m^2)	239.450
		J0l (kg-m^2)	240.706
		d (m)	1.146

Pitch Gyradius Only

Inclining Angles (degrees)			**Inclining Angles (degrees)**		
PITCH BOW DOWN		Theta (deg)	***PITCH BOW UP***		Theta (deg)
Initial	0.0000	0.0000	Initial	0.0000	
Weight Fwd 1	4.3600	4.3600	Weight Aft 1	-4.3600	4.3600
Initial	0.0000	4.3600	Initial	0.0000	4.3600
Weight Fwd 2	4.3600	4.3600	Weight Aft 2	-4.3600	4.3600
Initial	0.0000	4.3600	Initial	0.0000	4.3600
Theta (mean)		4.3600	Theta (mean)		4.3600

Theta (mean) for bow up and bow down= 4.360

	PITCH
TRIMMING MASS (kg)	0
DISTANCE FROM KE (X) (m, + fwd)	0
DISTANCE FROM KE (Y) (m, + stbd)	0
DISTANCE FROM KE (Z) (m, + down)	0
Correction to Inertia of System (kg-m^2):	0
Restoring Moment of System (G1b1) (Nm):	6242.95
Restoring Moment of Frame (G0b0) (Nm):	772.44
Restoring Moment of Inclinometer (Gibi) (Nm):	0.00
Restoring Moment of Model (Gb) (Nm):	5470.51
CG of Model and Trim Weight from KE (m):	0.838
VCG of Model and Trim Weight from keel (m):	0.308
VCG of Model from keel (m):	0.3084

Inertia of Model

PITCH IN AIR		
Cycles	Time (sec)	Period (sec)
10	28.26	2.826
10	28.26	2.826
10	28.26	2.826
	MEAN	**2.826**

	PITCH
Inertia of Entire System about KE (kg-m^2)	1262.92
Inertia of Frame about KE (kg-m^2)	234.92
Inertia of Model about KE (kg-m^2)	1028.00
Parallel Axis Correction (kg-m^2)	467.20
Inertia of Model about own CG (kg-m^2)	560.80
Radius of Gyration (m)	0.918
Radius of Gyration/Length	**0.267**

Roll Gyradius Only

Inclining Mass: 63.5kg

Inclining Angles (degrees)			Inclining Angles (degrees)		
ROLL PORT DOWN		Theta (deg)	***ROLL STBD DOWN***		Theta (deg)
Initial	0.0000		Initial	0.0000	
Weight Fwd 1	4.3700	4.3700	Weight Aft 1	-4.3600	4.3600
Initial	0.0000	4.3700	Initial	0.0000	4.3600
Weight Fwd 2	4.3700	4.3700	Weight Aft 2	-4.3600	4.3600
Initial	0.0000	4.3700	Initial	0.0000	4.3600
Theta (mean)		4.3700	Theta (mean)		4.3600

Theta (mean) for bow up and bow down= 4.365

	ROLL
TRIMMING MASS (kg)	0
DISTANCE FROM KE (X) (m, + fwd)	0
DISTANCE FROM KE (Y) (m, + stbd)	0
DISTANCE FROM KE (Z) (m, + down)	0
Correction to Inertia of System (kg-m^2):	0
Restoring Moment of System (G1b1) (Nm):	6237.81
Restoring Moment of Frame (G0b0t) (Nm):	770.81
Restoring Moment of Inclinometer (Gibi) (Nm):	-1.00
Restoring Moment of Model (Gbt) (Nm):	5468.00
CG of Model and Trim Weight from KE (m):	0.837
VCG of Model and Trim Weight from keel (m):	0.309
VCG of Model from keel (m):	0.3088

Inertia of Model

ROLL IN AIR		
Cycles	Time (sec)	Period (sec)
10	22	2.200
10	22	2.200
10	22	2.200
	MEAN	**2.200**

	ROLL
Inertia of Entire System about KE (kg-m^2)	764.75
Inertia of Frame about KE (kg-m^2)	239.45
Inertia of Model about KE (kg-m^2)	525.30
Parallel Axis Correction (kg-m^2)	466.77
Inertia of Model about own CG (kg-m^2)	58.53
Radius of Gyration (m)	0.297
Radius of Gyration/Beam	**0.370**

FINAL RESULTS	
VCG (Pitch) From keel (m)	**0.308**
VCG (Roll) From keel (m)	**0.309**
Radius of Gyration (Pitch) (m)	**0.918**
Radius of Gyration (Roll) (m)	**0.297**

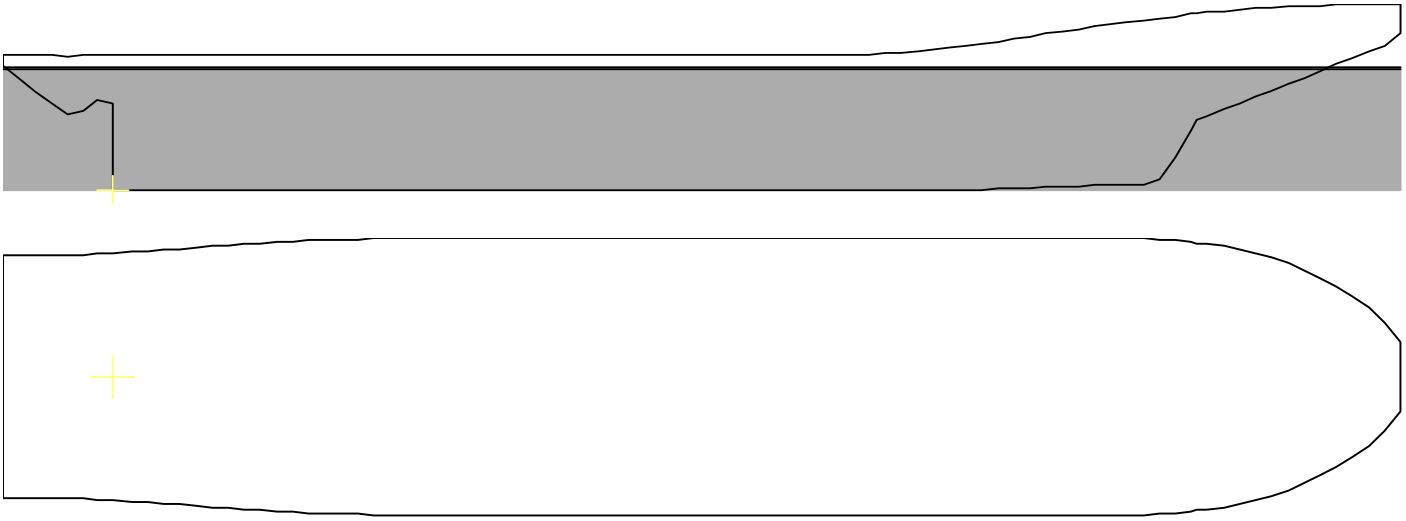

Hull Section Data (with appendages) No Trim, No heel

Location (m)	Draft (m)	Area (m^2)	WL Width (m)	Girth (m)
75.000f	8.200	0.077	0.821	0.902
73.125f	8.200	2.234	4.183	4.635
71.250f	8.200	6.838	6.821	7.737
69.375f	8.200	13.997	9.499	10.883
67.500f	8.200	22.830	11.545	13.506
65.625f	8.200	37.399	13.680	20.079
63.750f	8.200	56.009	15.566	23.543
61.875f	8.200	73.126	16.604	24.614
60.000f	8.200	87.952	16.967	25.439
58.125f	8.200	99.829	17.056	26.245
56.250f	8.200	109.806	17.089	27.050
54.375f	8.200	117.199	17.119	27.830
52.500f	8.200	122.555	17.148	28.617
50.625f	8.200	125.838	17.178	29.362
48.750f	8.200	127.696	17.205	30.005
46.875f	8.200	127.994	17.228	30.115
45.000f	8.200	128.106	17.247	30.095
43.125f	8.200	128.106	17.247	30.095
41.250f	8.200	128.106	17.247	30.095
39.375f	8.200	128.106	17.247	30.095
37.500f	8.200	128.106	17.247	30.095
35.625f	8.200	128.106	17.247	30.095
33.750f	8.200	128.106	17.247	30.095
31.875f	8.200	128.106	17.247	30.095
30.000f	8.200	128.106	17.247	30.095
28.125f	8.200	128.106	17.247	30.095
26.250f	8.200	127.578	17.247	30.144

24.375f	8.200	125.502	17.238	30.015
22.500f	8.200	121.670	17.220	29.782
20.625f	8.200	116.211	17.189	29.512
18.750f	8.200	110.112	17.144	29.459
16.875f	8.200	103.832	17.074	29.949
15.000f	8.200	97.408	16.972	31.138
13.125f	8.200	88.881	16.838	32.976
11.250f	8.200	77.287	16.651	35.328
9.375f	8.200	67.885	16.412	37.421
7.500f	8.200	59.068	16.120	40.068
5.625f	8.200	50.782	15.797	42.736
3.750f	8.200	40.063	15.447	47.199
1.875f	8.200	26.329	14.458	26.649
0.000	8.200	20.883	12.797	25.470

Volume = 6895.79m^3 LCG = 35.218f

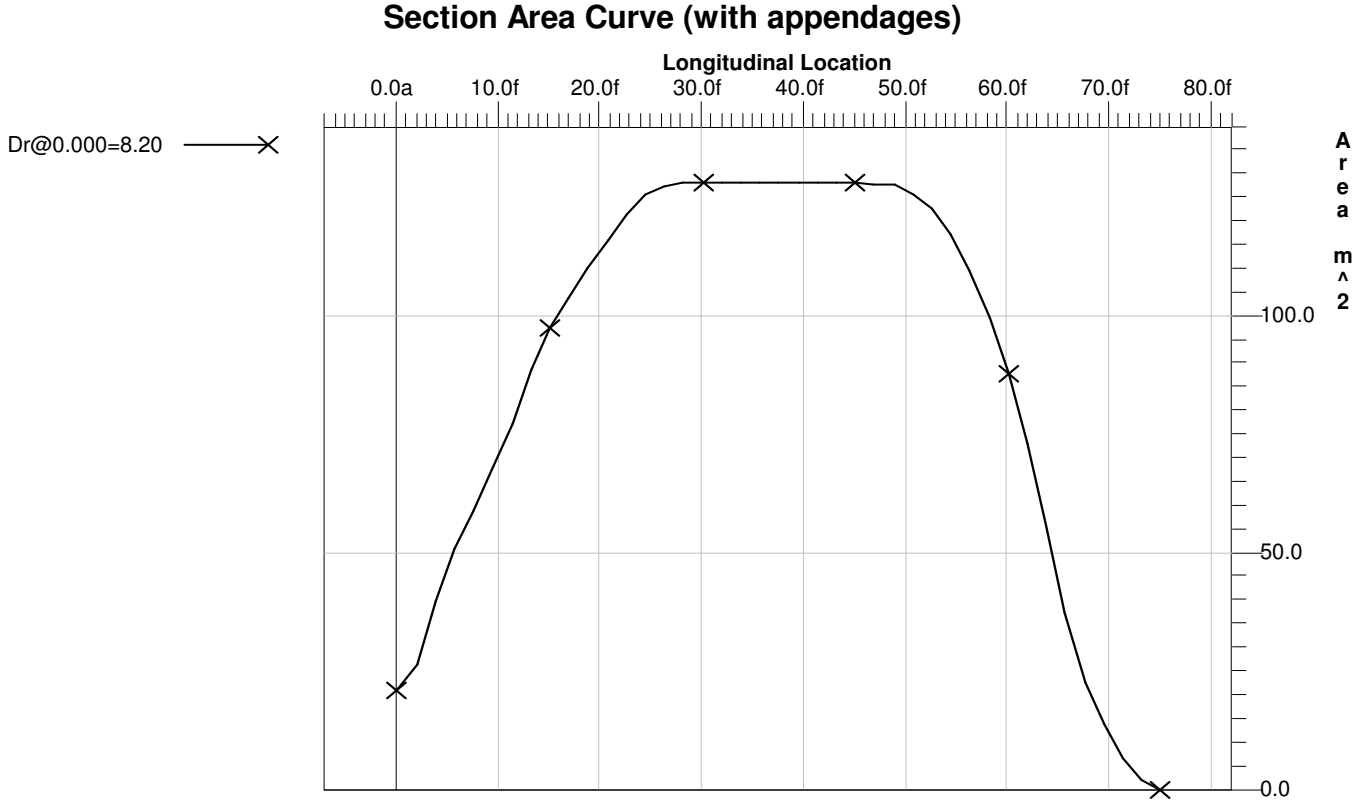

Appendix B

Instrumentation and Calibrations

The test program required measurements of the following 17 items:

i. Surge Center (N)…… Channel # 1.
ii. FWD Sway (N)…….. Channel # 2.
iii. AFT Sway (N)…….. Channel # 3.
iv. X Inline Load cell (N)…… Channel # 4.
v. Y Inline Load cell (N)…… Channel # 5.
vi. Yaw (degrees)…… Channel # 17.
vii. Sway Position (m)…….. Channel # 19.
viii. Sway Velocity (m/s)…… Channel # 20.
ix. FWD Heave (mm)…… Channel # 21.
x. AFT Heave (mm)…… Channel # 22.
xi. X (m/s^2)…… Channel # 25.
xii. Y (m/s^2)…… Channel # 26.
xiii. Z (m/s^2)…… Channel # 27.
xiv. Yaw Rate (deg/s)…... Channel # 28.
xv. Carriage Position (m)…… Channel # 33.
xvi. Carriage Velocity (m/s)…… Channel # 34.
xvii. Carriage Velocity (F/V) (m/s)……... Channel # 35.

Test Configuration

DACON File: PJ953_NMS_Dec03
Project: Marine Structural Fragility and Software Validation
Facility: Icetank

Channel No.	Sensor Name	Sensor Model	Serial No.	Data Description
1	SURGE CENTER	SSB-HN-250	B88024	Force (N)
2	FWD Sway	SSB-AJ-500	C65397	Force (N)
3	AFT Sway	SSB-AJ-500	C65391	Force (N)
4	X Inline Load	60001-100	A10501 S/N 683212	Force (N)
5	Y Inline Load cell	60001-100	NRC A10500 S/N 00083211	Force (N)
17	Yaw	DG57-0302-1	IMD20098	Angle (deg)
19	Sway POSITION	DV301-0500-111-1110	NRC168567 A54581	Displacement (m)
20	SWAY Velocity	DV301-0500-111-1110	NRC NRC168567 A54581	Velocity (m/s)
21	FWD HEAVE	pt-101-0010-111-1110	A55549 nrc# 168628	Displacement (mm)
22	AFT HEAVE	PT-101-0010-111-1110	A56015 NRC# 168630	Displacement (mm)
25	X	QFLEX QA700 9790700001	13702	Acceleration (m/s^2)
26	Y	QFLEX QA1400 979-1400-001	942 8710	Acceleration (m/s^2)
27	Z	QFLEX QA1400-AA01-01,9791400001	2149	Acceleration (m/s^2)
28	Yaw Rate	Northrop dac7836978	28 nrc 166870	Angular Velocity (deg/s)
33	Carriage position	ITC Carriage A/D output (CnE)	N/A	Displacement (m)
34	Carriage Velocity	Carriage A/D output (CnE)	N/A	Velocity (m/s)
35	Carriage Speed (F/V)	Ono Sokki 132 Wheel en fv801	60302876	Velocity (m/s)

Calibration of ICEDAS Channel 1 — 15:13 09 December 2003

Project: Marine Structural Fragility and Software Validation
Facility: Ice Tank
Sensor: SURGE CENTER
Model: SSB-HN-250
Serial Number: B88024
Programmable Gain: 1
Plug-In Gain: 200
Filter Frequency: 10.0 Hz

Data Point No.	Input Signal (volts)	Physical Value (N)	Fitted Curve Value (N)	Error (N)	
1	5.359	1000.8	1000.9	0.09186	
2	2.971	556.0	555.9	−0.12476	⇐ Maximum Error
3	−0.013	0.0	0.0	−0.02280	
4	−2.996	−556.0	−556.0	0.07465	
5	−5.384	−1000.8	−1000.9	−0.01892	
Maximum Error = −0.00623 % of Calibration Range.					

Definition of Calibration Curve
Polynomial Degree = 1 (Linear Fit)

$$Y = C_0 + C_1 \cdot V$$

where $Y(t)$ = Force (N),
$V(t)$ = input signal at A/D converter (volts),
C_0 = 2.33367 N,
and C_1 = 186.331 N/volt .

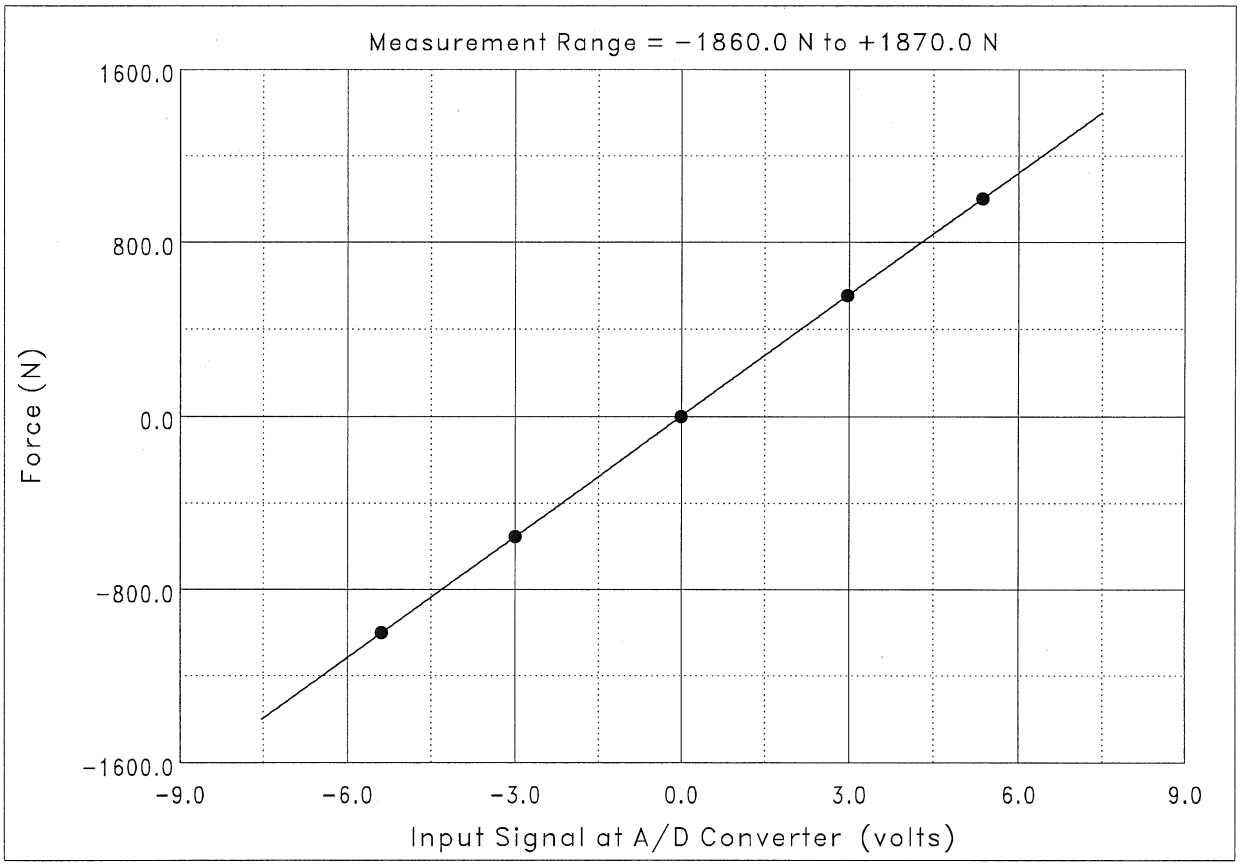

Calibration of ICEDAS Channel 2 — 15:18 09 December 2003

Project: Marine Structural Fragility and Software Validation
Facility: Ice Tank
Sensor: FWD. Sway
Model: SSB-AJ-500
Serial Number: C65397
Programmable Gain: 1
Plug-In Gain: 1000
Filter Frequency: 10.0 Hz

Data Point No.	Input Signal (volts)	Physical Value (N)	Fitted Curve Value (N)	Error (N)	
1	−5.476	−2001.7	−2001.8	−0.11694	
2	−3.052	−1112.1	−1112.1	−0.01477	
3	−0.021	0.0	0.3	0.30813	⇐ Maximum Error
4	3.007	1112.1	1111.9	−0.11487	
5	5.431	2001.7	2001.6	−0.06152	
Maximum Error = 0.00770 % of Calibration Range.					

Definition of Calibration Curve
Polynomial Degree = 1 (Linear Fit)

$$Y = C_0 + C_1 \cdot V$$

where $Y(t)$ = Force (N),
$V(t)$ = input signal at A/D converter (volts),
C_0 = 8.09692 N,
and C_1 = 367.037 N/volt .

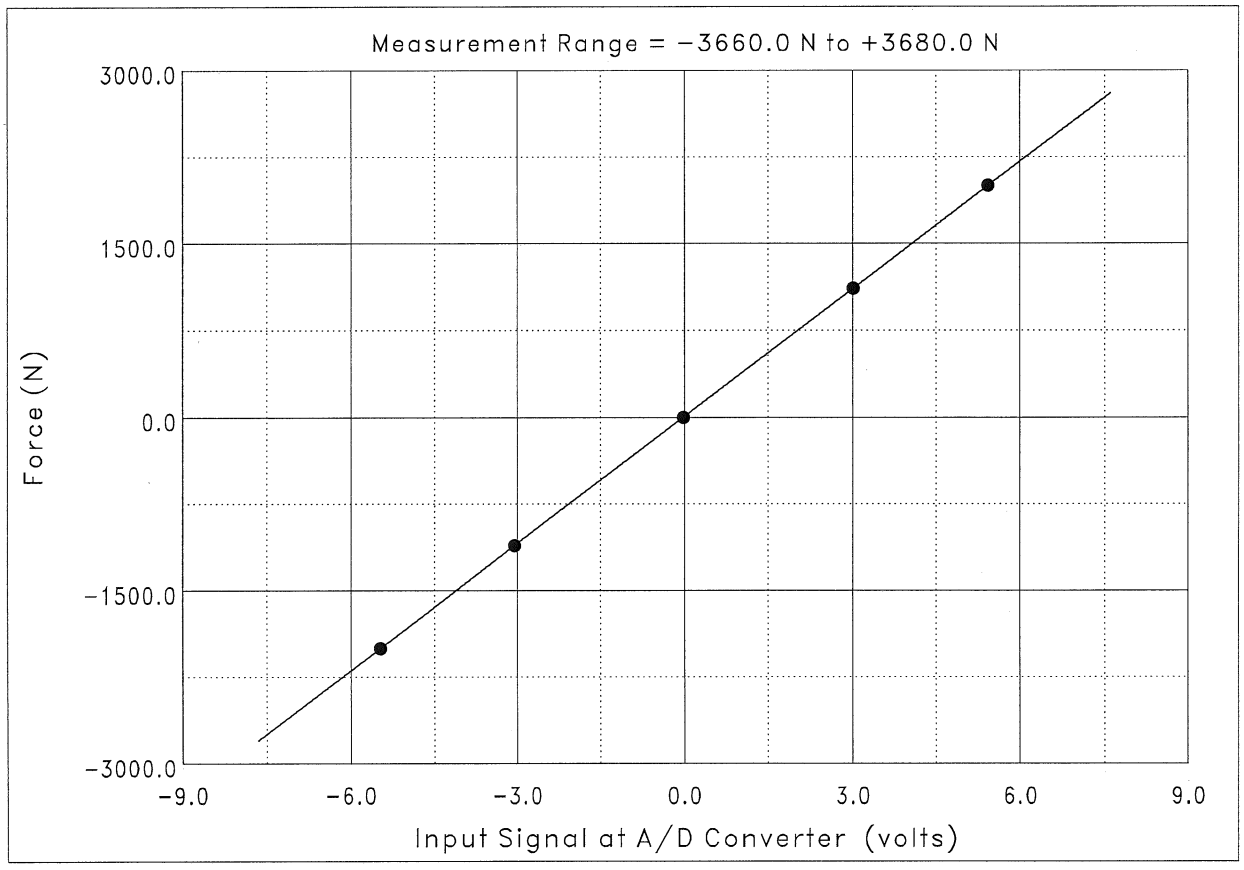

Calibration of ICEDAS Channel 3 — 15:25 09 December 2003

Project: Marine Structural Fragility and Software Validation
Facility: Ice Tank
Sensor: AFT.Sway
Model: SSB-AJ-500
Serial Number: C65391
Programmable Gain: 1
Plug-In Gain: 1000
Filter Frequency: 10.0 Hz

Data Point No.	Input Signal (volts)	Physical Value (N)	Fitted Curve Value (N)	Error (N)	
1	−5.673	2001.7	2001.7	−0.036499	
2	−3.157	1112.1	1112.1	0.023315	
3	−0.011	0.0	0.0	0.042977	⇐ Maximum Error
4	3.134	−1112.1	−1112.1	−0.013672	
5	5.650	−2001.7	−2001.7	−0.015991	
Maximum Error = 0.00107 % of Calibration Range.					

Definition of Calibration Curve
Polynomial Degree = 1 (Linear Fit)

$$Y = C_0 + C_1 \cdot V$$

where $Y(t)$ = Force (N),
$V(t)$ = input signal at A/D converter (volts),
C_0 = −3.99404 N,
and C_1 = −353.556 N/volt .

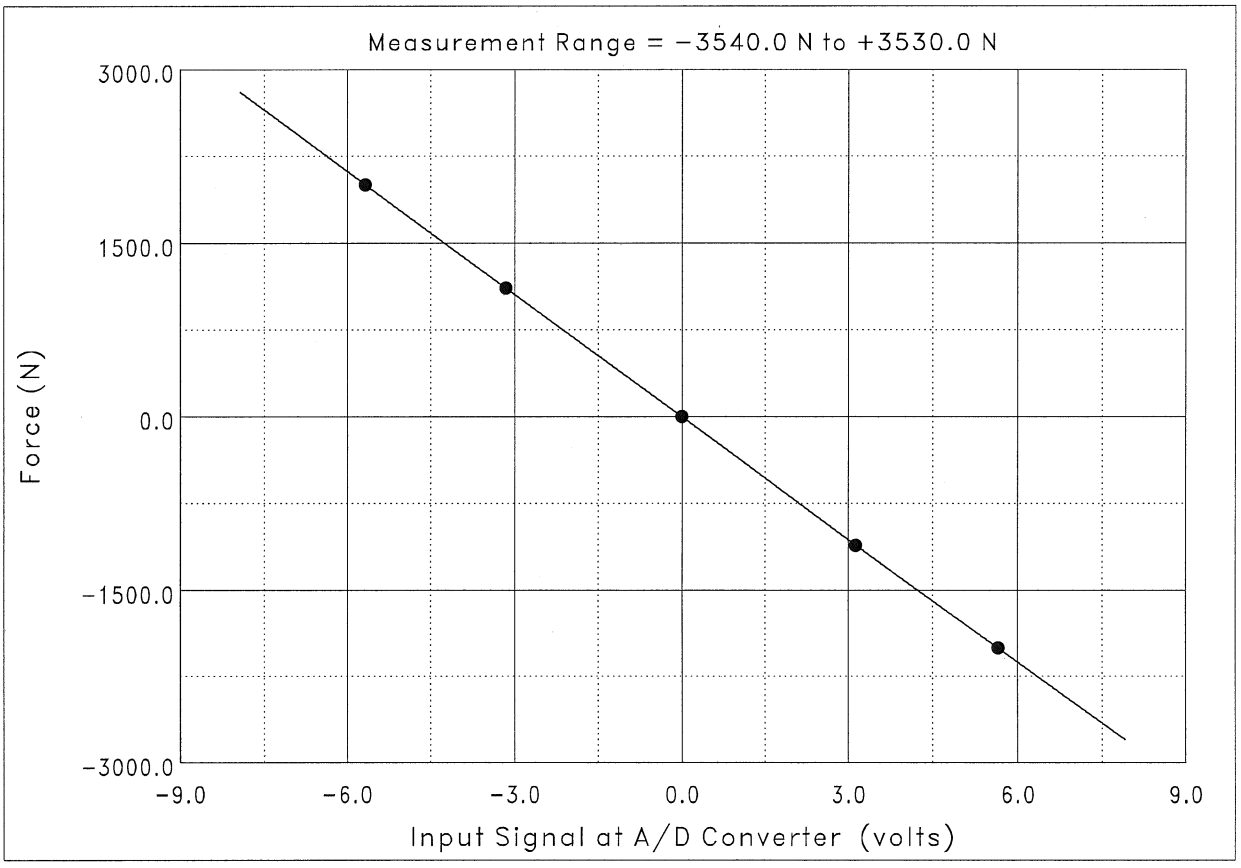

Calibration of ICEDAS Channel 4 — 16:00 09 December 2003

Project: Marine Structural Fragility and Software Validation
Facility: Ice Tank
Sensor: X Inline Load
Model: 60001-100
Serial Number: A10501 S/N 683212
Programmable Gain: 1
Plug-In Gain: 200
Filter Frequency: 10.0 Hz

Data Point No.	Input Signal (volts)	Physical Value (N)	Fitted Curve Value (N)	Error (N)	
1	0.682	0.00	−0.08	−0.08144	
2	1.369	49.03	48.89	−0.14052	
3	2.060	98.07	98.10	0.03813	
4	2.746	147.10	147.00	−0.09511	
5	3.436	196.13	196.18	0.04904	
6	4.129	245.17	245.53	0.36099	
7	4.818	294.20	294.68	0.48422	⇐ Maximum Error
8	5.495	343.23	342.88	−0.35342	
9	6.184	392.27	392.00	−0.26187	
Maximum Error = 0.123 % of Calibration Range.					

Definition of Calibration Curve
Polynomial Degree = 1 (Linear Fit)

$$Y = C_0 + C_1 \cdot V$$

where $Y(t)$ = Force (N),
$V(t)$ = input signal at A/D converter (volts),
C_0 = −48.7054 N,
and C_1 = 71.2668 N/volt .

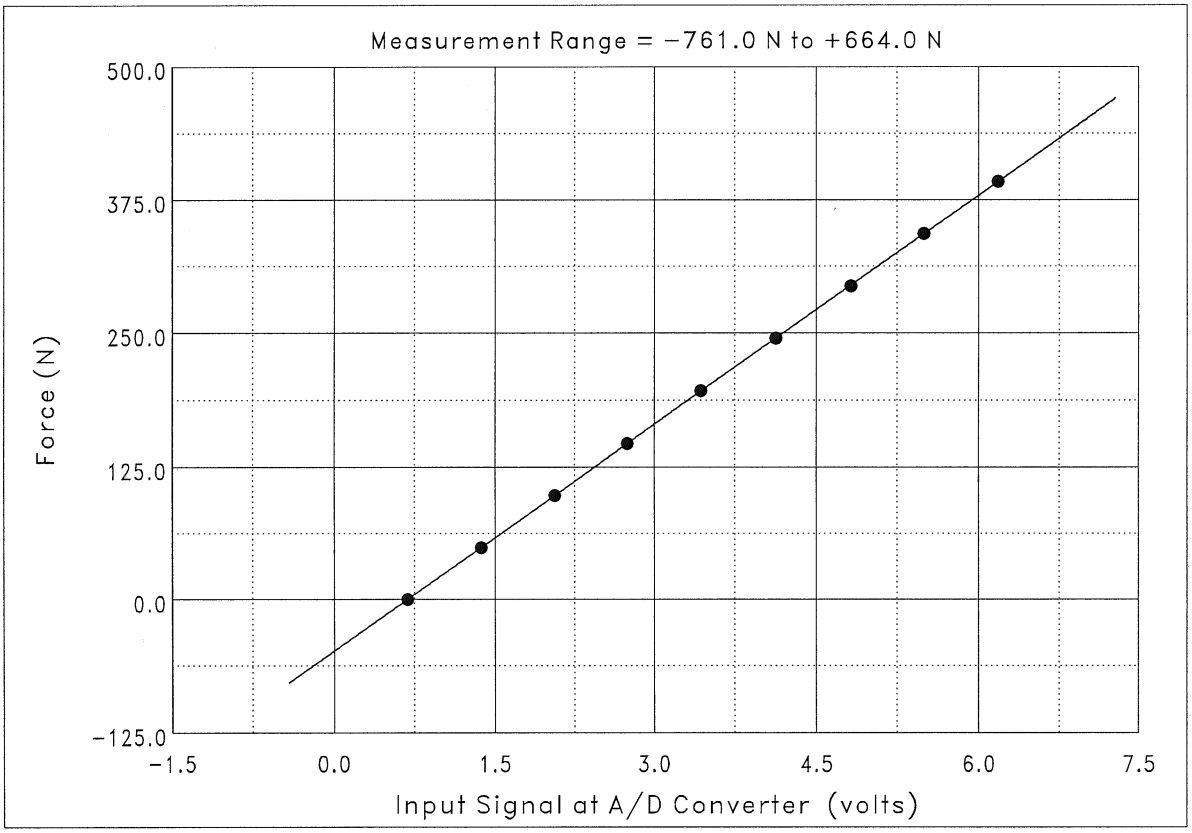

Calibration of ICEDAS Channel 5 16:00 09 December 2003

Project: Marine Structural Fragility and Software Validation **Facility:** Ice Tank

Sensor: Y Inline Load cell **Model:** 6001-100 **Serial Number:** NRC A10500 S/N 00083211

Programmable Gain: 1 **Plug-In Gain:** 200 **Filter Frequency:** 10.0 Hz

Data Point No.	Input Signal (volts)	Physical Value (N)	Fitted Curve Value (N)	Error (N)	
1	0.403	0.00	−0.03	−0.03161	
2	1.043	49.03	49.49	0.45797	⇐ Maximum Error
3	1.668	98.07	97.88	−0.19124	
4	2.301	147.10	146.83	−0.26707	
5	2.935	196.13	195.86	−0.27354	
6	3.573	245.17	245.26	0.09845	
7	4.209	294.20	294.51	0.30521	
8	4.836	343.23	342.96	−0.26959	
9	5.475	392.27	392.44	0.17136	
Maximum Error = 0.117 % of Calibration Range.					

Definition of Calibration Curve

Polynomial Degree = 1 (Linear Fit)

$$Y = C_0 + C_1 \cdot V$$

where $Y(t)$ = Force (N),
$V(t)$ = input signal at A/D converter (volts),
C_0 = −31.2063 N,
and C_1 = 77.3780 N/volt .

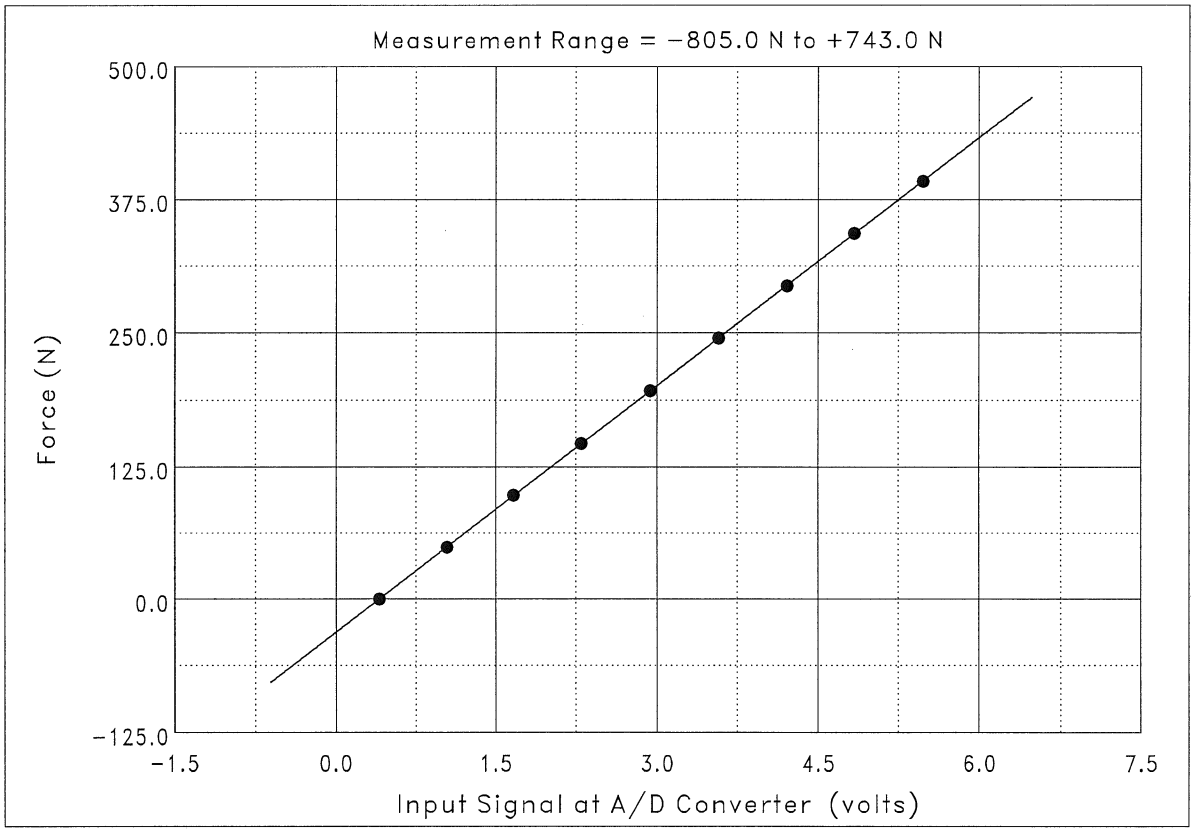

Calibration of ICEDAS Channel 17 16:58 11 December 2003

Project: Marine Structural Fragility and Software Validation **Facility:** Ice Tank

Sensor: Yaw **Model:** DG57-0302-1 **Serial Number:** IMD20098

Programmable Gain: 1 **Plug-In Gain:** 1 **Filter Frequency:** 10.0 Hz

Data Point No.	Input Signal (volts)	Physical Value (deg)	Fitted Curve Value (deg)	Error (deg)	
1	2.895	−90.000	−90.025	−0.02460	
2	4.180	−45.000	−44.884	0.11562	⇐ Maximum Error
3	5.455	0.000	−0.094	−0.09433	
4	6.737	45.000	44.941	−0.05917	
5	8.021	90.000	90.062	0.06245	
Maximum Error = 0.0642 % of Calibration Range.					

Definition of Calibration Curve
Polynomial Degree = 1 (Linear Fit)

$$Y = C_0 + C_1 \cdot V$$

where $Y(t)$ = Angle (deg),
$V(t)$ = input signal at A/D converter (volts),
C_0 = −191.706 deg,
and C_1 = 35.1274 deg/volt .

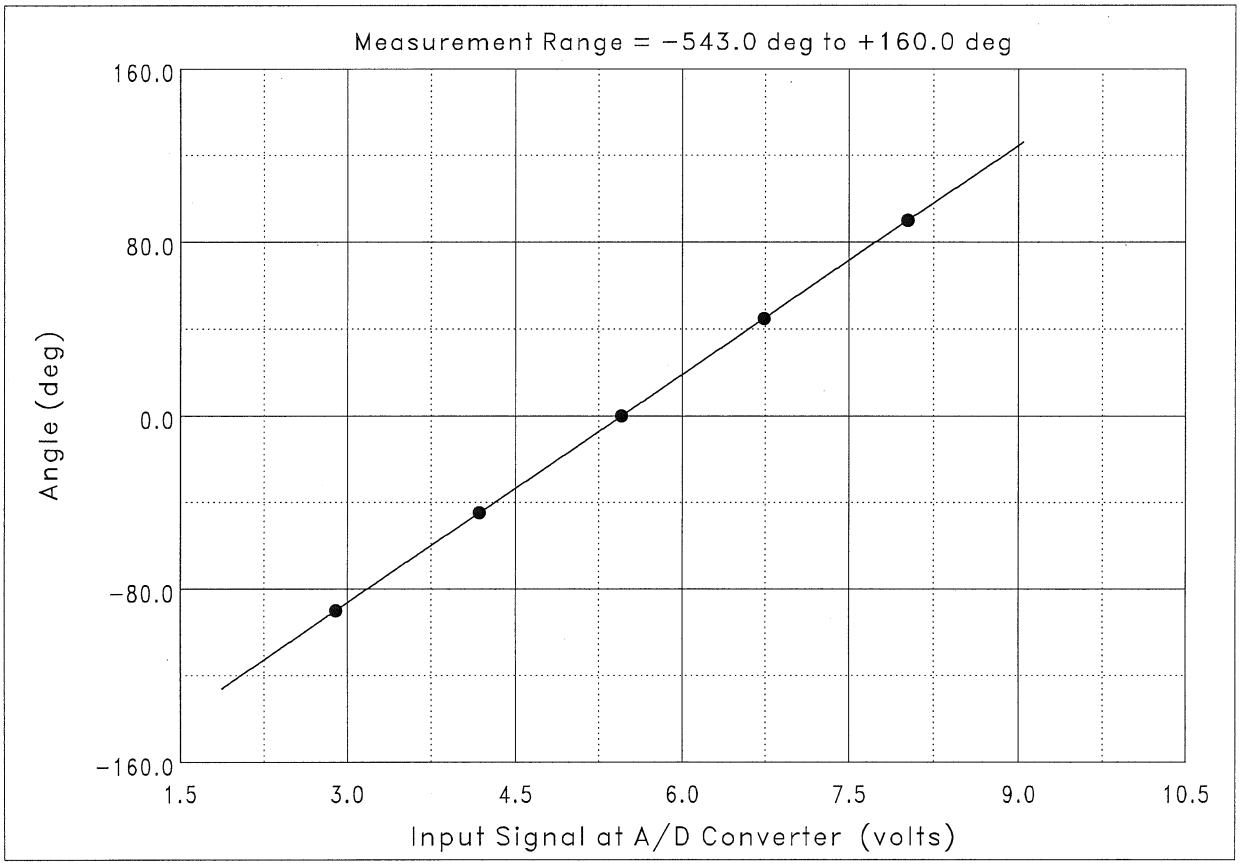

Calibration of ICEDAS Channel 19 — 09:50 10 December 2003

Project: Marine Structural Fragility and Software Validation **Facility:** Ice Tank

Sensor: Sway POSITION **Model:** DV301-0500-111-1110 **Serial Number:** NRC168567 A54581

Programmable Gain: 1

Data Point No.	Input Signal (volts)	Physical Value (m)	Fitted Curve Value (m)	Error (m)	
1	0.538	−3.5000	−3.4997	0.0003138	
2	0.920	−3.0000	−3.0016	−0.0016077	
3	2.073	−1.5000	−1.4982	0.0018070	⇐ Maximum Error
4	3.222	0.0000	−0.0008	−0.0008292	
5	4.374	1.5000	1.5007	0.0006876	
6	4.758	2.0000	2.0013	0.0013289	
7	5.140	2.5000	2.4988	−0.0012407	
8	5.907	3.5000	3.4995	−0.0004606	
Maximum Error = 0.0258 % of Calibration Range.					

Definition of Calibration Curve
Polynomial Degree = 1 (Linear Fit)

$$Y = C_0 + C_1 \cdot V$$

where $Y(t)$ = Displacement (m),
$V(t)$ = input signal at A/D converter (volts),
C_0 = −4.20079 m,
and C_1 = 1.30351 m/volt .

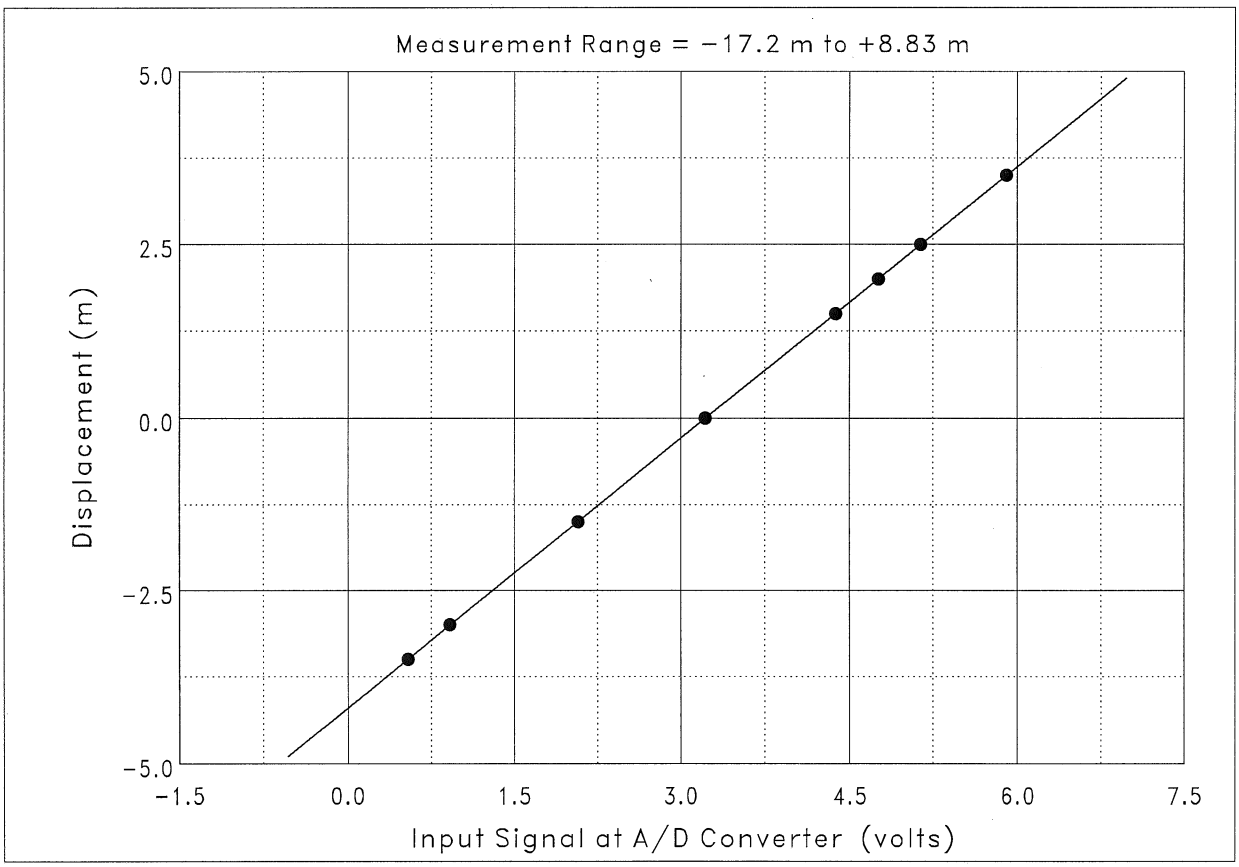

Calibration of ICEDAS Channel 20 10:20 03 November 2003

Project: Marine Structural Fragility and Software Validation **Facility:** Ice Tank

Sensor: SWAY Velocity **Model:** DV301-0500-111-1110 **Serial Number:** NRC NRC168567 A54581

Programmable Gain: 1

Data Point No.	Input Signal (volts)	Physical Value (m/s)	Fitted Curve Value (m/s)	Error (m/s)	
1	−0.008	0.00000	0.00015	0.00014710	
2	−0.850	−0.10000	−0.10049	−0.00048641	
3	0.830	0.10000	0.10043	0.00042554	
4	−0.175	−0.02000	−0.01981	0.00018959	
5	−0.566	−0.06700	−0.06657	0.00043124	
6	0.185	0.02300	0.02324	0.00023602	
7	0.563	0.06950	0.06856	−0.00094309	⇐ Maximum Error
Maximum Error = −0.472 % of Calibration Range.					

Definition of Calibration Curve

Polynomial Degree = 1 (Linear Fit)

$$Y = C_0 + C_1 \cdot V$$

where $Y(t)$ = Velocity (m/s),
$V(t)$ = input signal at A/D converter (volts),
C_0 = 0.00116103 m/s,
and C_1 = 0.119639 (m/s)/volt .

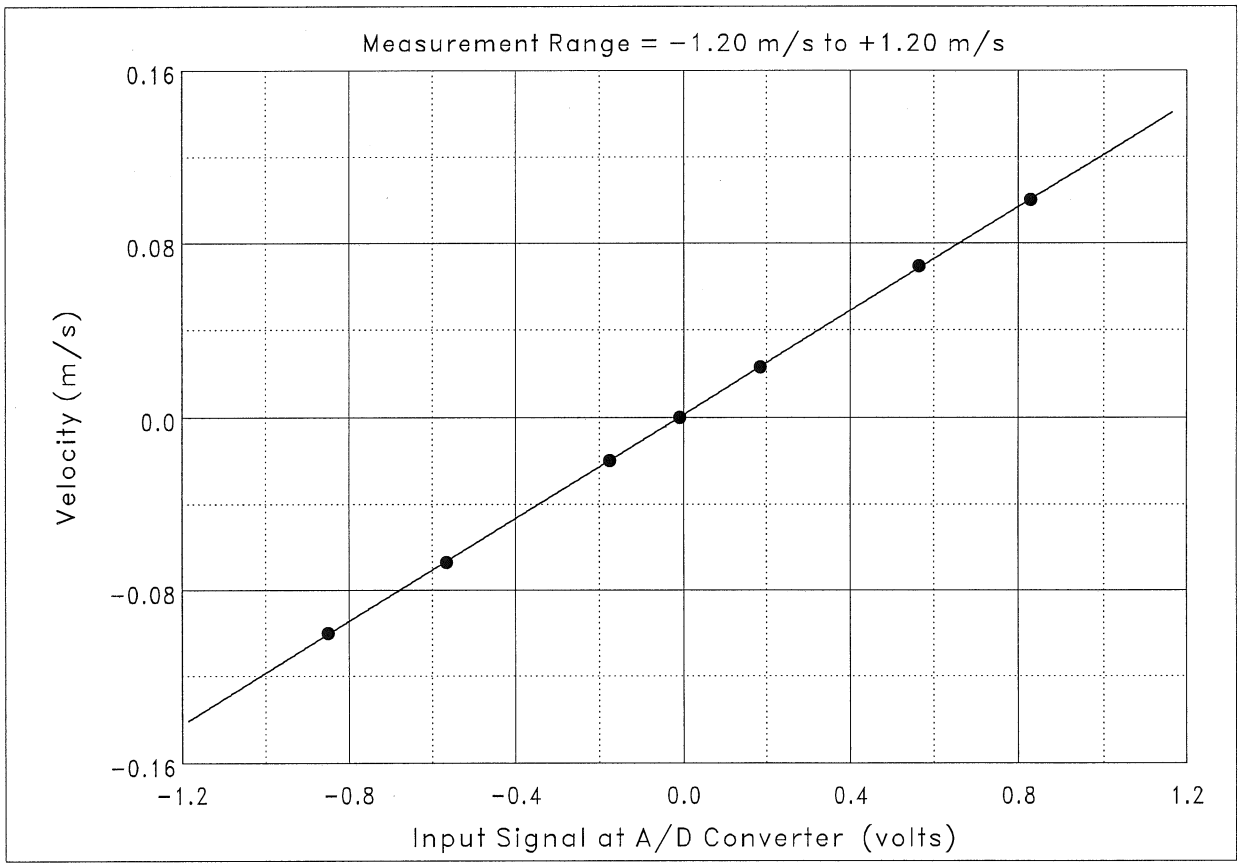

Calibration of ICEDAS Channel 21 — 08:48 10 December 2003

Project: Marine Structural Fragility and Software Validation **Facility:** Ice Tank

Sensor: FWD HEAVE **Model:** pt-101-0010-111-1110 **Serial Number:** a55549 nrc# 168628

Programmable Gain: 1 **Plug-In Gain:** 1 **Filter Frequency:** 10.0 Hz

Data Point No.	Input Signal (volts)	Physical Value (mm)	Fitted Curve Value (mm)	Error (mm)	
1	0.828	0.00	0.17	0.17174	
2	1.734	50.00	49.94	−0.05975	
3	2.652	100.00	100.29	0.29124	
4	3.551	150.00	149.65	−0.34860	
5	4.455	200.00	199.23	−0.76944	⇐ Maximum Error
6	5.393	250.00	250.71	0.71478	
Maximum Error = −0.308 % of Calibration Range.					

Definition of Calibration Curve

Polynomial Degree = 1 (Linear Fit)

$$Y = C_0 + C_1 \cdot V$$

where $Y(t)$ = Displacement (mm),
$V(t)$ = input signal at A/D converter (volts),
C_0 = −45.2486 mm,
and C_1 = 54.8830 mm/volt .

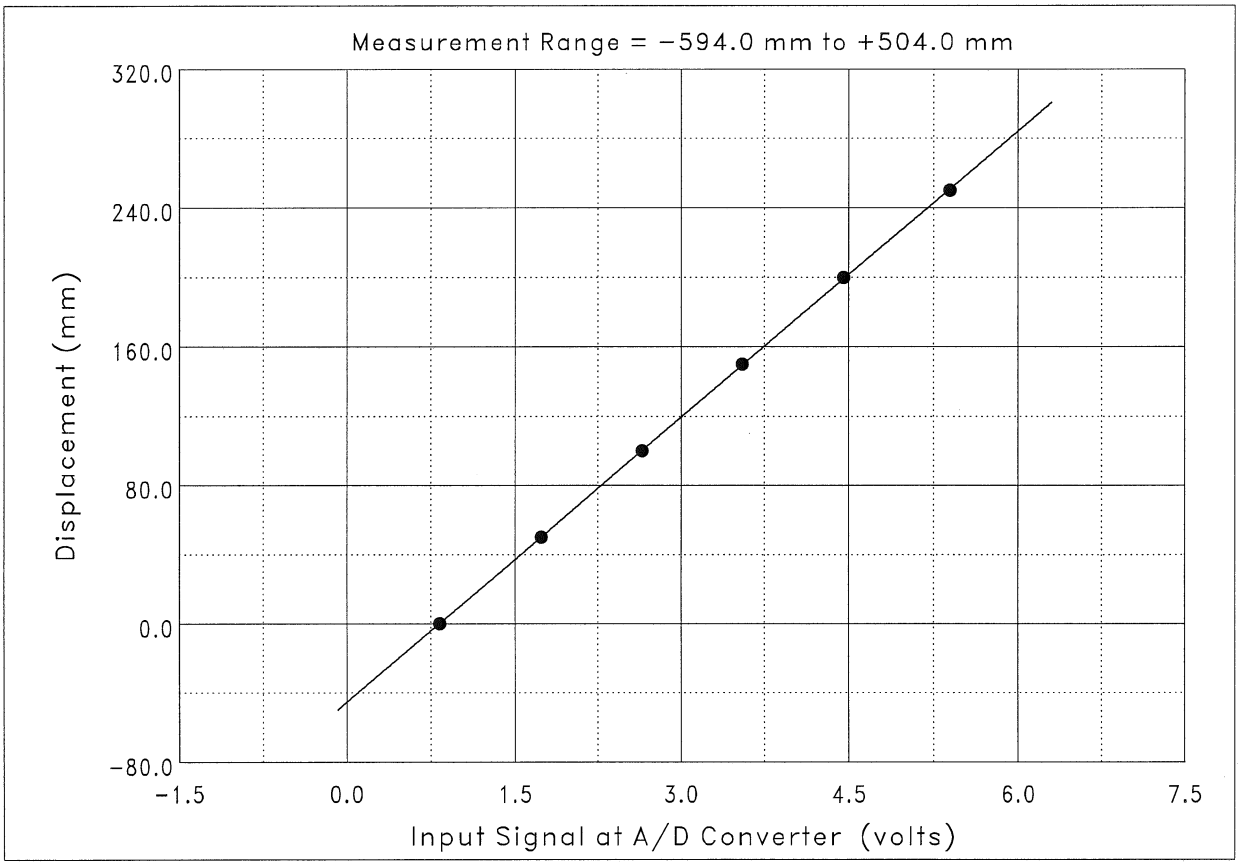

Calibration of ICEDAS Channel 22 — 08:51 10 December 2003

Project: Marine Structural Fragility and Software Validation
Facility: Ice Tank
Sensor: AFT HEAVE
Model: PT101-0010-111-1110
Serial Number: A56015 NRC# 168630
Programmable Gain: 1
Plug-In Gain: 1
Filter Frequency: 10.0 Hz

Data Point No.	Input Signal (volts)	Physical Value (mm)	Fitted Curve Value (mm)	Error (mm)	
1	0.765	0.00	0.69	0.6947	
2	1.674	50.00	50.00	0.0023	
3	2.591	100.00	99.71	−0.2868	
4	3.509	150.00	149.52	−0.4821	
5	4.411	200.00	198.46	−1.5424	
6	5.391	250.00	251.61	1.6143	⇐ Maximum Error
Maximum Error = 0.646 % of Calibration Range.					

Definition of Calibration Curve
Polynomial Degree = 1 (Linear Fit)

$$Y = C_0 + C_1 \cdot V$$

where $Y(t)$ = Displacement (mm),
$V(t)$ = input signal at A/D converter (volts),
C_0 = −40.7959 mm,
and C_1 = 54.2361 mm/volt .

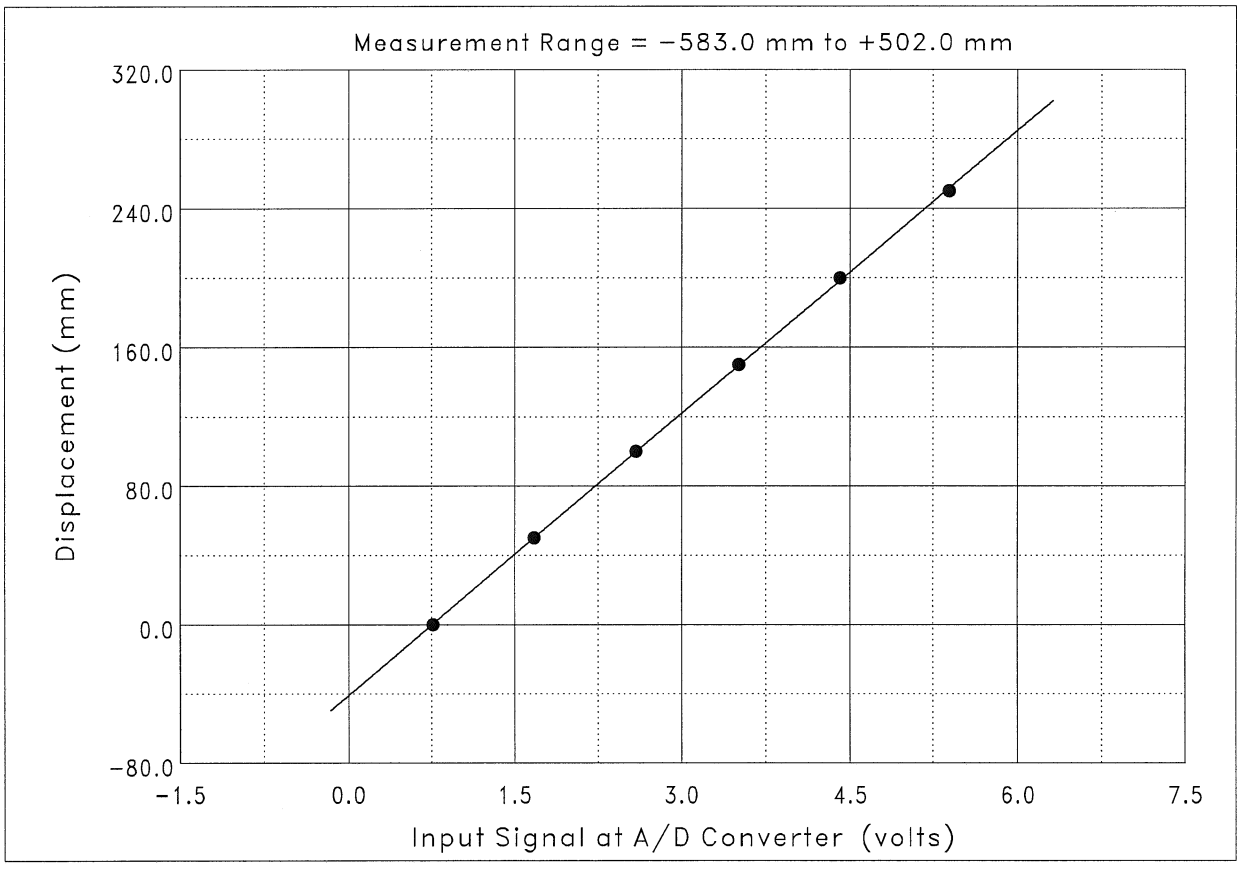

Calibration of ICEDAS Channel 25 14:19 09 December 2003

Project: Marine Structural Fragility and Software Validation **Facility:** Ice Tank

Sensor: X **Model:** QFLEX QA700 9790700001 **Serial Number:** 13702

Programmable Gain: 1 **Plug-In Gain:** 1 **Filter Frequency:** 10.0 Hz

Data Point No.	Input Signal (volts)	Physical Value (m/s**2)	Fitted Curve Value (m/s**2)	Error (m/s**2)	
1	−0.016	0.0000	0.0033	0.0033010	⇐ Maximum Error
2	−4.486	9.8080	9.8063	−0.0016508	
3	4.458	−9.8080	−9.8096	−0.0016499	
Maximum Error = 0.0168 % of Calibration Range.					

Definition of Calibration Curve

Polynomial Degree = 1 (Linear Fit)

$$Y = C_0 + C_1 \cdot V$$

where $Y(t)$ = Acceleration (m/s**2),
$V(t)$ = input signal at A/D converter (volts),
C_0 = −0.0326240 m/s**2,
and C_1 = −2.19335 (m/s**2)/volt .

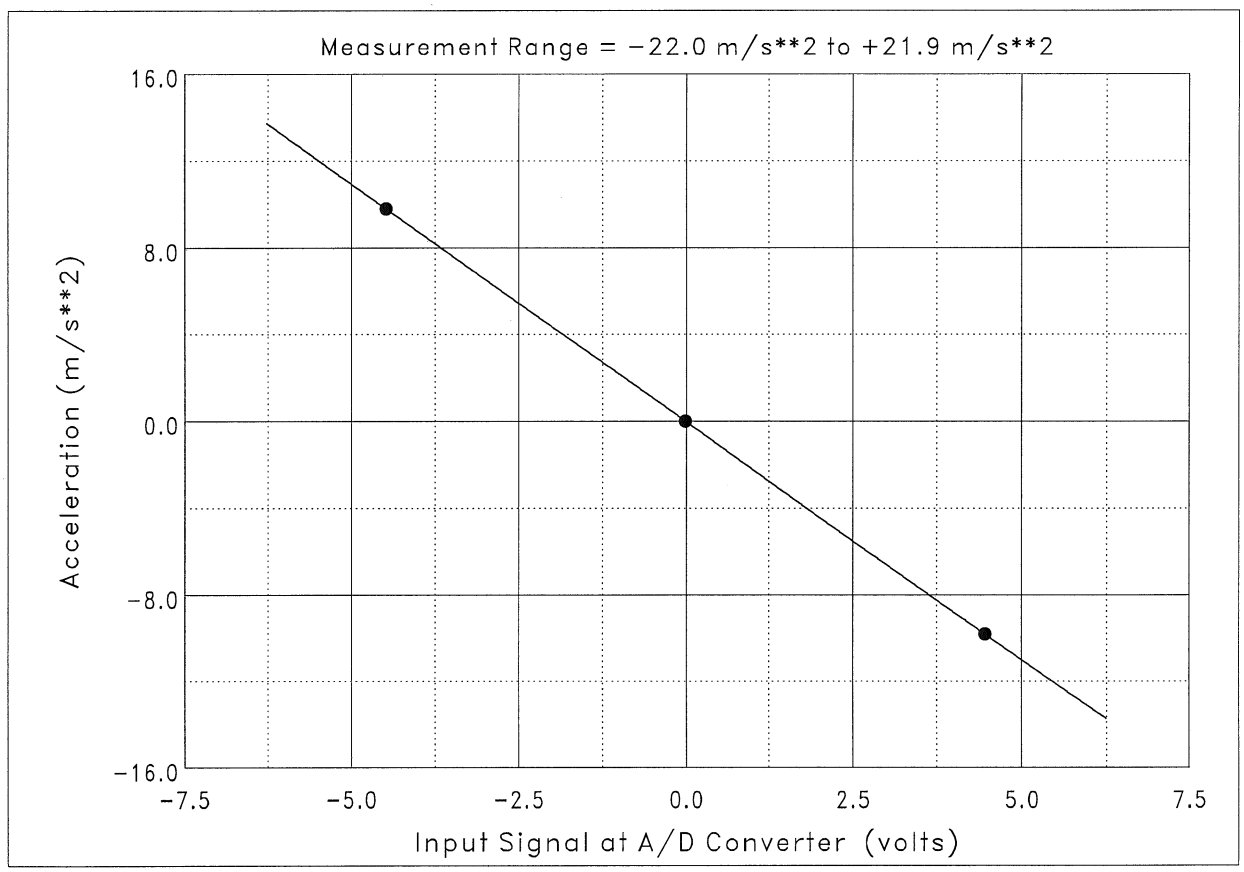

Calibration of ICEDAS Channel 26 14:15 09 December 2003

Project: Marine Structural Fragility and Software Validation **Facility:** Ice Tank

Sensor: Y **Model:** QFLEX QA1400 979-1400-001 **Serial Number:** 942 8710

Programmable Gain: 1 **Plug-In Gain:** 1 **Filter Frequency:** 10.0 Hz

Data Point No.	Input Signal (volts)	Physical Value (m/s**2)	Fitted Curve Value (m/s**2)	Error (m/s**2)	
1	−0.013	0.0000	−0.0043	−0.0043424	⇐ Maximum Error
2	4.507	9.8080	9.8102	0.0021696	
3	−4.526	−9.8080	−9.8058	0.0021734	
Maximum Error = −0.0221 % of Calibration Range.					

Definition of Calibration Curve

Polynomial Degree = 1 (Linear Fit)

$$Y = C_0 + C_1 \cdot V$$

where $Y(t)$ = Acceleration (m/s**2),
$V(t)$ = input signal at A/D converter (volts),
C_0 = 0.0230729 m/s**2,
and C_1 = 2.17172 (m/s**2)/volt .

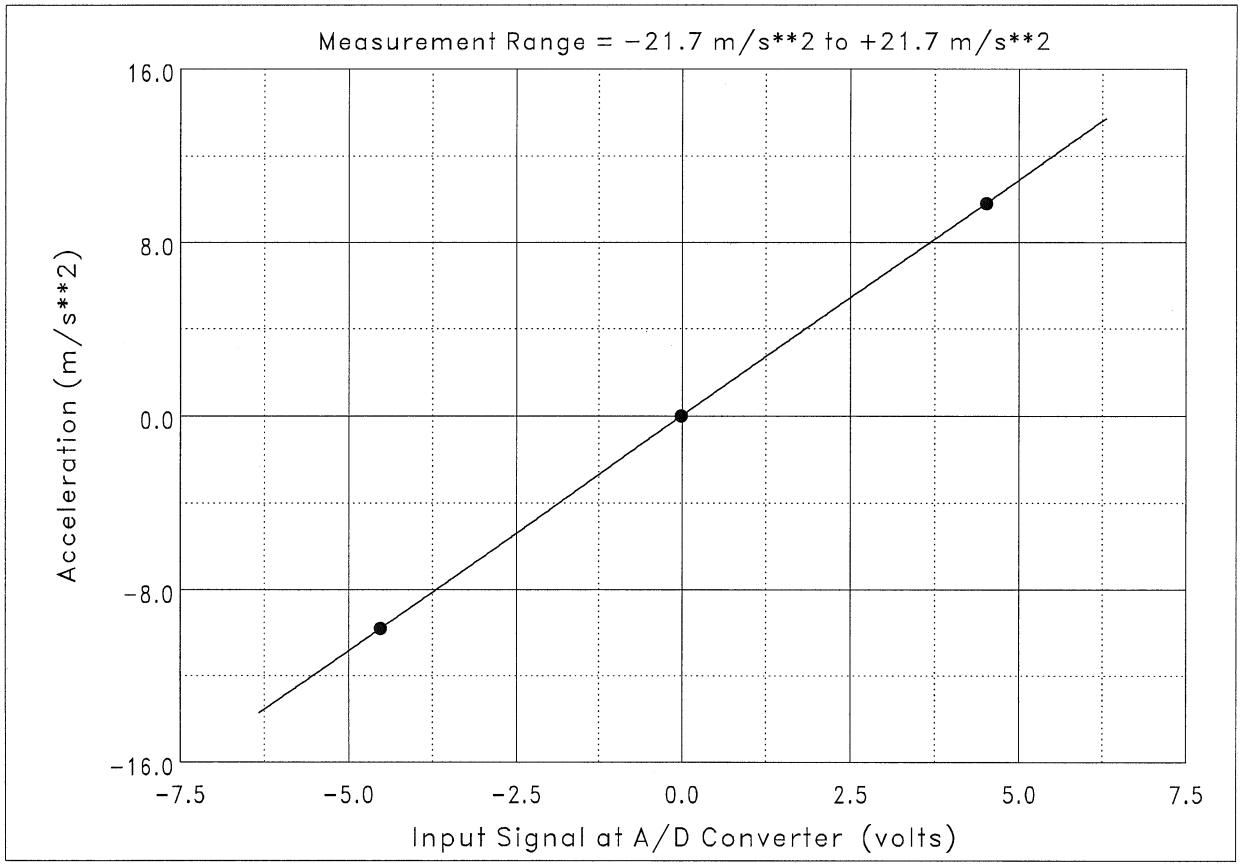

Calibration of ICEDAS Channel 27 — 14:30 09 December 2003

Project: Marine Structural Fragility and Software Validation **Facility:** Ice Tank

Sensor: Z **Model:** QFLEX QA1400-AA01-01,9791400001 **Serial Number:** 2149

Programmable Gain: 1 **Plug-In Gain:** 1 **Filter Frequency:** 10.0 Hz

Data Point No.	Input Signal (volts)	Physical Value (m/s**2)	Fitted Curve Value (m/s**2)	Error (m/s**2)	
1	−0.007	0.0000	−0.0070	−0.0070275	⇐ Maximum Error
2	4.514	9.8080	9.8115	0.0035105	
3	−4.519	−9.8080	−9.8045	0.0035181	
Maximum Error = −0.0358 % of Calibration Range.					

Definition of Calibration Curve

Polynomial Degree = 1 (Linear Fit)

$$Y = C_0 + C_1 \cdot V$$

where $Y(t)$ = Acceleration (m/s**2),
$V(t)$ = input signal at A/D converter (volts),
C_0 = 0.00879919 m/s**2,
and C_1 = 2.17170 (m/s**2)/volt .

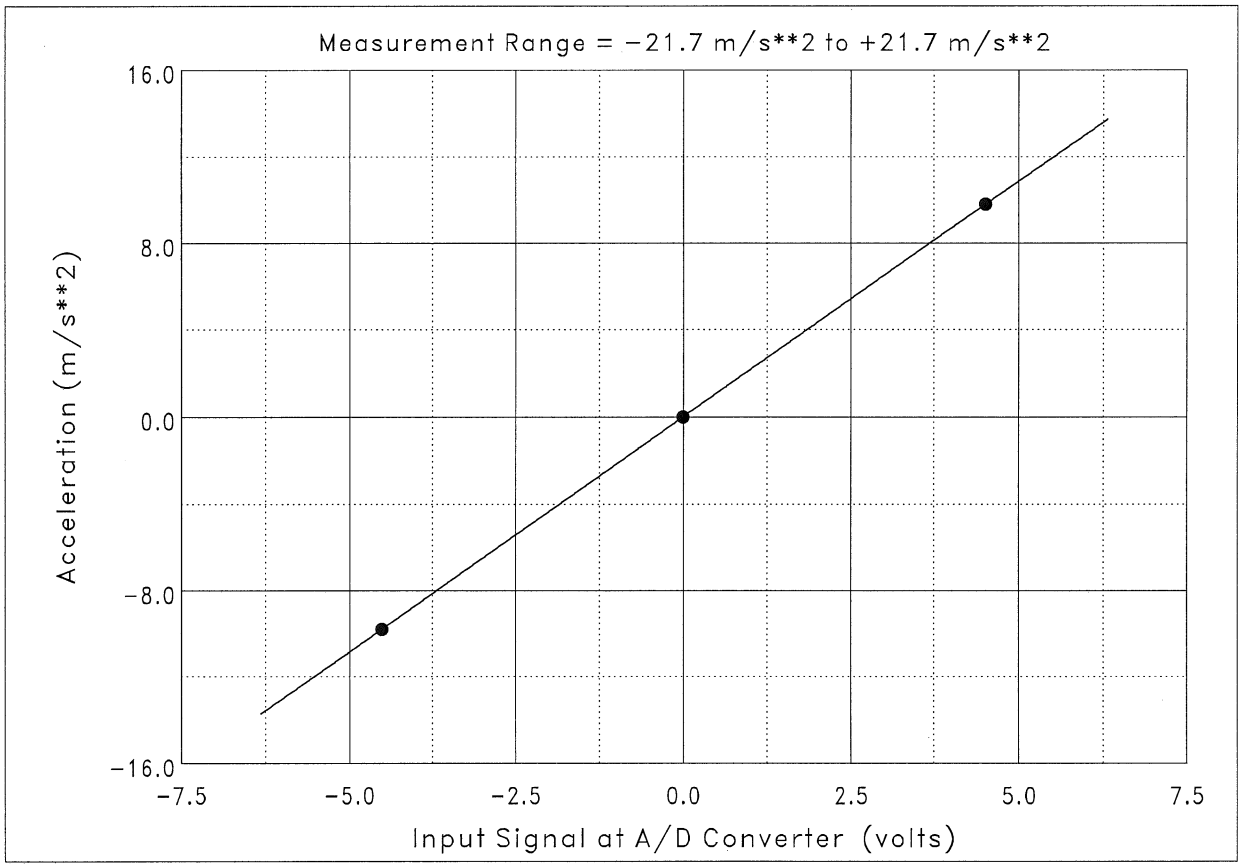

Calibration of ICEDAS Channel 28 16:29 12 December 2003

Project: Marine Structural Fragility and Software Validation **Facility:** Ice Tank

Sensor: Yaw Rate **Model:** Northrop dac7836978 **Serial Number:** 28 nrc 166870

Programmable Gain: 2 **Plug-In Gain:** 1 **Filter Frequency:** 10.0 Hz

Data Point No.	Input Signal (volts)	Physical Value (deg/s)	Fitted Curve Value (deg/s)	Error (deg/s)	
1	4.980	0.0000	0.0104	0.010433	
2	5.031	0.2000	0.2175	0.017508	
3	5.106	0.5000	0.5217	0.021727	
4	5.234	1.0000	1.0474	0.047403	
5	4.720	−1.0000	−1.0509	−0.050898	⇐ Maximum Error
6	4.849	−0.5000	−0.5270	−0.027029	
7	4.926	−0.2000	−0.2132	−0.013173	
8	4.489	−2.0000	−1.9942	0.005789	
9	5.464	2.0000	1.9860	−0.013994	
10	4.618	−1.5000	−1.4661	0.033871	
11	5.338	1.5000	1.4684	−0.031631	
Maximum Error = −1.27 % of Calibration Range.					

Definition of Calibration Curve
Polynomial Degree = 1 (Linear Fit)

$$Y = C_0 + C_1 \cdot V$$

where $Y(t)$ = Angular Velocity (deg/s),
$V(t)$ = input signal at A/D converter (volts),
C_0 = −20.3109 deg/s,
and C_1 = 4.08033 (deg/s)/volt .

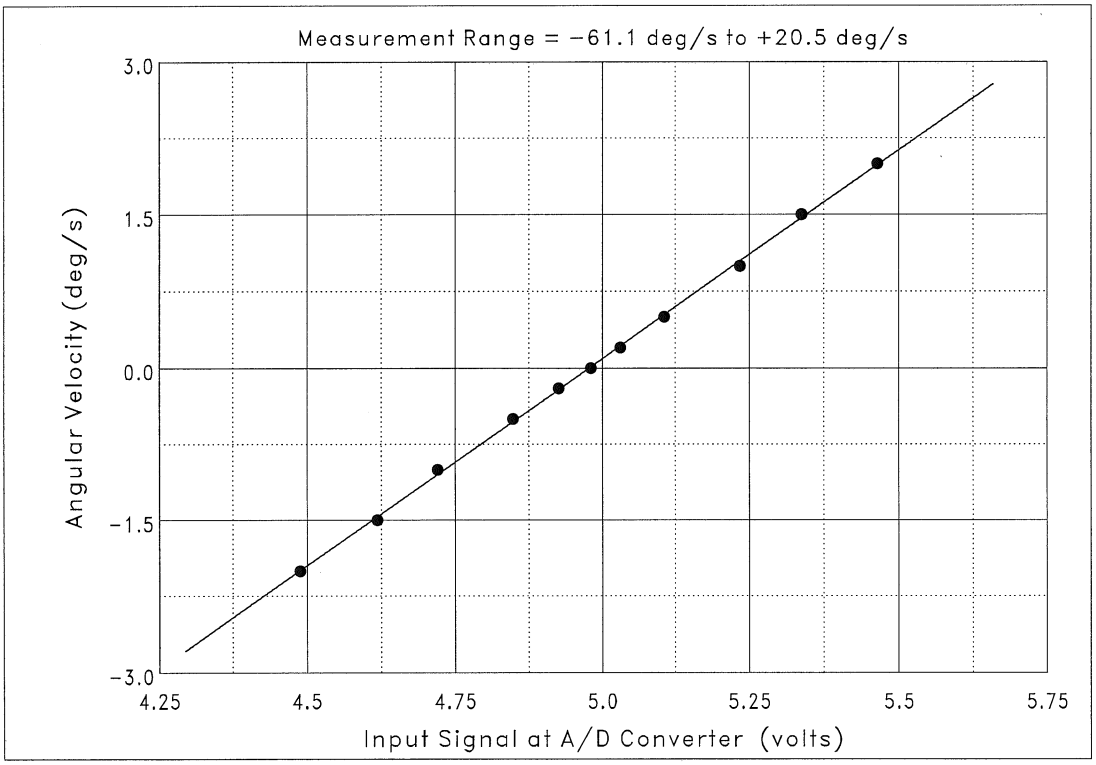

Calibration of ICEDAS Channel 33 12:10 19 November 2003

Project: Marine Structural Fragility and Software Validation **Facility:** Ice Tank

Sensor: Carriage position **Model:** ITC Carriage A/D output (CnE) **Serial Number:** N/A

Programmable Gain: 1 **Plug-In Gain:** 1 **Filter Frequency:** 10.0 Hz

Data Point No.	Input Signal (volts)	Physical Value (m)	Fitted Curve Value (m)	Error (m)	
1	−7.319	9.999	9.993	−0.0063848	
2	−4.664	19.996	20.006	0.0095901	⇐ Maximum Error
3	0.632	39.986	39.983	−0.0032005	
Maximum Error = 0.0320 % of Calibration Range.					

Definition of Calibration Curve
Polynomial Degree = 1 (Linear Fit)

$$Y = C_0 + C_1 \cdot V$$

where $Y(t)$ = Displacement (m),
$V(t)$ = input signal at A/D converter (volts),
C_0 = 37.6003 m,
and C_1 = 3.77227 m/volt .

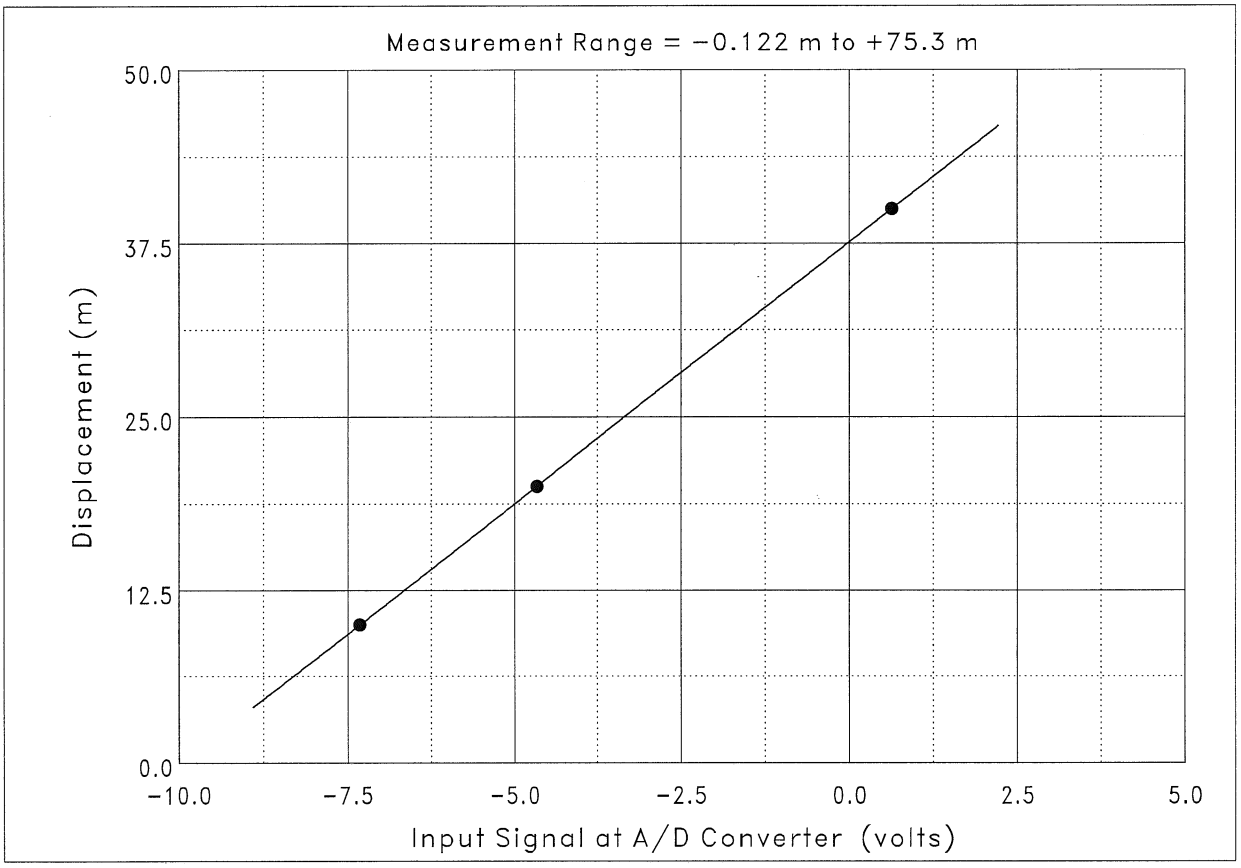

Calibration of ICEDAS Channel 34 — 15:54 10 December 2003

Project: Marine Structural Fragility and Software Validation
Facility: Ice Tank
Sensor: Carriage Velocity
Model: Carriage A/D Output (CnE)
Serial Number: N/A
Programmable Gain: 1
Plug-In Gain: 1
Filter Frequency: 10.0 Hz

Data Point No.	Input Signal (volts)	Physical Value (m/s)
1	−6.010	0.0000
2	−0.011	1.5000

Definition of Calibration Curve
Polynomial Degree = 1 (Linear Fit)

$$Y = C_0 + C_1 \cdot V$$

where $Y(t)$ = Velocity (m/s),
$V(t)$ = input signal at A/D converter (volts),
C_0 = 1.50263 m/s,
and C_1 = 0.250007 (m/s)/volt .

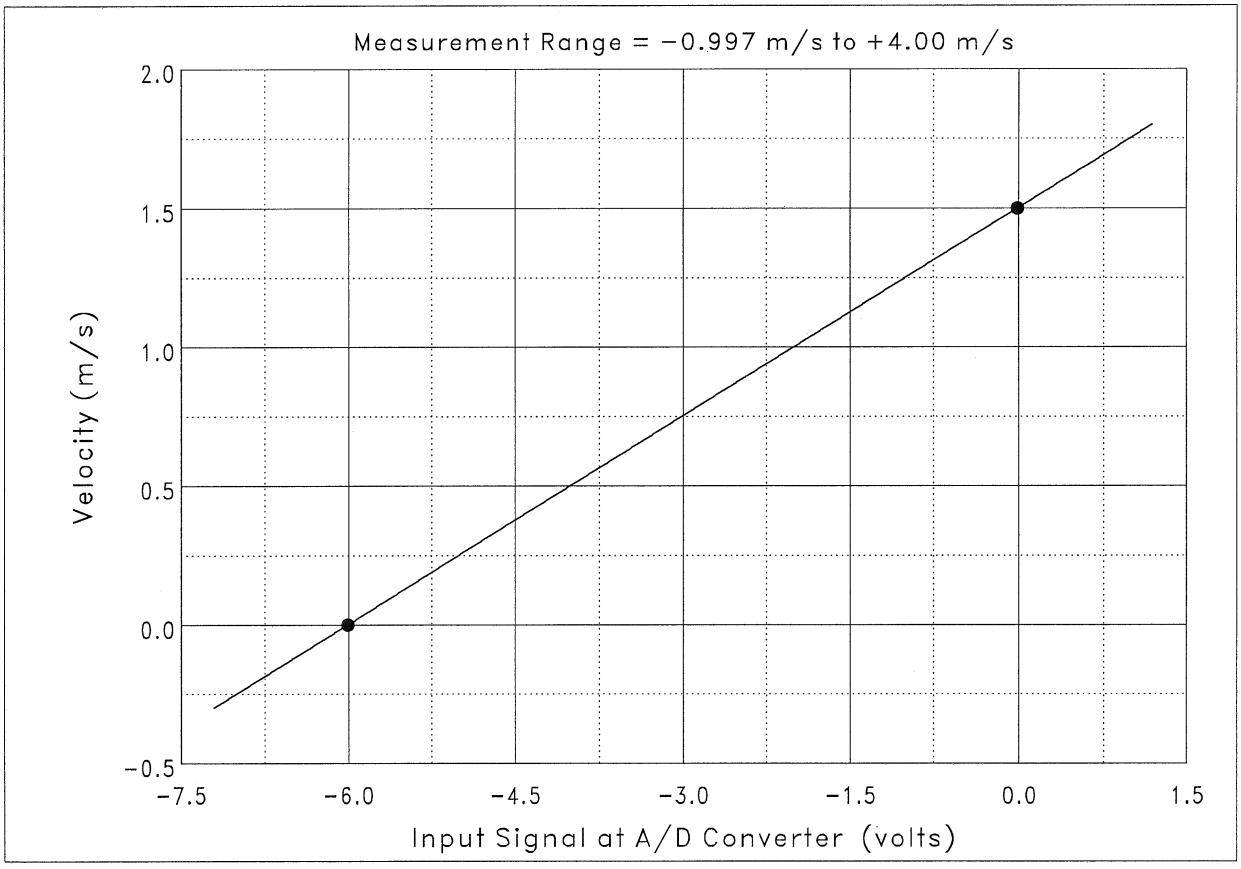

Calibration of ICEDAS Channel 35 11:24 27 November 2003

Project: Marine Structural Fragility and Software Validation **Facility:** Ice Tank

Sensor: Carriage Speed (F/V) **Model:** Ono Sokki 132 Wheel en fv801 **Serial Number:** 60302876

Programmable Gain: 1 **Plug-In Gain:** 1 **Filter Frequency:** 100.0 Hz

Data Point No.	Input Signal (volts)	Physical Value (m/s)	Fitted Curve Value (m/s)	Error (m/s)	
1	0.095	0.0250	0.0253	0.00026187	
2	4.979	1.0000	1.0001	0.00012660	
3	2.471	0.5000	0.4996	−0.00044927	⇐ Maximum Error
4	7.484	1.5000	1.5001	0.00006080	
Maximum Error = −0.0305 % of Calibration Range.					

Definition of Calibration Curve
Polynomial Degree = 1 (Linear Fit)

$$Y = C_0 + C_1 \cdot V$$

where $Y(t)$ = Velocity (m/s),
$V(t)$ = input signal at A/D converter (volts),
C_0 = 0.00628002 m/s,
and C_1 = 0.199592 (m/s)/volt .

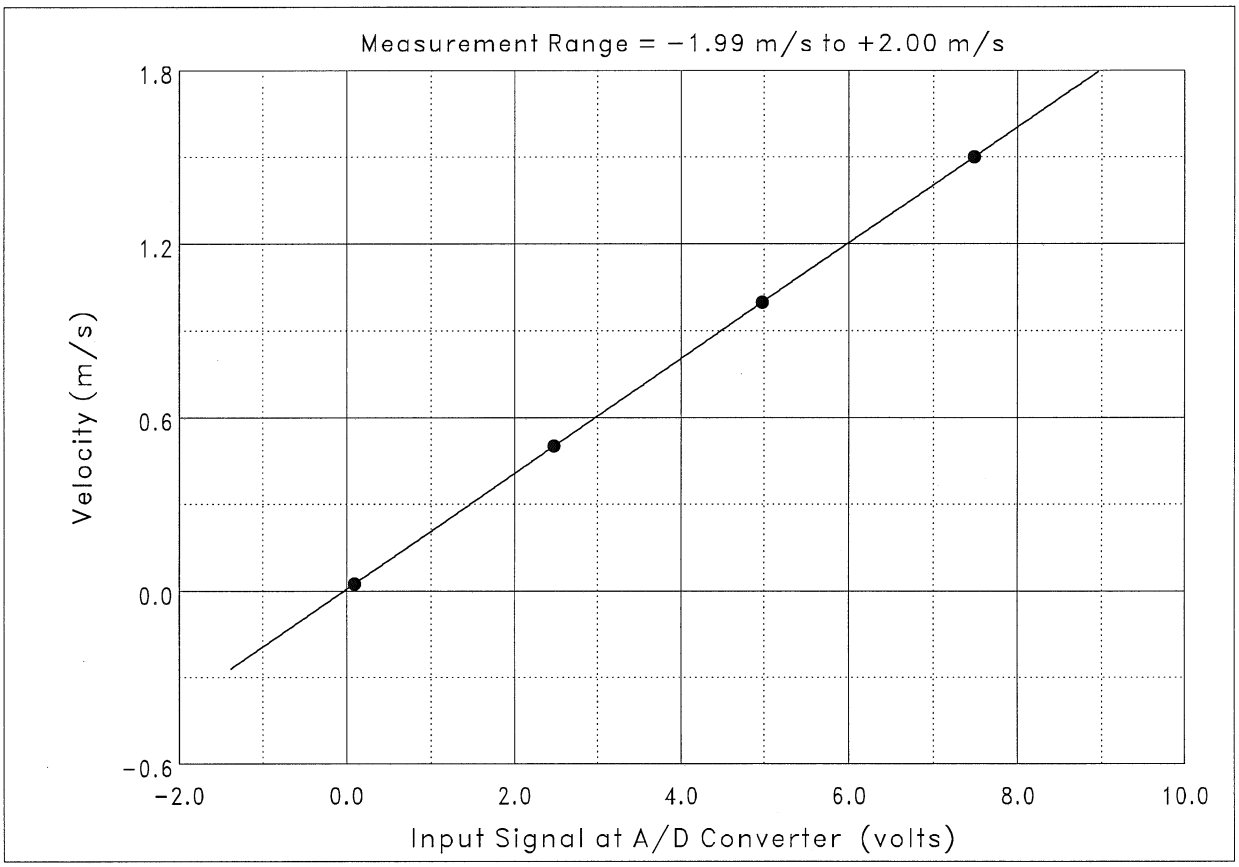

Appendix C

Ice Sheet Summaries

NRC - INSTITUTE FOR MARINE DYNAMICS

ARCTIC VESSEL RESEARCH SECTION

ICE MECHANICAL PROPERTIES SUMMARY

Test Name: NMS1 Project Number: 953

Warm up commenced: 23:00 14-DEC-2003

Time	Warm-up hrs	Loc	hi mm	Sf kPa	Lc cm	E MPa	E/Sf	Lc/hi	K1c N/m	Sf/K1c m-.5	Sc/s kPa	Rhoi Mg/m3
0820	9.33	N	39.3± 0.6 n= 3									
		S	40.5± 3.8 n= 3									
0834	9.57	40N	40.4		63.	258.6	3881	15.7				
0855	9.92	40S	38.8	49.± 4.7								
			38.5	30.(u/d 61%)								
0905	10.08	40N	39.4	64.± 1.4								
			39.4	41.(u/d 63%)								
1025	11.42	38N	39.9	53.± 3.3								
			40.5	29.(u/d 54%)								
1030	11.50	38S	39.1	48.± 3.0								
			38.3	34.(u/d 70%)								
1138	12.63	39N	40.1	47.± 6.3								
			39.9	24.(u/d 50%)								
1142	12.70	39S	38.5	37.± 1.3								
			38.5	28.(u/d 74%)								
1215	13.25	N	40.9± 1.3 n=32									
		S	40.2± 1.2 n=32									
1355	14.92	N	39.3± 1.5 n=33									
		S	39.1± 1.4 n=33									
1415	15.25	35N	40.0	42.±10.6								
			40.0	18.(u/d 43%)								
1420	15.33	35S	37.8	24.± 3.4								
			38.8	12.(u/d 48%)								
1433	15.55	66N	36.4									.841
1435	15.58	66S	35.7									.906

Run #	Date	Time	Hours from Warm-up	Flexural Strength north	south	mean
LIR_022	12/15/2003	1204	13.07	45.8	35.2	40.5
PS_LIR_023	12/15/2003	1327	14.45	45.1	27.0	36.1
AR_R10_V0P02_024	12/15/2003	1457	15.95	40.2	21.9	31.1
AR_R10_V0P1_025	12/15/2003	1521	16.35	39.0	20.7	29.9
AR_R10_V0P6_026	12/15/2003	1539	16.65	38.2	19.9	29.0
CR_R10_V0P6_027	12/15/2003	1547	16.78	37.8	19.5	28.6
CR_R10_V0P9_028	12/15/2003	1600	17.00	37.1	18.9	28.0

NRC - INSTITUTE FOR MARINE DYNAMICS

ARCTIC VESSEL RESEARCH SECTION

ICE MECHANICAL PROPERTIES SUMMARY

Test Name: NMS2 Project Number: 04953

Warm up commenced: 00:37 7-JAN-2004

Time	Warm-up hrs	Loc	hi mm	Sf kPa	Lc cm	E MPa	E/Sf	Lc/hi	K1c N/m	Sf/K1c m-.5	Sc/s	kPa	Rhoi Mg/m3
0805	7.45	N	39.2± 4.3 n= 3										
		S	35.1± 0.8 n= 3										
0830	7.87	40S	36.8		50.	136.4	1629	13.7					
0900	8.37	40N	37.1	69.± 2.2									
			37.1	67.(u/d 97%)									
0903	8.42	40S	36.7	76.± 3.5									
			36.2	40.(u/d 52%)									
1031	9.89	39N	37.0	53.± 1.2									
			37.1	57.(u/d108%)									
1035	9.95	39S	37.0	54.± 7.0									
			36.4	37.(u/d 68%)									
1114	10.60	39S	37.6							s	50.4±	6.4	
1120	10.70	39N	37.6							s	40.0_	2.9	
1129	10.85	38S	36.9	36.± 2.4									
			36.3	32.(u/d 89%)									
1137	10.99	38N	36.3	40.± 1.8									
			35.6	34.(u/d 83%)									
1220	11.70	N	38.2± 1.6 n=31										
		S	38.8± 1.5 n=31										
1318	12.67	62S	40.9										.819
1400	13.37	N	38.2± 1.3 n=31										
		S	36.9± 1.1 n=31										
1420	13.70	70S	39.1										.888
1432	13.90	66N	40.3										.845
1435	13.95	N	38.0± 2.0 n=32										
		S	38.2± 2.0 n=32										
1500	14.37	42S	36.6	27.± 2.2									

			36.2	21.(u/d 78%)
1501	14.39	42N	37.2	39.± 4.5
			37.3	32.(u/d 82%)

Run #	Date	Time	Hours from Warm-up	Flexural Strength north	south	mean
LIR_CC_111	01/07/2004	1202	11.40	39.0	32.6	35.8

NRC - INSTITUTE FOR MARINE DYNAMICS

ARCTIC VESSEL RESEARCH SECTION

ICE MECHANICAL PROPERTIES SUMMARY

Test Name: NMS3 Project Number: 04953

Warm up commenced: 22:34 8-JAN-2004

Time	Warm-up hrs	Loc	hi mm	Sf kPa	Lc cm	E MPa	E/Sf	Lc/hi	K1c N/m	Sf/K1c m-.5	Sc/s kPa	Rhoi Mg/m3
0836	10.02	N	39.3± 2.2 n= 3									
		S	39.4± 1.9 n= 3									
0846	10.19	40S	38.7		47.	90.1	1658	12.2				
0913	10.64	40N	39.8	74.± 4.3								
			40.1	44.(u/d 60%)								
0917	10.70	40S	39.1	51.± 4.8								
			39.0	36.(u/d 70%)								
1054	12.32	39N	39.8	65.± 3.7								
			39.5	36.(u/d 55%)								
1058	12.39	39S	39.6	46.± 4.4								
			40.1	31.(u/d 65%)								
1106	12.52	39N	39.3									.844
1112	12.62	39S	39.9									.850
1121	12.77	39S	39.8							s	63.2± 9.8	
1208	13.55	38N	40.2	52.± 4.0								
			40.3	32.(u/d 61%)								
1212	13.62	38S	40.1	43.± 1.2								
1317	14.70	N	40.3± 1.8 n=12									
		S	39.8± 1.8 n=12									
1418	15.72	37N	40.8	45.± 3.1								
			40.8	32.(u/d 71%)								
1420	15.75	37S	39.9	32.± 4.1								
			40.1	26.(u/d 81%)								
1430	15.92m	N	41.4± 1.9 n=19									
		S	40.8± 1.2 n=19									
1535	17.00	N	40.1± 1.0 n=13									

		S	39.7± 0.8	n=13
1623	17.80	N	40.5± 1.8	n= 5
		S	40.3± 1.9	n= 5
1642	18.12	41N	40.2	26.± 4.0
			40.1	19.(u/d 71%)
1644	18.15	41S	40.0	20.± 1.9
			39.9	15.(u/d 76%)
1650	18.25	N	38.9± 2.0	n=20
		S	38.8± 0.9	n=20

Run #		Date	Time	Hours from Warm-up	Flexural Strength north	south	mean
LIR CC	128	01/09/2004	1245	14.17	48.2	39.8	44.0
LIR CC	129	01/09/2004	1342	15.12	48.3	34.4	41.3
LIR CC	130	01/09/2004	1351	15.27	47.3	33.7	40.5
LIR CC	131	01/09/2004	1451	16.27	41.3	29.8	35.5
LIR CC	132	01/09/2004	1502	16.45	40.3	29.1	34.7
LIR CC	133	01/09/2004	1554	17.32	28.9	22.4	25.6

NRC - INSTITUTE FOR MARINE DYNAMICS

ARCTIC VESSEL RESEARCH SECTION

ICE MECHANICAL PROPERTIES SUMMARY

Test Name: NMS4 Project Number: O4953

Warm up commenced: 22:37 11-JAN-2004

Time	Warm-up hrs	Loc	hi mm	Sf kPa	Lc cm	E MPa	E/Sf	Lc/hi	K1c N/m	Sf/K1c m-.5	Sc/s kPa	Rhoi Mg/m3
0823	9.75	N	39.4± 3.0 n= 3									
		S	40.6± 2.3 n= 3									
0837	9.99	40S	39.1		48.	90.9	1467	12.2				
0855	10.29	40N	39.2	64.± 1.3								
			39.4	42.(u/d 65%)								
0904	10.44	40S	39.6	57.± 2.9								
			39.6	42.(u/d 74%)								
0943	11.09	39N	39.3	56.± 3.6								
			39.7	105.(u/d187%)								
0959	11.35	39S	39.8	55.± 2.9								
			40.0	40.(u/d 73%)								
1047	12.15	39S	40.1							s	60.9±11.4	
1102	12.40	39S	40.1									.844
1110	12.54	39N	41.1									.809
1119	12.69	38N	39.9	54.± 4.0								
			40.4	40.(u/d 74%)								
1122	12.74	38S	40.2	47.± 4.8								
			40.7	33.(u/d 70%)								
1330	14.87	N	41.0± 2.1 n=14									
		S	40.9± 2.1 n=14									
1351	15.22	37N	40.6	41.± 1.7								
			41.0	28.(u/d 68%)								
1352	15.24	37S	40.3	34.± 2.1								
			40.5	25.(u/d 72%)								
1432	15.90	N	41.7± 1.8 n=12									
		S	41.2± 1.0 n=12									

1511	16.55	N	40.3± 0.4	n= 5
		S	40.5± 0.4	n= 5
1536	16.97	N	39.7± 0.5	n= 5
		S	39.8± 0.5	n= 5
1655	18.29	N	39.0± 0.9	n= 4
		S	39.4± 0.2	n= 4
1717	18.65	N	39.2± 0.2	n= 4
		S	39.3± 0.4	n= 4
1732	18.90	35N	40.1	16.± 2.0
1735	18.95	35S	40.5	11.± 0.8
			40.8	10.(u/d 87%)

Run #	Date	Time	Hours from Warm-up	Flexural Strength north	south	mean
LIR CC 144	01/12/2004	1309	14.52	45.5	39.1	42.3
LIR CC 145	01/12/2004	1356	15.30	40.3	33.6	36.9
LIR CC 146	01/12/2004	1408	15.50	39.1	32.3	35.7
LIR CC 147	01/12/2004	1446	16.14	35.4	28.6	32.0
LIR CC 148	01/12/2004	1528	16.84	31.8	25.0	28.4

NRC - INSTITUTE FOR OCEAN TECHNOLOGY

ICE TANK FACILITIES

ICE MECHANICAL PROPERTIES SUMMARY

Test Name: NMS5 Project Number: 04953

Warm up commenced: 22:40 13-JAN-2004

Time	Warm-up hrs	Loc	hi mm	Sf kPa	Lc cm	E MPa	E/Sf	Lc/hi	K1c N/m	Sf/K1c m-.5	Sc/s kPa	Rhoi Mg/m3
0823	9.70	N	38.5± 1.4 n= 3									
		S	40.3± 1.4 n= 3									
0832	9.85	40N	38.2		41.	51.2	1448	10.6				
0854	10.22	40N	39.4	34.± 0.6								
			39.4	25.(u/d 73%)								
0858	10.29	40S	39.1	37.± 5.5								
			39.5	28.(u/d 74%)								
1028	11.79	N	39.4± 1.5 n= 4									
		S	40.0± 1.2 n= 4									
1051	12.17	N	38.5± 0.9 n= 4									
		S	38.2± 0.8 n= 4									
1105	12.40	N	39.0± 1.8 n= 4									
		S	39.1± 2.3 n= 4									
1122	12.69	38N	40.9	38.± 5.0								
			41.1	32.(u/d 83%)								
1129	12.80	38N	40.1	32.± 1.3								
			39.1	17.(u/d 54%)								
1138	12.95	38S	40.0							s	44.2± 5.8	
1222	13.69	N	41.8± 0.7 n= 5									
		S	41.1± 0.8 n= 5									
1316	14.59	37N	39.1	28.± 3.6								
			38.7	18.(u/d 63%)								
1317	14.60	37S	40.4	29.± 4.2								
			40.5	20.(u/d 70%)								
1324	14.72	N	41.2± 0.7 n= 5									
		S	40.9± 1.7 n= 5									
1437	15.94	N	40.3± 0.7 n= 5									

		S	41.0± 0.7 n= 5		
1508	16.45	36N	41.0		.867
1511	16.50	37S	40.4		.915
1514	16.55	N	40.4± 0.2 n= 5		
		S	40.4_ 0.4 n= 5		
1523	16.70	34N	39.0 18.± 2.6		
			39.1 10.(u/d 57%)		
1525	16.74	34S	40.2 16.± 0.6		
			40.0 12.(u/d 71%)		
1559	17.30	N	38.6± 0.5 n= 5		
		S	39.6± 0.5 n= 5		
1623	17.70	N	38.8± 0.8 n= 5		
		S	39.2± 0.7 n= 5		
1648	18.12	N	39.8± 0.7 n= 6		
		S	40.4± 1.2 n= 6		
1703	18.37	41N	39.0 18.± 1.3		
			39.3 13.(u/d 70%)		
1708	18.45	41S	39.1 15.± 0.9		
			39.0 7.(u/d 50%)		

Run #	Date	Time	Hours from Warm-up	Flexural Strength north	south	mean
LIR_YAW00_0P6_CC_156	01/14/2004	1050	12.15	33.0	31.7	32.3
LIR_YAW2_0P6_SQP_157	01/14/2004	1050	12.15	33.0	31.7	32.3
LIR_YAWM2_0P6_NQP_158	01/14/2004	1050	12.15	33.0	31.7	32.3
LIR31_0P6_AR10_164	01/14/2004	1206	13.42	29.1	27.1	28.1
LIR31_0P6_AR10_165	01/14/2004	1236	13.92	27.7	25.5	26.6
LIR33_0P4_AR10_168	01/14/2004	1424	15.72	23.1	20.5	21.8
LIR34_0P3_AR10_169	01/14/2004	1457	16.27	21.8	19.2	20.5
LIR35_0P2_AR10_170	01/14/2004	1543	17.04	20.2	17.4	18.8
LIR36_0P1_AR10_171	01/14/2004	1613	17.54	19.2	16.4	17.8
LIR37_0P05_AR10_172	01/14/2004	1635	17.90	18.5	15.7	17.1

Appendix D

Test Matrix

Test type	Name
Level Ice Resistance Runs	**Name: LIR_'Channel'_Inc.dac** • LIR = Level Ice Resistance • Channel = test location (CC, NQP, or SQP) If not stated assume CC • Inc = Incremented File Number (automatically) • dac = extension for GEDAP files. **Example: LIR_CC_111** • Level ice resistance, Center Channel, 111th run sequence.

Pre-sawn Resistance Runs	**Name: PS_'SQP'_'Cut'_Inc.dac**
	• PS = Pre-sawn Ice Resistance
	• SQP = test performed in South Quarter Point
	• Cut = HB or SC. If not stated assume HB
	  ○ HB = Herring Bone
	  ○ SC = Straight Cut
	• Inc = Incremented File Number (automatically)
	• dac = extension for GEDAP files.
	Example: PRESAWN_SQP_HB_112
	• Pre-sawn ice resistance, South Quarter Point, Herring Bone, 112th run sequence.

Arc Ice Runs	**Name: 'LIR##'_'V_m'_'AR#'_Inc.dac** • LIR = Level Ice Resistance • ## = Ice sheet #, Arc # • V_m = Velocity of the model (example: 0P1 = 0.1 m/s) • RA# = Rudder Angle (degrees) • AR# = Arc Radius (m) • Inc = Incremented File Number (automatically) • dac = extension for GEDAP files. **Example: LIR23_OP6_AR10_147** • Level ice test, Ice Sheet # 2, Run # 3, Model Speed = 0.6 m/s, Arc radius = 10 m, 147th run sequence.
Open Water Runs	**Name: 'OW#'_'V_m'_'RA#'_'AR#'_inc.dac** • OW = Open Water • V_m = Model Speed • Inc = Incremented File Number **Example: OW1_OP1_RA0_AR999_053** • Open Water Test, Speed of 0.1m/s, Rudder Angle of 0°, and Arc radius of 999 m, 53rd run sequence

Experiments in Level Ice:

Run name	Test Date	Test Time	Model Velocity (m/s)	Arc Radius (m)
LIR_022	15-Dec-03	12:04:34	0.1	Straight
LIR_022	15-Dec-03	12:04:34	0.6	Straight
LIR_022	15-Dec-03	12:04:34	0.9	Straight
LIR_022	15-Dec-03	12:04:34	0.02	Straight
LIR_CC_111	7-JAN-2004	12:02:05	0.1	Straight
LIR_CC_111	7-JAN-2004	12:02:05	0.3	Straight
LIR_CC_111	7-JAN-2004	12:02:05	0.6	Straight
LIR_CC_111	7-JAN-2004	12:02:05	0.02	Straight
LIR_NQP_114	7-JAN-2004	14:20:35	0.1	Straight
LIR_NQP_114	7-JAN-2004	14:20:35	0.6	Straight
LIR_NQP_114	7-JAN-2004	14:20:35	0.9	Straight
LIR_NQP_114	7-JAN-2004	14:20:35	0.02	Straight
LIR11_0P1_AR50_128	9-JAN-2004	12:45:07	0.1	50
LIR11A_0P1_129	9-JAN-2004	13:42:14	0.1	Straight
LIR12_0P3_AR50_130	9-JAN-2004	13:51:13	0.3	50
LIR12A_0P3_131	9-JAN-2004	14:51:09	0.3	Straight
LIR13_0P3_AR10_132	9-JAN-2004	15:02:01	0.3	10
LIR14_0P1_AR10_133	9-JAN-2004	15:54:43	0.1	10
LIR_SQP_134	9-JAN-2004	16:29:41	0.1	Straight
LIR_SQP_134	9-JAN-2004	16:29:41	0.3	Straight
LIR_SQP_134	9-JAN-2004	16:29:41	0.6	Straight
LIR21_OP6_AR50_144	12-Jan-04	13:09:49	0.6	50
LIR21A_OP6_145	12-Jan-04	13:56:30	0.6	Straight
LIR22_OP02_AR50_146	12-Jan-04	14:08:37	0.02	10
LIR23A_OP6_AR10_148	12-Jan-04	15:26:37	0.6	10
LIR24A_SQP_149	12-Jan-04	16:13:52	0.1	Straight
LIR24A_SQP_149	12-Jan-04	16:13:52	0.3	Straight
LIR24A_SQP_149	12-Jan-04	16:13:52	0.6	Straight
LIR24A_SQP_149	12-Jan-04	16:13:52	0.02	Straight
LIR24B_SQP_150	12-Jan-04	16:20:47	0.1	Straight
LIR24B_SQP_150	12-Jan-04	16:20:47	0.02	Straight
LIR25_0P3_AR10_152	12-Jan-04	16:46:56	0.3	10
LIR24_0P02_AR10_153	12-Jan-04	17:07:13	0.02	10
LIR31_0P6_AR10_164	14-Jan-04	12:06:49	0.6	10
LIR31_0P6_AR10_165	14-Jan-04	12:36:36	0.5	10
LIR33_0P4_AR10_168	14-Jan-04	14:24:42	0.4	10
LIR34_0P3_AR10_169	14-Jan-04	14:57:49	0.3	10
LIR35_0P2_AR10_170	14-Jan-04	15:43:54	0.2	10
LIR36_0P1_AR10_171	14-Jan-04	16:13:08	0.1	10
LIR37_0P05_AR10_172	14-Jan-04	16:35:16	0.05	10

Experiments in Pre-sawn Ice:

Run Name	Test Date	Test Time	Model Velocity (m/s)	Run Pattern
PS_SQP_023	15-Dec-03	13:27:19	0.1	Straight
PS_SQP_023	15-Dec-03	13:27:19	0.6	Straight
PS_SQP_023	15-Dec-03	13:27:19	0.9	Straight
PS_SQP_023	15-Dec-03	13:27:19	0.02	Straight
PRESAWN_SQP_HB_112	7-JAN-2004	13:26:04	0.1	Straight
PRESAWN_SQP_HB_112	7-JAN-2004	13:26:04	0.3	Straight
PRESAWN_SQP_HB_112	7-JAN-2004	13:26:04	0.6	Straight
PRESAWN_SQP_HB_112	7-JAN-2004	13:26:04	0.02	Straight
PRESAWN_SQP_SC_113	7-JAN-2004	13:38:01	0.1	Straight
PRESAWN_SQP_SC_113	7-JAN-2004	13:38:01	0.3	Straight
PRESAWN_SQP_SC_113	7-JAN-2004	13:38:01	0.6	Straight
PRESAWN_SQP_SC_113	7-JAN-2004	13:38:01	0.02	Straight

Experiments in Open Water:

Open Water Test	Test Date	Test Time	Model Speed (m/s)	Arc Radius (m)	Rudder Angle (degrees)
OW1_OP1_RA0_AR999_053	22-Dec-03	15:48:41	0.1	Straight	0
OW1_OP6_RA0_AR999_054	22-Dec-03	16:00:08	0.6	Straight	0
OW2_0P9_RA0_AR999_057	23-Dec-03	8:45:41	0.9	Straight	0
OW4_0P1_RA0_AR50_058	23-Dec-03	9:05:41	0.1	50	0
OW5_0P6_RA0_AR50_059	23-Dec-03	9:40:34	0.6	50	0
OW6_0P9_RA0_AR50_060	23-Dec-03	9:49:42	0.9	50	0
OW7_0P1_RA0_AR10_061	23-Dec-03	9:57:38	0.1	10	0
OW8_0P6_RA0_AR10_062	23-Dec-03	10:08:16	0.6	10	0
OW9_0P9_RA0_AR10_063	23-Dec-03	10:18:20	0.9	10	0
OW9A_0P9_RA0_CR10_064	23-Dec-03	10:28:18	0.9	10	0
OW10_0P1_RA20_CR999_065	23-Dec-03	10:54:59	0.1	Straight	20
OW10_0P6_RA20_CR999_066	23-Dec-03	11:05:01	0.6	Straight	20
OW12_0P9_RA20_CR999_067	23-Dec-03	11:15:29	0.9	Straight	20
OW13_0P1_RA20_AR50_068	23-Dec-03	11:25:25	0.1	50	20
OW14_0P6_RA20_AR50_069	23-Dec-03	11:35:22	0.6	50	20
OW15_0P9_RA20_AR50_070	23-Dec-03	11:42:59	0.9	50	20
OW16_0P1_RA20_CR10_071	23-Dec-03	11:49:30	0.1	10	20
OW17_0P6_RA20_CR10_072	23-Dec-03	12:00:02	0.6	10	20
OW18_0P9_RA20_CR10_073	23-Dec-03	12:10:43	0.9	10	20
OW19_0P1_RA30_CR999_074	23-Dec-03	12:20:45	0.1	Straight	20
OW20_0P6_RA30_CR999_075	23-Dec-03	12:31:15	0.6	Straight	30
OW21_0P9_RA30_CR999_076	23-Dec-03	12:41:11	0.9	Straight	30
OW22_0P1_RA30_AR50_077	23-Dec-03	12:50:59	0.1	50	30
OW23_0P6_RA30_AR50_078	23-Dec-03	12:59:23	0.6	50	30
OW24_0P9_RA30_AR50_079	23-Dec-03	13:05:46	0.9	50	30
OW25_0P1_RA30_CR10_080	23-Dec-03	13:18:26	0.1	10	30
OW25A_0P1_RA30_CR10_083	23-Dec-03	13:44:18	0.1	10	30
OW26_0P6_RA30_CR10_081	23-Dec-03	13:28:54	0.6	10	30
OW27_0P9_RA30_CR10_082	23-Dec-03	13:38:36	0.9	10	30
OW28_0P1_OP6_0P9_RA00_CR999_084	23-Dec-03	13:55:08	0.1	Straight	0
OW28_0P1_OP6_0P9_RA00_CR999_084	23-Dec-03	13:55:08	0.6	Straight	0
OW28_0P1_OP6_0P9_RA00_CR999_084	23-Dec-03	13:55:08	0.9	Straight	0
OW29_0P6_RA0_AR999_096	5-JAN-04	13:31:25	0.6	Straight	0
OW30_0P3_RA0_AR999_097	5-JAN-04	13:41:20	0.3	Straight	0
OW31_0P1_RA0_AR50_101	5-JAN-04	15:11:15	0.1	50	0
OW32_0P6_RA0_AR50_102	5-JAN-04	15:20:38	0.6	50	0
OW33_0P3_RA0_AR50_098	5-JAN-04	14:17:29	0.3	50	0
OW34_0P1_RA0_AR10_103	5-JAN-04	15:28:34	0.1	10	0
OW35A_0P6_RA0_AR10_105	5-JAN-04	15:49:43	0.6	10	0
OW36_0P3_RA0_AR10_099	5-JAN-04	14:49:55	0.3	10	0

Appendix E

Channel Width Measurements in Ice Tests

The actual measured data for channel edge positions in the model tests are discontinuous and unavoidable with human errors. It is expected that the two edges of the channel width were parallel and concentric to the model path that was controlled by the PMM. Concentric circles of various radii were then fitted to the measurements to obtain the best match.

Example

For Run LIR31_0P6_AR10_165, the circling radius was 10m, and the model speed was 0.6m/s. The radii of the best fitted circular arcs for the inner and the outer edges were 9.45 and 10.65 m, respectively, with a channel width of 1.2 m, as shown in Figure E.1.

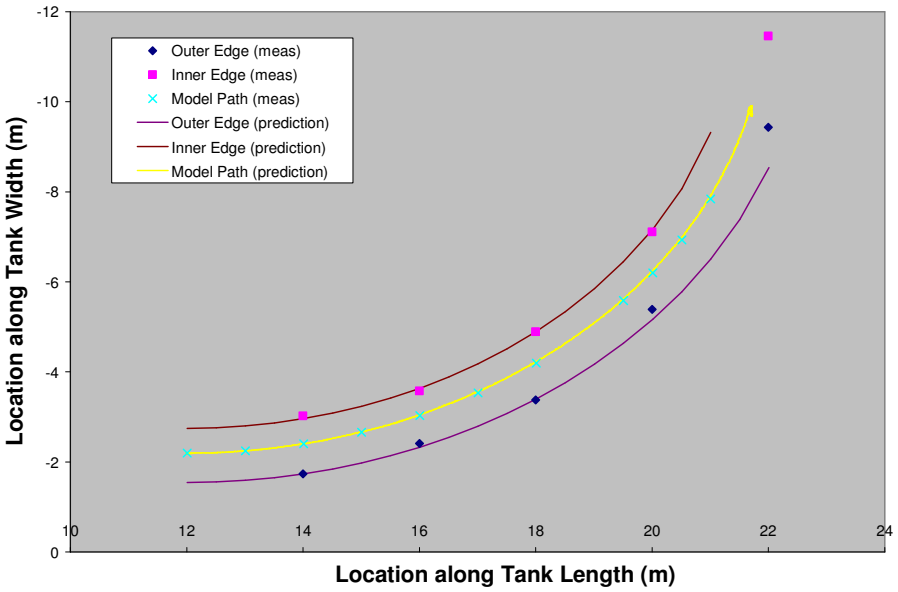

Figure E.1: The measured and predicted channel edge positions

Summary of Channel Width Measurements

Run Name: LIR11_0P1_AR50_128
Data: 9-Jan-04
Circle Radius (m): 50
Model Velocity (m/s): 0.1
Channel Width (m): 1.0

Position X (m)	North Edge Y_N (m)	South Edge Y_S (m)
2	1.83	2.73
4	1.91	2.90
6	2.22	3.16
8	2.56	3.52
10	2.91	3.97
12	3.25	4.36
14	3.77	4.88
16	4.44	5.65
18	5.09	6.23
20	5.81	7.28
22	6.85	8.15
24	8.39	8.84

Run Name: LIR12_0P3_AR50_130
Data: 9-Jan-04
Circle Radius (m): 50
Model Velocity (m/s): 0.3
Channel Width (m): 1.05

Position X (m)	North Edge Y_N (m)	South Edge Y_S (m)
24	1.93	2.85
26	1.81	3.01
28	2.32	3.36
30	2.55	3.62
32	3.03	3.98
34	3.60	4.61
36	4.18	5.29
38	4.64	5.91
40	5.44	6.67
42	6.56	7.55
44	7.44	8.57
46	8.33	9.69
48	9.81	10.75

Run Name: LIR13_0P3_AR10_132
Data: 9-Jan-04
Circle Radius (m): 10
Model Velocity (m/s): 0.3
Channel Width (m): 1.02

Position X (m)	North Edge Y_N (m)	South Edge Y_S (m)
48	2.16	3.52
50	3.02	4.33
52	4.59	6.14
54	6.88	10.30

Run Name: LIR14_0P1_AR10_133
Data: 9-Jan-04
Circle Radius (m): 10
Model Velocity (m/s): 0.1
Channel Width (m): 1.2

Position X (m)	North Edge Y_N (m)	South Edge Y_S (m)
54	1.97	3.20
56	2.83	4.08
58	3.86	5.79
60	6.49	8.89
62	11.35	11.35

Run Name: LIR21_OP6_AR50_144
Data: 12-Jan-04
Circle Radius (m): 50
Model Velocity (m/s): 0.6
Channel Width (m): 1.1

Position X (m)	North Edge Y_N (m)	South Edge Y_S (m)	Position X (m)	North Edge Y_N (m)	South Edge Y_S (m)
2	1.89	2.71	16	4.46	5.53
4	1.90	2.94	18	5.13	6.39
6	2.02	3.18	20	6.05	7.19
8	2.35	3.54	22	6.93	8.04
10	2.84	3.84	24	8.08	9.25
12	3.28	4.43	26	9.09	10.61
14	3.76	4.89	28	10.79	10.79

Run Name: LIR22_OP02_AR50_146
Data: 12-Jan-04
Circle Radius (m): 50
Model Velocity (m/s): 0.02
Channel Width (m): 1.0

Position X (m)	North Edge Y_N (m)	South Edge Y_S (m)
28	1.88	2.92
30	1.90	2.93
32	1.96	3.06
34	2.35	2.86

Run Name: LIR23A_OP6_AR10_148
Data: 12-Jan-04
Circle Radius (m): 10
Model Velocity (m/s): 0.6
Channel Width (m): 1.35

Position X (m)	North Edge Y_N (m)	South Edge Y_S (m)
40	1.60	3.14
42	2.16	3.57
44	3.14	4.69
46	4.76	6.47
48	7.34	8.86

Run Name: LIR25_0P3_AR10_152
Data: 12-Jan-04
Circle Radius (m): 10
Model Velocity (m/s): 0.3
Channel Width (m): 1.3

Position X (m)	North Edge Y_N (m)	South Edge Y_S (m)
48	1.94	3.23
50	2.71	4.36
52	4.16	6
54	5.65	9.44
56	11.53	11.53

Run Name: LIR24_0P02_AR10_153
Data: 12-Jan-04
Circle Radius (m): 10
Model Velocity (m/s): 0.02
Channel Width (m): 1.1

Position X (m)	North Edge Y_N (m)	South Edge Y_S (m)
52	1.89	3.08
54	1.89	3.08
56	2.62	3.89
58	4.16	4.16

Run Name: LIR31_0P6_AR10_164
Data: 14-Jan-04
Circle Radius (m): 10
Model Velocity (m/s): 0.6
Channel Width (m): 1.25

Position X (m)	North Edge Y_N (m)	South Edge Y_S (m)
8	1.63	3.07
10	2.39	3.81
12	3.67	5.22
14	5.27	7.44
15.5	7.7	8.93

Run Name: LIR31_0P6_AR10_165
Data: 14-Jan-04
Circle Radius (m): 10
Model Velocity (m/s): 0.5
Channel Width (m): 1.2

Position X (m)	North Edge Y_N (m)	South Edge Y_S (m)
14	1.74	3.02
16	2.41	3.58
18	3.38	4.89
20	5.39	7.11
22	9.43	11.46

Run Name: LIR33_0P4_AR10_168
Data: 14-Jan-04
Circle Radius (m): 10
Model Velocity (m/s): 0.4
Channel Width (m): 1.15

Position X (m)	North Edge Y_N (m)	South Edge Y_S (m)
22	1.77	2.99
24	1.99	3.49
26	3.39	4.77
28	5.47	7.46
30	8.43	10.99

Run Name: LIR34_0P3_AR10_169
Data: 14-Jan-04
Circle Radius (m): 10
Model Velocity (m/s): 0.3
Channel Width (m): 1.25

Position X (m)	North Edge Y_N (m)	South Edge Y_S (m)
28	1.83	2.94
30	2.26	3.45
32	2.89	4.42
34	4.73	6.49
36	6.41	10.09
36.5	10.92	10.92

Run Name: LIR35_0P2_AR10_170
Data: 14-Jan-04
Circle Radius (m): 10
Model Velocity (m/s): 0.2
Channel Width (m): 1.1

Position X (m)	North Edge Y_N (m)	South Edge Y_S (m)
40	1.84	3.02
42	2.42	3.92
44	3.57	5.18
46	6.02	7.85
47.5	8.36	10.85

Run Name: LIR36_0P1_AR10_171
Data: 14-Jan-04
Circle Radius (m): 10
Model Velocity (m/s): 0.1
Channel Width (m): 1.05

Position X (m)	North Edge Y_N (m)	South Edge Y_S (m)
46	1.9	3.06
48	2.25	3.43
50	3.41	4.71
52	4.87	6.66
54	8.37	10.75

Run Name: LIR37_0P5_AR10_172
Data: 14-Jan-04
Circle Radius (m): 10
Model Velocity (m/s): 0.05
Channel Width (m): 1.15

Position X (m)	North Edge Y_N (m)	South Edge Y_S (m)
54	2.05	3.4
56	2.91	4.37
58	4.7	6.35
60	8	9.95
60.5	10.15	10.15

Channel widths of straight model tests

The channel widths for the straight test runs were not obtained with the exception of LIR_022. The average channel width for this run is 0.99 m.

Run Name: LIR_022
Data: 15-Dec-03
Straight Test Run
Model Velocity (m/s): 0.1, 0.6, 0.9 and 0.02
Channel width (m): 0.99

Position (X) (m)	Channel Width (m)
2	1.04
4	1.02
6	1.02
8	1.015
10	0.96
12	0.97
14	1
16	1.05
18	1.03
20	0.92
22	0.99
24	0.93
26	0.965
28	1.05
30	0.95
32	1.05
34	1.01
36	0.98
38	0.95
40	0.95
42	0.943
44	0.945
46	0.91
48	1.09
50	0.99
52	1.065
54	0.94
56	1.06
58	1.06
60	0.99
62	0.98
64	1

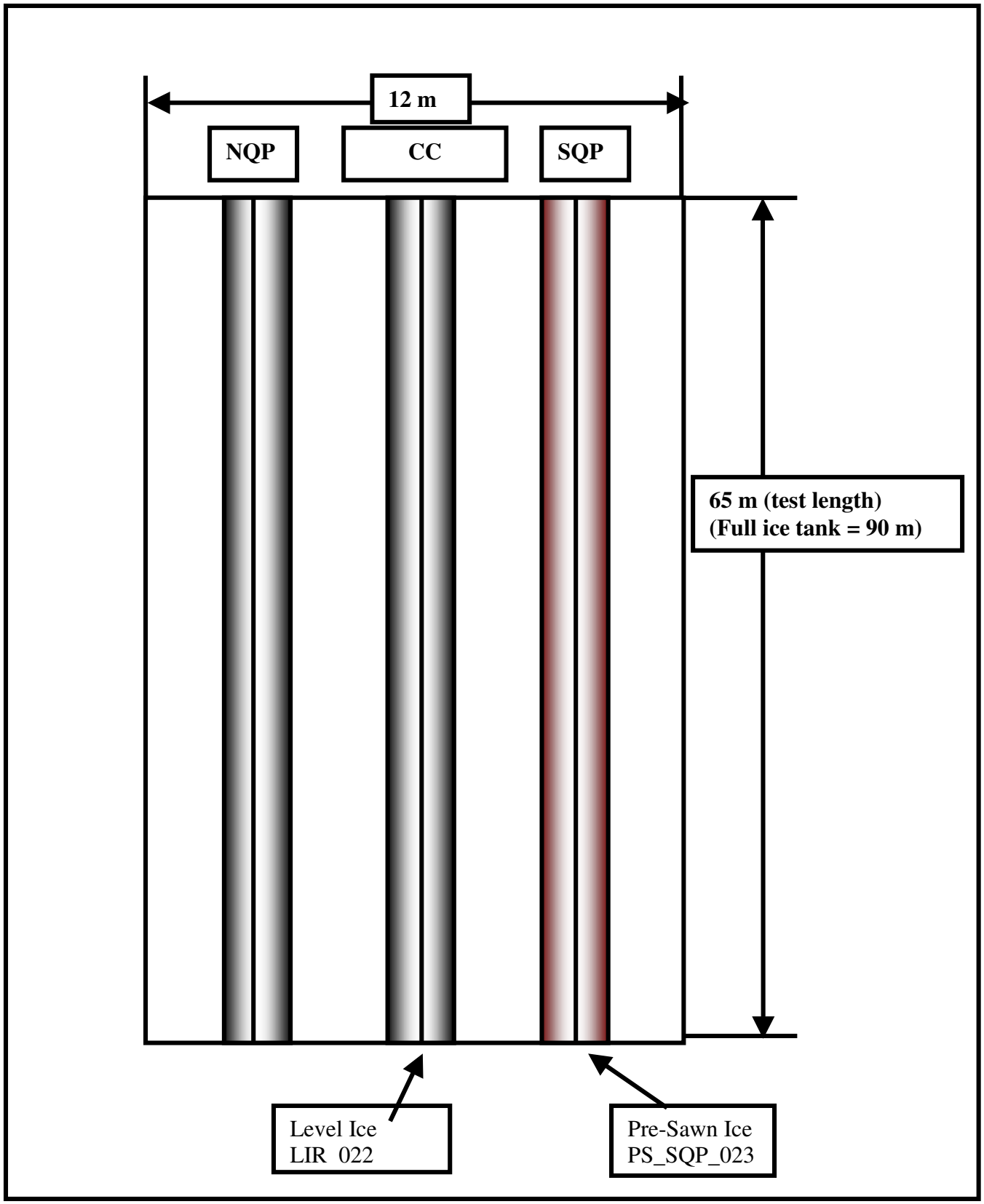

Figure E.2 : Run schematic for NMS1

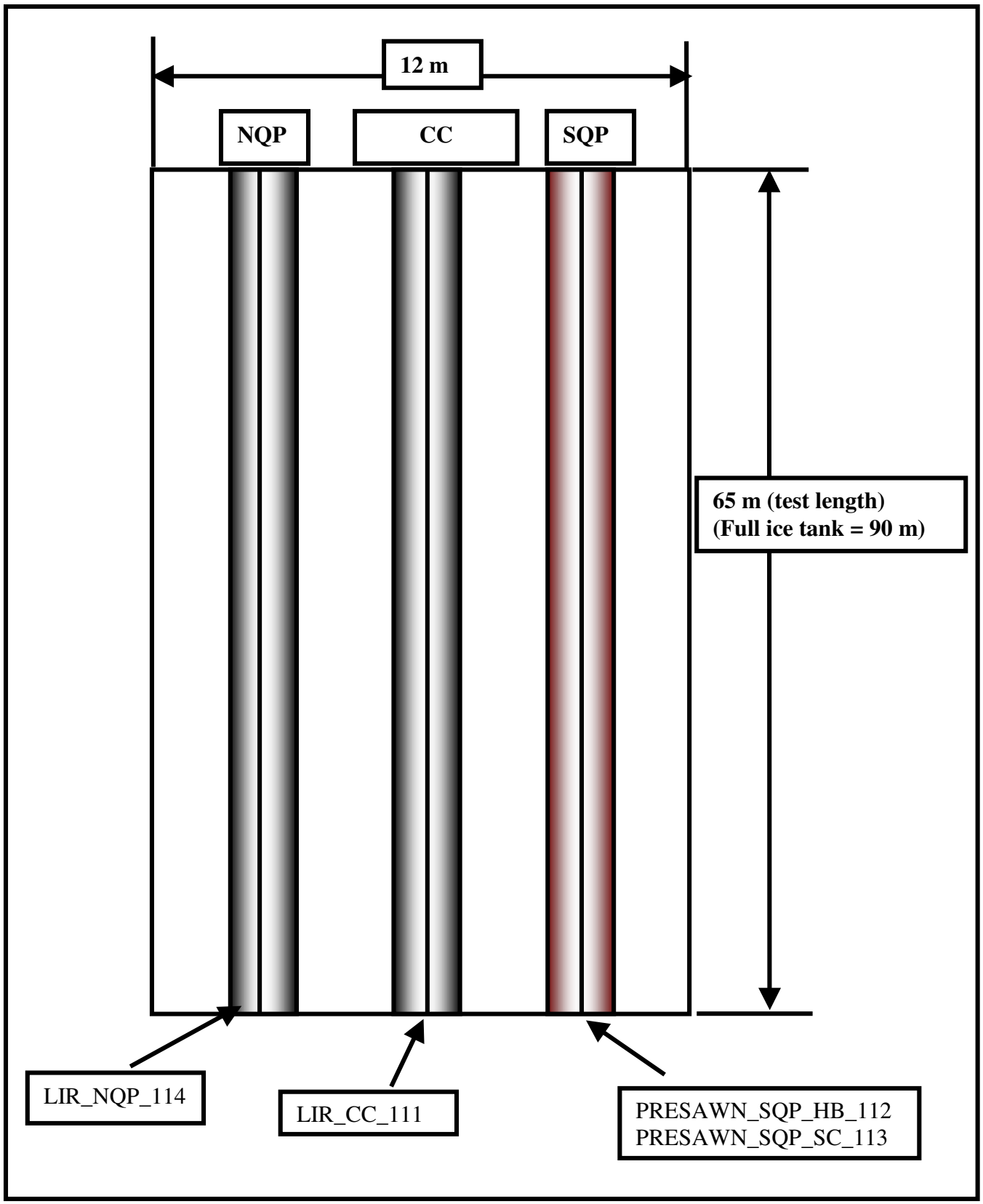

Figure E.3: Run schematic for NMS2

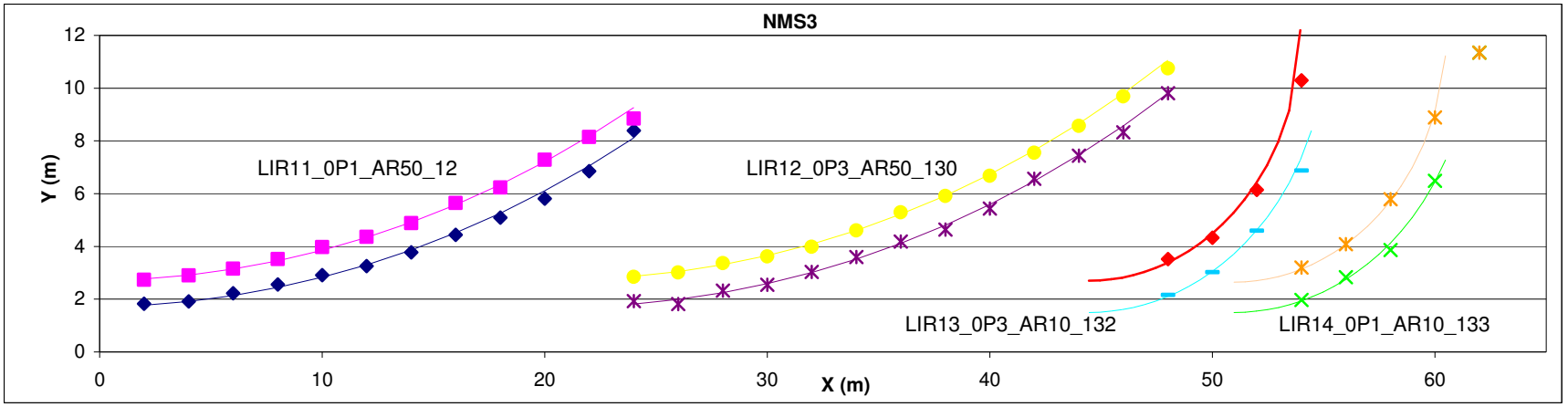

Figure E.4: Run schematic for NMS3

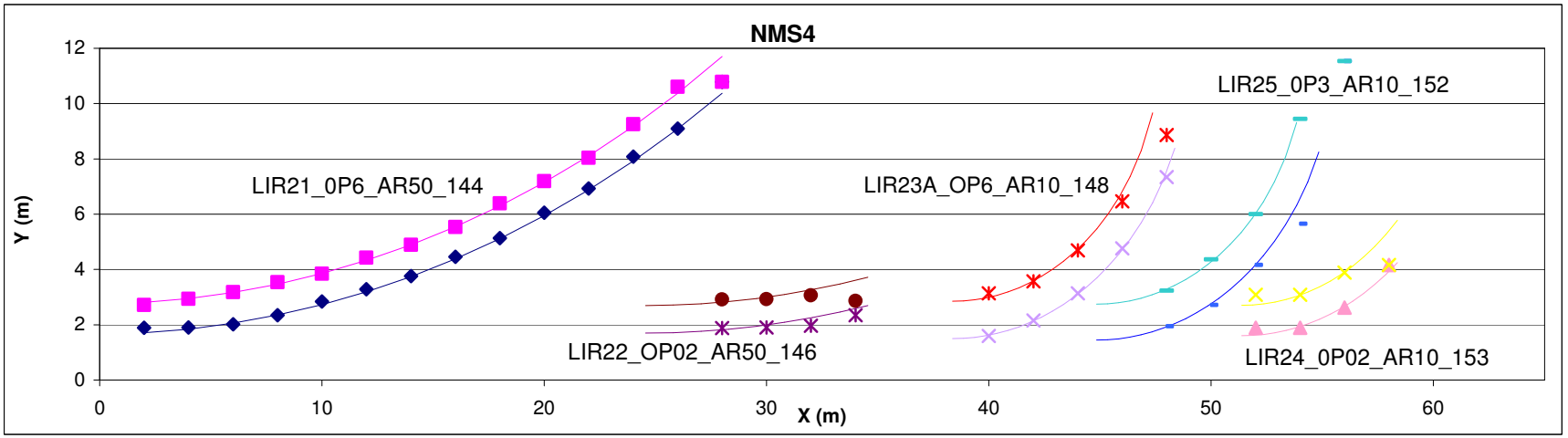

Figure E.5: Run schematic for NMS4

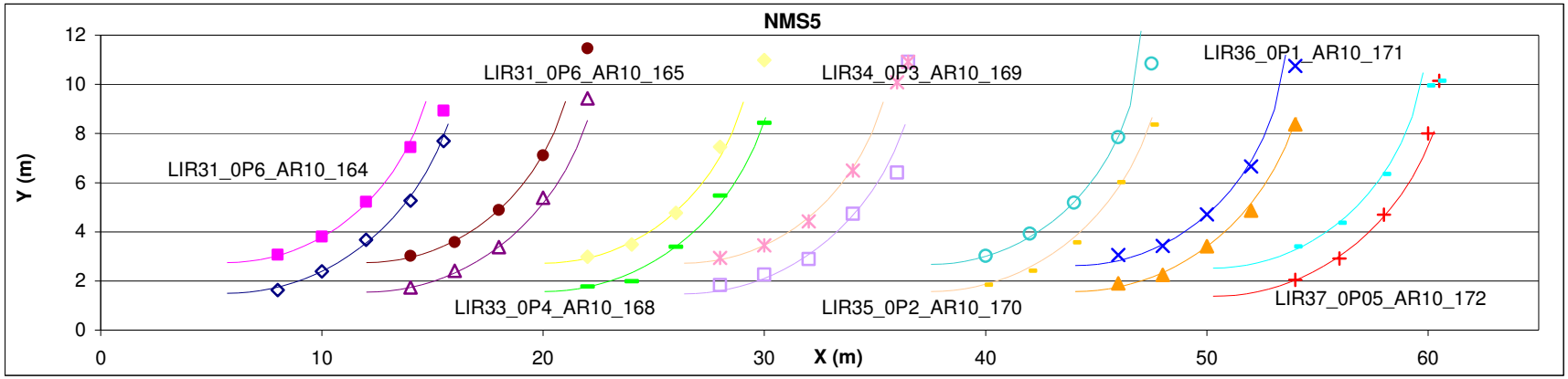

Figure E.6: Run schematic for NMS5

Appendix F

Typical Test Results

---- Tared Data ----

Analysis Date/Time = 4-NOV-2004 15:06:52
Acquired Date/Time = 9-JAN-2004 13:51:13
Input File = SHORT_S1
Output File = LIR12_0P3_AR50_130_STAT
Number of Samples = 3823
Segment Start Time = 46.060 seconds
Segment End Time = 122.50 seconds

Description	Unit	Min	Max	Mean	S.D.	Chan
Carriage Pos	m	32.728	54.380	43.823	6.2798	1
Surge Force	N	-321.74	42.141	-40.422	43.589	2
Fwd Sway Force	N	-280.78	401.37	-2.9793	69.398	3
Aft Sway Force	N	-123.36	58.446	-27.552	27.383	4
Sway Force	N	-318.65	372.47	-30.532	75.458	5
Yaw Moment	N-m	-277.74	427.40	25.955	71.160	6
Yaw	deg	-1.0460	0.028460	-0.44232	0.16563	7
Yaw Rate	deg/s	-0.91877	0.30031	-0.34316	0.14598	8
Sway Position	m	-7.2319	-0.18155	-2.8765	2.0751	9
Sway Velocity	m/s	-0.15904	-0.023292	-0.092805	0.037904	10
Fwd Heave	mm	-25.435	14.294	-3.5443	7.5967	11
Aft Heave	mm	1.7785	23.577	14.203	6.3322	12
Heave	mm	-38.884	-4.8861	-22.481	7.8800	13
Pitch	deg	-0.028460	1.0460	0.44232	0.16563	14
Surge Accel	m/s**2	-0.42561	0.098509	-0.057883	0.064508	15
Sway Accel	m/s**2	-0.11114	0.17385	0.028358	0.045376	16
Heave Accel	m/s**2	-0.20268	0.24203	-0.00077895	0.066082	17
Carriage Speed	m/s	0.25358	0.30048	0.28210	0.012611	18
Tangential Vel	m/s	0.29517	0.30406	0.29964	0.0012147	19
Cal_Yaw	deg	-31.807	-4.4612	-18.206	7.6650	20
Cal_Yaw - Yaw	deg	-1.2399	2.0189	0.66486	0.37142	21

Marine Structural Fragility and Software Validation
TERRY FOX – PMM/MANEUVER/ICE IOT

Analyzed: 04-NOV-2004 15:06:55
Acquired: 9-JAN-2004 13:51:13

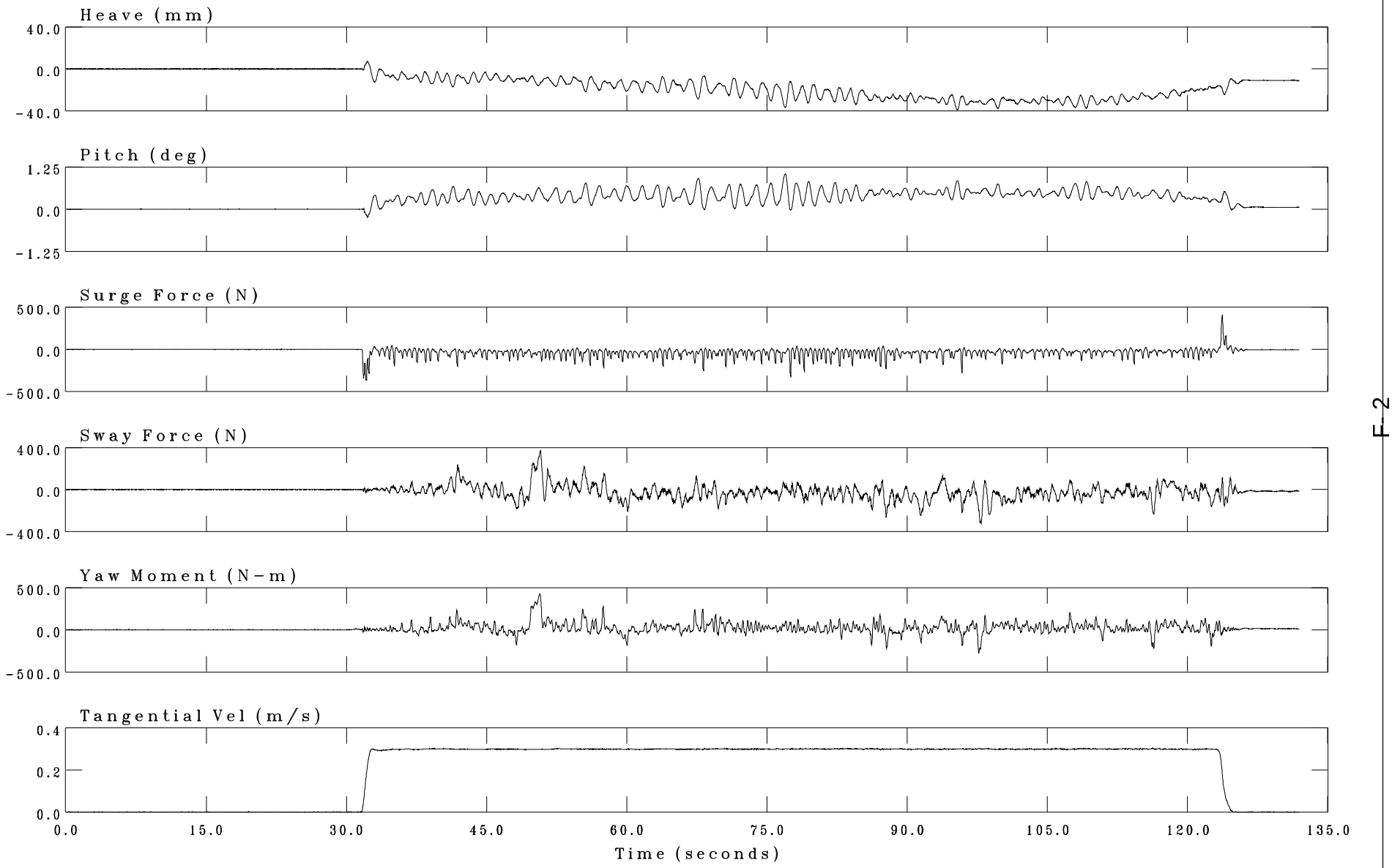

F-2

National Research Council Canada
Institute for Ocean Technology

GENERATED BY: LAUM	CHECKED BY:	APPROVED BY:

Figure 1 LIR12_0P3_AR50_130

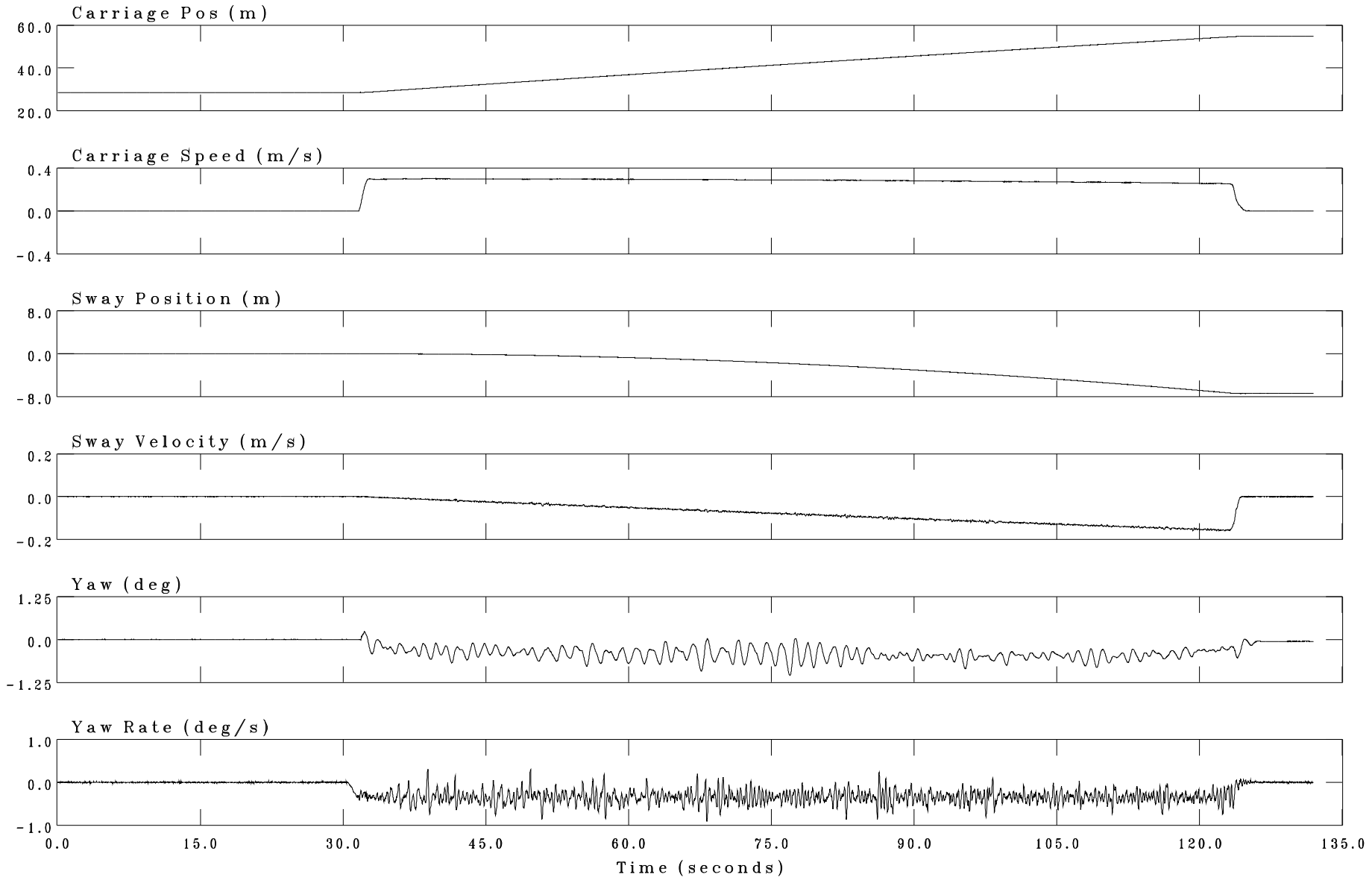

F-3

National Research Council Canada
Institute for Ocean Technology

GENERATED BY: LAUM	CHECKED BY:	APPROVED BY:

Figure 2 LIR12_0P3_AR50_130

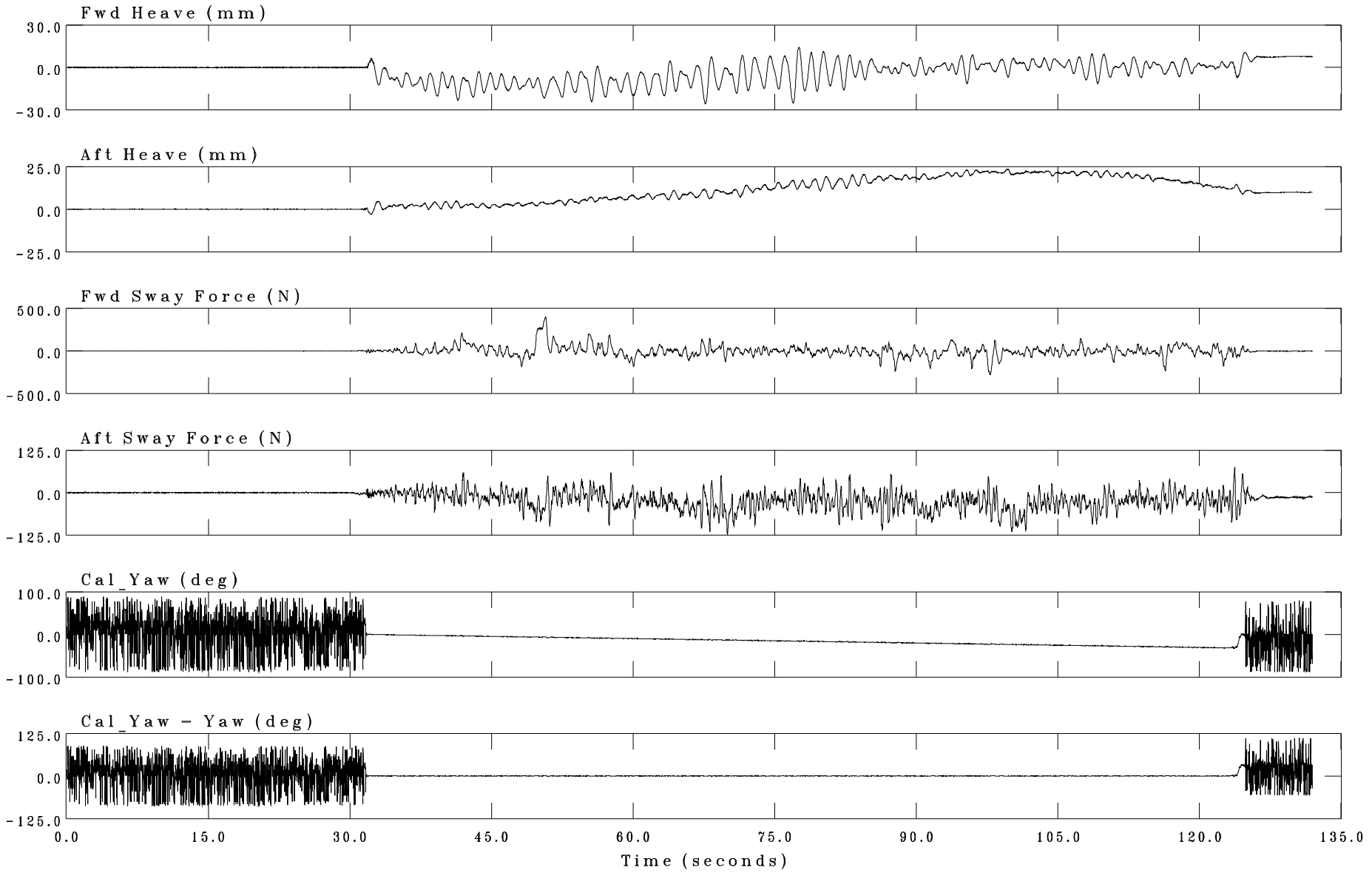

F-4

National Research Council Canada
Institute for Ocean Technology

GENERATED BY: LAUM	CHECKED BY:	APPROVED BY:

Figure 3 LIR12_0P3_AR50_130

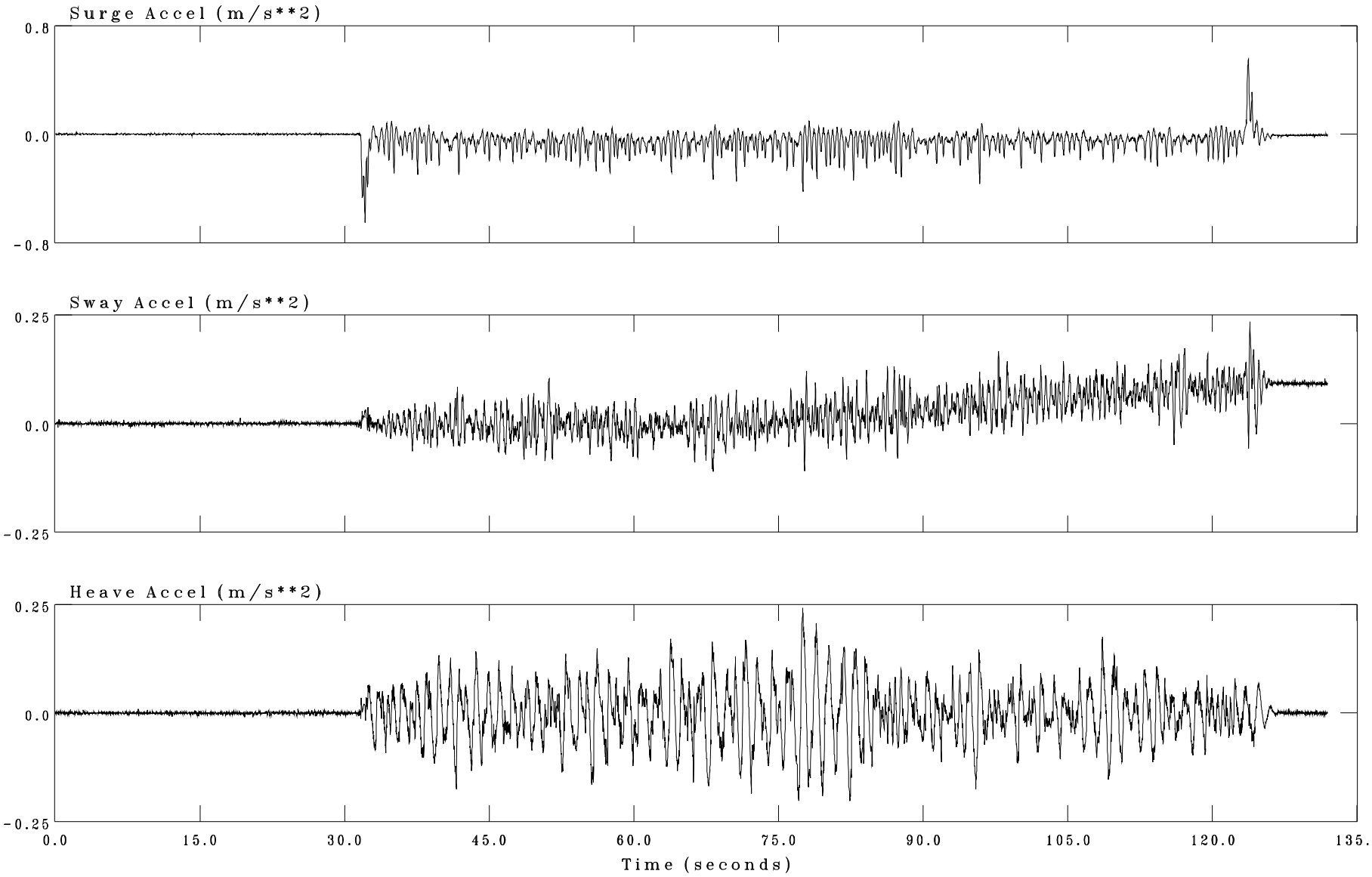

National Research Council Canada
Institute for Ocean Technology

GENERATED BY: LAUM	CHECKED BY:	APPROVED BY:

Figure 4 LIR12_0P3_AR50_130